10th International Conference

POLAND 2020 LUBLIN UNIVERSITY OF TECHNOLOGY

AMCM

ADVANCED MODELS AND NEW CONCEPTS IN CONCRETE AND MASONRY STRUCTURES

PROCEEDINGS

under auspices

Ministry of Science and Higher Education

Republic of Poland

Co-financed from the programme "Doskonała nauka"
Minister of Science and Higher Education.

HONORABLE PATRONAGE

MAYOR OF LUBLIN CITY
KRZYSZTOF ŻUK

RECTOR OF LUBLIN UNIVERSITY OF TECHNOLOGY
PROF. PIOTR KACEJKO

leading sponsors

SOLBET LUBARTÓW S.A.

Sika BUDUJĄCE ROZWIĄZANIA

sponsors

TS PROJEKTY EKSPERTYZY BUDOWLANE

CBiC Centrum Badań i Certyfikacji

10th International Conference AMCM
2020 Lublin, October 21–23, 2020

Advances Models and New Concepts in Concrete and Masonry Structures

Proceeding

Edited by:

Anna Halicka
Marta Słowik
Piotr Smarzewski
Ewa Zarzeka-Raczkowska

Publikacja wydana za zgodą Rektora Politechniki Lubelskiej

ISBN: 978-83-7947-414-1

Wydawca: Wydawnictwo Politechniki Lubelskiej
www.biblioteka.pollub.pl/wydawnictwa
ul. Nadbystrzycka 36C, 20-618 Lublin
tel. (81) 538-46-59

Druk: DjaF – 30-092 Kraków, ul. Kmietowicza 1/1
www.djaf.pl

Preface

The collection of abstracts published in this volume introduces the subject matter and contents of papers presented during the 10th International Conference on Advanced Models and New Concepts in Concrete and Masonry Structures **AMCM2020.** The conference has been organized online from 21st to 23rd October 2020 by Faculty of Civil Engineering and Architecture, Lublin University of Technology.
The objective of the **AMCM2020** conference is to bring together scientists and engineers from around the world to share recent achievements and the latest developments in the fields of concrete and masonry engineering, mechanics and computation. The **AMCM2020** intends to be a forum for discussion of the present and future trends in experimental, analytical and numerical investigations on concrete and masonry structures. The conference provides an opportunity to disseminate cross-disciplinary knowledge among researchers and civil engineers from Europe and numerous other countries outside the continent. It is organized once every three years to track and update developments in concrete and masonry structures research. After successful nine editions held in Białystok (1993), Łódź (1996), Wrocław/Świeradów (1999), Kraków (2002), Ustroń/Gliwice (2005), Łódź (2008), Kraków (2011), Wrocław (2014) and Gliwice (2017), the conference in 2020 is being organized by **Lublin University of Technology in cooperation with International Federation for Structural Concrete – Polish Group and Polish Union of Civil Engineers and Technicians – Lublin Scientific Committee**.

The main topics covered in the accepted papers include the following:

1. Models and numerical simulations for concrete and masonry at macro/meso/micro-scales.
2. Experiments, analytical and numerical models for concrete and masonry structures.
3. Advances in reinforced and pre-stressed concrete and masonry structures.
4. Behavior and application of HPC structures.
5. Application of FRP materials – theory, practice.
6. Durability assessment and environmental impact upon concrete and masonry structures.
7. Performance-based design of concrete and masonry structures.
8. Impact of cyclic and long-term loading on concrete and masonry structures.
9. Safety and reliability of concrete and masonry structures.

The volume contains abstracts of papers submitted and accepted by the Scientific Committee of AMCM2020 conference and 4 extended abstracts of plenary lectures. Particular thanks are due to plenary speakers and all authors of the papers to be presented during the event. Grateful thanks are extended to members of the Honorary Advisory Committee and Scientific Committee for their significant help in reviewing the papers and sharing their extensive knowledge and experience.
The tireless efforts and creative attitude of the members of the Organizing Committee during preparations for this event are highly appreciated. Last but not least, special credit is due to invited sponsors for their invaluable contribution and financial support.
We sincerely hope that the papers presented during the 10th International Conference on Advanced Models and New Concepts in Concrete and Masonry Structures will contribute to the development of science and technology in the field of concrete and masonry structures.

Anna Halicka	Marta Słowik
Chair of the Scientific Committee	Chair of the Organizing Committee

HONORARY ADVISORY COMMITTEE

Flaga Kazimierz (Poland)

Kaszyńska Maria (Poland)

Kowalczyk Ryszard (Poland)

Madryas Cezary (Poland)

Mróz Zenon (Poland)

Radomski Wojciech (Poland)

SCIENTIFIC COMMITTEE

Halicka Anna (Poland) – Chair of the Scientific Committee

Ajdukiewicz Andrzej (Poland)

Balázs György (Hungary)

Blikharskyy Zinoviy (Ukraine)

Capozucca Roberto (Italy)

Derkowski Wit (Poland)

Destrebecq Jean-F. (France)

Drobiec Łukasz (Poland)

Falikman Vyacheslav R. (Russia)

Fardis Michael N. (Greece)

Görgün Halil (Turkey)

Klemczak Barbara (Poland)

Klemm Agnieszka J. (United Kingdom)

Knauff Michał (Poland)

Kotynia Renata (Poland)

Kubica Jan (Poland)

Lantsoght Eva (Ecuador)

Leonovich Sergei N. (Bielaruss)

Lourenço Paulo B. (Portugal)

Mang Herbert A. (Austria)

Mojsilović Nebojsa (Switzerland)

Műller Harald S. (Germany)

Noakowski Piotr (Germany)

Novák Drahomír (Czech Republic)

Nowak Andrzej S. (USA)

Oliveira Daniel V. (Portugal)

Peiretti Hugo Corres (Spain)

Pesavento Francesco (Italy)

Pichler Bernhard (Austria)

Pietruszczak Stanislaw (Canada)

Randl Norbert (Austria)

Sakai Koji (Japan)

Seitl Stanislav (Czech Republic)

Śliwiński Jacek (Poland)

Woliński Szczepan (Poland)

ORGANIZING COMMITTEE

Słowik Marta – Chair of the Organizing Committee

Golewski Grzegorz L. – Vice-Chair of the Organizing Committee

Akram Amanada

Bartosik Paweł

Franczak-Balmas Dominika

Górecki Marcin

Jabłoński Łukasz

Rozner Aleksandra

Smarzewski Piotr

Snela Małgorzata

Szerafin Jerzy

Szulej Jacek

Śledziewski Krzysztof

Ślósarz Szymon

Zarzeka-Raczkowska Ewa

ORGANIZERS

Lublin University of Technology – Faculty of Civil Engineering and Architecture

The International Federation for Structural Concrete – Polish Group

Polish Association of Civil Engineers and Technicians – Lublin Committee of Science

Table of content

Experimental response of historic masonry under compression and shear loading: damage and strengthening with FRP

Roberto Capozucca[1,*]

[1]Structural Section, Dept. DICEA, University Polytechnic of Marche, Ancona, Italy.

1 Introduction

The preservation of the historical masonry buildings as architectural heritage is one of the duties appointed to structural engineering and, given the geometric complexity of the structures involved, the variability of materials used and the loading history of the same buildings, this objective may be carried out knowing the behaviour of historic unreinforced and reinforced masonry walls under in-plane loading. The failure of masonry walls under combined compression and shear is one dangerous failure mechanism of historic buildings under seismic actions. The mechanism of resistance in shear depends on the geometry of masonry panels, their boundary conditions, the magnitude of the vertical loads and, finally, on the characteristics of the interface bond between bricks or stones and the mortar.

This paper describes experimental researches carried out from author in last decades to investigate the behaviour of historic masonry walls un-strengthened and strengthened using Fiber Reinforced Polymers (FRPs) under compression and shear loading until failure.

Several studies were carried out in the past in order to establish the behaviour of unreinforced masonry walls subjected to combined compression and shear [1-6]. Investigations regarding the shear behaviour of full-scale and model brick masonry walls led to the important conclusion that the scale effect has no significance on ultimate strength in shear [1,2,6].

In recent years, composite materials such as Fibre Reinforced Polymers (FRPs) seem to represent a valid solution in masonry building rehabilitation. FRPs are a class of materials having the potential to significantly improve the masonry response of buildings in seismic areas. FRPs consist in high strength fibres embedded in a resin matrix. The fibres are usually Carbon, Glass or Aramid, but more recently Basalt and other Bio-fibers. The fibres are strong in their direction and generally weak laterally. Fibres typically show no ductility and the stress-strain behaviour is linear elastic up to the failure. For the construction industry, FRPs are available in sheets, strips, tendons, reinforcing bars and meshes. Externally bonded FRP strips are usually used as a technique for strengthening shear masonry walls by increasing tensile capacity for supporting shear actions during earthquakes. The strengthening of masonry walls with FRPs is opening new venues for experimental research focusing on the possible performance of masonry subjected to seismic loading. The use of FRPs for enhancing the performance of masonry walls under monotonic or seismic loading has been addressed in recent works experimentally [8-12] and theoretically [13,14]. Unfortunately, the behaviour of HURM strengthened by FRPs continues to be insufficiently known even if many works have investigated the main aspects of this strengthening technique. The topic of adhesion between FRPs and masonry with the dangerous mechanism of delamination, both due to tensile stress and compression stress with dangerous effect of delamination buckling have experimentally and theoretical exanimated [15,16]. Delamination of FRP strips can limit condition in design especially in the case of adhesion of FRPs with the surface of historic clay bricks. Adequate surface preparation is required to avoid unfilled cracks or unsmoothed irregularities which can cause premature debonding.

* Corresponding author: r.capozucca@pm.univpm.it

In this paper, the behaviour of masonry wall models experimentally studied by using walls built with historic bricks in scale 1/3rd and strengthened with different composite material is described. The walls were subjected to in-plane cyclic loading; following shear damage with diagonal cracking, the walls were strengthened using Carbon-Glass-Steel-FRP strips bonded to only one of the surfaces of the wall. The behaviour of un-strengthened and strengthened walls under in-plane cyclic loading is discussed below based on the obtained experimental results.

2 Experimental tests

Static tests were performed on wall models, built with solid clay bricks in scale 1/3rd obtained from full scale handmade bricks measuring about 50÷60 mm × 150 mm × 300 mm recovered from the restoration of a historic building. The dimensions of tested models are shown in Figure 1; the width of web was about 50 mm. The compression and shear test set-up is shown in Figures 1(a), (b). Vertical loads were applied to the wall through a load distribution system by three hydraulic jacks to a steel plate placed on the top of the model. The steel plate, positioned on the top of the wall, distributes both vertical load and horizontal cyclic load to brickwork wall. The horizontal load was applied using double phase jack. Bases to measure vertical strains were located at five positions along the length, labelled A, B, C on the web. Measuring bases were used to evaluate principal strains in the centre of wall; for this Rosetta was positioned. The measurement of lateral deflection was achieved with inductive linear displacement transducers (LVTDs) (Fig. 1(b)).

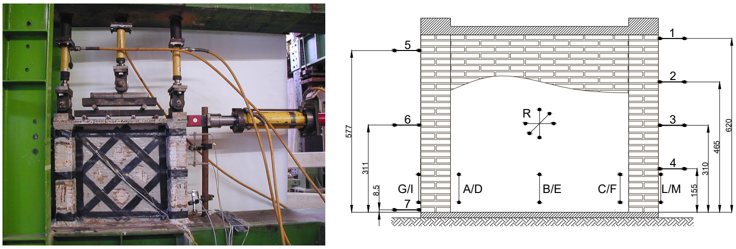

(a) (b)

Figure 1. (a) Set-up of experimental masonry model under in plane loading strengthened with CFRP strips; (b) instruments of measurement.

It is known from literature that Benjamin and Williams (1958) [1] investigated the shear behaviour of full-scale and model brick masonry walls. Their results led to the important conclusion that the scale effect has no significance on the ultimate strength in shear. Further a set of experimental research tests were carried out on brick wall models, clearly showing that the strength of full scale in shear can be conveniently predicted through testing on small scale models [2,5]. The masonry wall models were tested under combined compression and cyclic shear load as described below. The choice of using double T shape sections was connected to the need to avoid bending cracking at the base of the wall model, so that failure is initiated only due to shear. A cement: lime: sand (1:1:5) mortar by volume was used for the wall models with historic solid bricks in scale. In Table 1 main experimental results are shown obtained by shear tests on wall model strengthened with CFRP strips. In Table 1 the coefficient of ductility obtained assuming a bilinear behaviour is shown.

Table 1. Values of exp. horizontal load vs. displacements for tested walls with CFRP strips.

Wall Models		Cracking Load H_{cr} (kN)	d_{cr} Cracking (*) (mm)	Elastic Stiffness K_e (kN/m)·10^3	Load H_{max} (kN)	d_e Elastic (*) (mm)	d_u Ultimate (*) (mm)	Coeff. of Ductility μ_u
A	Unreinforced	40.66	1.745	23.30	56.11	2.167	2.80	**1.29**
	CFRP strips	45.00	2.70	16.60	70.04	3.789	9.14	**2.41**
B	Unreinforced	40.00	0.362	110.50	51.00	0.428	1.096	**2.56**
	CFRP strips	60.00	2.705	22.18	118.4	4.183	7.366	**1.76**

(*) Displacement measured during tests; H= horizontal load

Shear tests involved not only models with CFRP strips but also strengthening with GFRP and SRP strips. In Figure 2(a) one of wall models tested with and without GFRP strips is shown. Damaged by cracking walls under shear tests have been reinforced with GFRP strips glued to the surface of masonry and the walls have been again subjected to the same loading path. In Figure 2(b) the mechanisms of delamination under tensile stresses is shown which is cause of failure of GFRP strips close to the strain gauge E1.

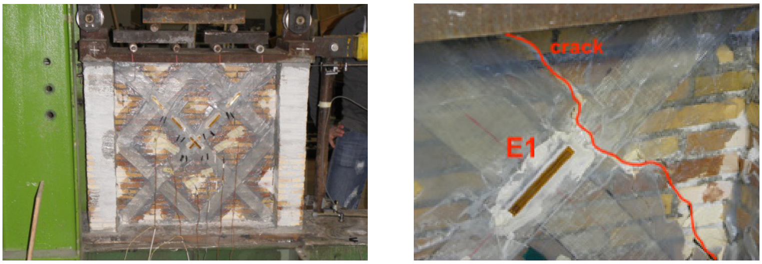

(a) (b)

Figure 2. (a) Wall model strengthened with GFRP strips - strain gauges E1,…,E6 on the GFRP strips of main diagonals; (b) view of strengthened side.

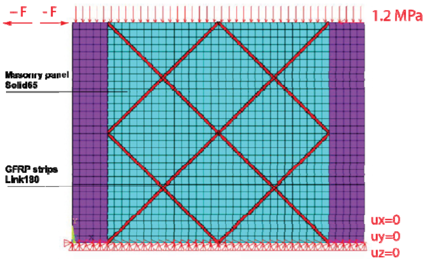

Figure 3. Macromodelling of wall model for FE analysis and load's assignment.

In Figure 3 the macro-modelling of one wall model with strengthening by diagonal GFRP strips is shown; theoretical results obtained by modelling are compared with experimental data. In Figure 4 a comparison between strains is shown for two strain gauges positions.

3 Conclusions

The experimental analysis of masonry walls has been developed in many years through combined vertical and cyclic horizontal loading tests on masonry wall models damaged and strengthened by FRP strips utilizing different fibers. Experimental results have confirmed the availability of strengthening with high values of displacements and ductility for strengthened walls but pointed out also the dangerous mechanism of delamination of FRP strips.

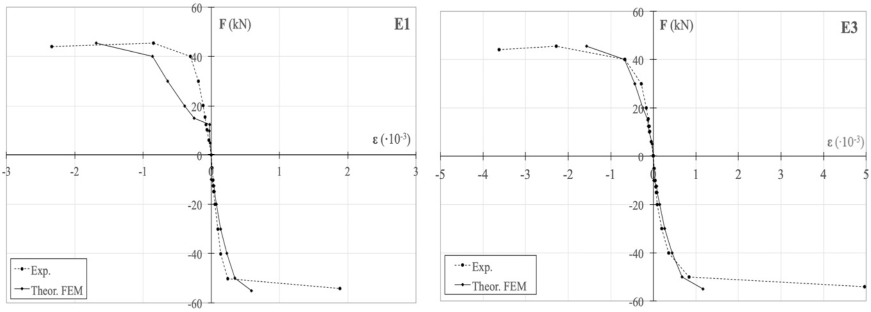

Figure 4. Comparison of exp. and theor. data of strains measured at strain gauges E1, E3.

References

1. Benjamin R., Williams H.A. The behaviour of one-story brick shear walls, Jour. of Struct. Division ASCE. **84**(1723): 130 (1958)
2. Hendry A.W., Sinha B.P. Shear tests on full scale single storey brickwork structures subjected to pre-compression. Civil Eng. Public Works Review. 1339–1334 (1971)
3. Tomazevic M. Earthquake-resistant design of masonry buildings. London Imperial College Press (1999)
4. Capozucca R., Sinha B.P. Strength and Behaviour of Historic Masonry under Lateral Loading. In: Proc. 13th IBMaC, Amsterdam. vol. 1: 277–284 (2004)
5. Magenes G., Calvi G.M. In-plane seismic response of brick masonry walls. Earthq Eng Struct Dyn. **26**(11):1091–112 (1997)
6. Capozucca R. Shear behavior of historic masonry made of clay bricks. Open Construction and Building Technology Journal. 5, Special Issue 1: 89–96 (2011)
7. Triantafillou TC. Strengthening of masonry structures using epoxy bonded FRP laminates Jour. Composites for Construction, **2**(5): 96–104 (1998)
8. Ehsani M., Saadatmanesh H., Velazquez-Dimas J. Behavior of retrofitted URM walls under simulated earthquake loading. J. Compos. Constr. ASCE (3): 134–142 (1999)
9. Shrive N.G. The use of fibre reinforced polymers to improve seismic resistance of masonry. Construction and Building Materials. **20**: 269–277 (2006)
10. Capozucca R. Experimental analysis of historic masonry walls reinforced by CFRP under in-plane cyclic loading, Composite Structures. **94**: 277–289 (2011)
11. Aiello M.A., Sciolti M.S. Analysis of bond performance between FRP sheets and calcarenite stones under service and ultimate conditions. Mas. Int. **21**(1): 15–28 (2008)
12. Capozucca R. Double-leaf masonry walls under in-plane loading strengthened with GFRP/SRG strips. Engineering Structures. **128**: 453–473 (2016)
13. Fedele R., Milani G. A numerical insight into the response of masonry reinforced by FRP strips. The case of perfect adhesion. Compos. Struct. **92**: 2345–2357 (2010)
14. Grande E., Imbimbo M., Sacco E. Modeling and numerical analysis of the bond behavior of masonry elements strengthened with SRP/SRG. Composites: Part B**55**: 128–138 (2013)
15. Capozucca R. Experimental FRP/SRP-historic masonry delamination. Composite Structures. **92**: 891–903 (2010)
16. Capozucca R., Ricci V. Bond of GFRP strips on modern and historic brickwork masonry. Composite Structures. **140**: 540–555 (2016)

Reliability assessment of concrete structures: Advanced stochastic FEM modelling and case studies

Drahomír Novák[1,*]

[1]Brno University of Technology, Faculty of Civil Engineering, Institute of Structural Mechanics, Veveří 95, 60200 Brno, Czech Republic

1 Introduction

Large number of concrete structures worldwide reached a stage in need of repair, rehabilitation, strengthening or replacement. Many countries are currently experiencing a problem of aging and deterioration of concrete structures such e.g. bridges. Naturally, uncertainties are involved, and questions of safety and advanced reliability assessment are becoming more and more important. An individual reliability approach which is nowadays supported by design codes (where design reliability measures are specified enabling the fully probabilistic approach) can save money comparing to the classical deterministic approach and thinking. An advanced complex methodology and software is needed for that. Such trend can be observed in literature already long time ago [1-6].

Several current standards advocate probabilistic approaches, utilization of mathematical models and design of structures for durability, i.e. time-dependent limit state approach (LS) with service life consideration: ISO 13823 and the fib-Model Code. In this respect it is important to develop relevant advanced assessment method, evaluation procedures and service life prognoses for concrete structures. In this area, mathematical modelling is often a useful tool together with relevant limit states for accomplishment of such tasks, utilizing stochastic approaches. Inverse analysis, identification of material parameters and generally model updating are important tasks, e.g. [7,8]. Such approaches go in hand with development of numerical methods and complex material models utilized for the numerical analyses.

The extended abstract describes keystones of complex methodology for statistical, reliability and risk analyses of concrete structures including advanced nonlinear finite element analysis, uncertainties simulation and degradation modelling. It presents virtual simulation used on the way from assessment of experimental results to reliability analysis of a civil engineering structure, based on randomization of nonlinear fracture mechanics finite element analysis.

2 Stochastic nonlinear analysis

2.1 Structural analysis and reliability assessment

For the global structural modelling advanced computational models are needed, where aspects of nonlinear behaviour of concrete and reliability modelling are combined. The problem involves uncertainties in material, geometry, loading and degradation phenomena and therefore the concept of reliability theory has to be applied. The combination of structural analysis and reliability assessment has been developed and is presented together as the SARA software [4,6] – a software shell which controls the communication between following individual programs: ATENA [9,10] – FEM nonlinear analysis

* Corresponding author: novak.d@fce.vutbr.cz

of concrete structures and FReET [11,12] – the probabilistic engine based on stratified Monte Carlo type Latin Hypercube Sampling.

2.2 Uncertainties simulation

The stochastic response calculation requires repeated analyses of the structure with stochastic input parameters, which reflects randomness and uncertainties in the input values. As the nonlinear structural analysis is computationally very demanding, a suitable technique of statistical sampling should be utilized, which allows relatively small number of simulations. Final results are statistical characteristics of response (stresses, deflections, crack width etc.), information on dominating and non-dominating variables (sensitivity analysis) and estimation of reliability using reliability index and theoretical failure probability).

The probabilistic software FReET [12] allows simulations of uncertainties of the analysed problem basically at random variables level (typically in civil engineering – material properties, loading, geometrical imperfections). The attention is paid to those techniques that are developed for analyses of computationally intensive problems; the nonlinear FEM analysis is here a typical example. Stratified simulation technique Latin hypercube sampling (LHS) is used in order to keep the number of required simulations at an acceptable level. This technique can be used for both random variables' and random fields' levels. Statistical correlation is efficiently imposed by the stochastic optimization technique – the simulated annealing [13]. Sensitivity analysis is based on nonparametric rank-order correlation coefficients and may serve e.g. for model reduction in subsequent analyses. State-of-the-art probabilistic algorithms are implemented to compute the probabilistic response and reliability.

2.3 Nonlinear FEM simulation

The ATENA software was developed for realistic simulation of reinforced concrete structures [9-10]. It is based on finite element method with non-linear material models, and utilized for analysis of beams and girders, plates and shells, bridges, tunnels, dams, composite structures, strengthening, structural details, fastenings, fibre-reinforced structures and masonry structures etc. The ATENA software consists of calculating core ensuring the non-linear numerical analysis, and a user-friendly graphical interface for an efficient communication between end-user and program core. The numerical core covers the finite element technology, non-linear material models and non-linear solution. The non-linear material models are based on the orthotropic damage theory and special concrete-related theory of plasticity. As one of the main features the non-linear fracture mechanics is employed for concrete cracking in tension. Based on the fracture energy approach the tensile cracks are modelled as smeared material damage which enables utilization of the continuum mechanics even for the damaged material. Objectivity of the solution is ensured using crack band method. The material law exhibits softening after reaching the tensile strength. The behaviour of concrete in compression is defined by special theory of plasticity (three-parameter model) with non-associated plastic flow rule and softening. This material model for concrete can successfully reproduce also other important effect, such as volume change under plastic compression or compressive confinement.

2.4 Degradation simulation

There are many predictive computational models for degradation modelling mainly carbonation of concrete, chloride ingress and corrosion of reinforcement at different sophistication levels. Frequently, heuristic models are employed using more or less simplified approaches and data. Common feature of all these models is that input data are very uncertain. There is a software implementation where all relatively well-known models are summarized within the framework of unified software environment. It is called FReET-D [12], where a combination of analytical models and simulation techniques has been amalgamated to form specialized software for assessing the potential degradation of newly designed as well as existing concrete structures. Models implemented (mainly simple-to-use 1D probabilistic models) for carbonation, chloride ingress, corrosion of reinforcement and others which may serve directly in the durability assessment of concrete structures in the form of a durability limit states in “hot-spots”, i.e. the assessment of service life and the level of the relevant reliability measure. Several features are offered including parametric studies and Bayesian updating. Altogether 32 models are implemented as pre-defined dynamic-link library functions (including models provided by new fib Model Code). FReET-D represents the specialized module of FReET software, mentioned above. Some applications are shown e.g. in [14].

3 Case studies

There are already many practical applications of tools described above during last decades worldwide. Let us mention only some recent selected examples solved by the software developer´s team:

- Analysis of Kristienberg bridge, Stockholm: Statistical analysis of crack width [15].
- Probabilistic and semi-probabilistic analysis o very large concrete beams (based on Toronto experiments) [16].
- Complex research on prestressed concrete girders failing in shear [17].
- Advanced stochastic analysis of 10 existing reinforced and prestressed concrete bridges in the Austria-Czech Republic region (project Interreg) [18].

4 Conclusion

The advanced methods for nonlinear, reliability and degradation analyses were integrated in a software package for reliability assessment of concrete structures. Methodology and software tools are prepared for a routine application. Tools have been used in many practical applications and they are continuously improved by implementation of new state of art methods.

The author acknowledges the financial support from project TAČR DELTA No. TF06000016.

References

1. M.G. Stewart, D.V. Rosowsky, Time dependent reliability of deteriorating reinforced concrete bridge decks. Structural Safety, 20(1): 129–139, (1998)
2. M. Mahsuli, T. Haukaas, Software for multi-model reliability analysis. In Application of Statistics and Probability in Civil Engineering, Faber, Kohler, Nishijima (eds), (Taylor & Francis Group): 1267–1275, (2011)
3. A. Strauss, K. Bergmeister, S. Hoffmann, R. Pukl, D. Novák, Advanced life-cycle analysis of existing concrete bridges. J. of Materials in Civil Eng., 20: 9–19, (2008)

4. K. Bergmeister, D. Novák, R. Pukl, An advanced tool for reliability assessment of concrete structures. In Progress in Structural Engineering, Mechanics and Computation, Zingoni (ed.), Proc. of 2nd int. conf., Cape Town, South Africa, (Taylor & Francis Group): 899–904, (2004)
5. I. Enevoldsen, Practical implementation of probability-based assessment methods for bridges. Structure and Infrastructure Engineering, 7 (7–8), 535–549, (2011)
6. A. Strauss, D. Novák, D. Lehký, M. Vořechovský, B. Teplý, R. Pukl, V. Červenka, E. M. Eichinger-Vill, U. Santa, Safety analysis and reliability assessment of engineering structures – The success story of SARA. ce/papers, 3(2), 38–47, (2019)
7. D. Novák, D. Lehký, ANN inverse analysis based on stochastic small-sample training set simulation. Eng. of Artificial Intelligence, Vol. 19, 731–740, (2006)
8. D. Lehký, Z. Keršner, D. Novák, FraMePID-3PB Software for Material Parameters Identification Using Fracture Test and Inverse Analysis, Advances in Engineering Software, Vol. 72, 147–154, (2014)
9. V. Červenka, L. Jendele, J. Červenka, ATENA Program Documentation – Part 1: Theory. Cervenka Consulting, Prague, Czech Republic, (2015)
10. V. Červenka, J. Červenka, R. Pukl, ATENA – A tool for engineering analysis of fracture in concrete', Sadhana 27(4): 485–492, (2002)
11. D. Novák, M. Vořechovský, R. Rusina, FReeT v.1.5 – program documentation. User´s and Theory Guides. Brno/Červenka Consulting, Czech Republic, http://www.freet.cz (2015)
12. D. Novák, M. Vořechovský, B. Teplý, FReeT: Software for the statistical and reliability analysis of engineering problems and FReeT-D: Degradation module. Advances in Engineering Software, Vol. 72, 179–192, (2014)
13. M. Vořechovský, D. Novák, Correlation control in small-sample Monte Carlo type simulations I: A simulated annealing approach. Probabilistic Engineering Mechanics, Vol. 24, 452–462, (2009)
14. B. Teplý, M. Chromá, P. Rovnaník, D. Novák, The role of modelling in the probabilistic durability assessment of concrete structures. Proc. Life-Cycle and Sustainability Infrastructure Systems (IALCCE 2012) – Strauss, Frangopol & Bergmeister (Eds), Taylor & Francis Group, London: 876–882 (2013)
15. R. Pukl, T. Sajdlová, L. Řoutil, D. Novák, P. Šeda, Case study - Nonlinear reliability analysis of a concrete bridge. Proc. Maintenance, Monitoring, Safety, Risk and Resilience of Bridges and Bridge Networks (Foz do Iguaçu). Taylor & Francis Group, 2503–2507, (2016)
16. L. Novák, D. Novák, R. Pukl, Probabilistic and semi-probabilistic design of large concrete beams failing in shear. In Advances in Engineering Materials, Structures and Systems: Innovations, Mechanics and Applications. 1st Edition. London: Taylor and Francis Group CRC Press, 2019. p. 1–6. ISBN: 9781138386969
17. D. Lehký, D. Novák, L. Novák, M. Šomodíková, Prestressed concrete roof girders: Part II: surrogate modelling and sensitivity analysis; D. Novák, L. Novák, A. Strauss, O. Slowik, Part III: semi-probabilistic design. In: Proceedings of the sixth Int. Symposium on Life-Cycle Civil Engineering IALCCE 2018. Ghent, Belgium, (2018)
18. E. Apostolidi, M. Šomodíková, A. Strauss, R. Pukl, D. Lehký, D. Novák, The Interreg „ATCZ190 Safebridge“ project… In: The 10th International Conference on Bridges in Danube Basin (Danube Bridges 2019), Vienna, Austria, 228–231 (2019)

Multiscale modelling of cementitious materials

Bernhard L.A. Pichler[1,*], *Markus* Königsberger[2,1], *Hui* Wang[3,1], and *Christian* Hellmich[1]

[1]Institute for Mechanics of Materials and Structures, Vienna University of Technology, Austria
[2]BATir Department, Université Libre de Bruxelles, Brussels, Belgium
[3]Department of Transportation Engineering, School of Naval Architecture, Ocean and Civil Engineering, Shanghai Jiao Tong University, China

1 Introduction

The Institute for Mechanics of Materials and Structures of Vienna University of Technology in Austria is renowned for having developed predictive multiscale models for microheterogeneous materials. The present contribution refers to cementitious materials and provides an overview over multiscale modeling focused on the elastic stiffness, the creep behavior, the compressive strength, and the thermal expansion. The required scale transitions are based on methods taken from continuum micromechanics.

2 Continuum micromechanics

Multiscale models establish quantitative links between key features of microstructures of materials and the macroscopic scale of engineering applications, and vice versa. Upscaled properties of microheterogeneous materials are defined on representative volume elements (RVEs). They satisfy the separation of scales principle:

$$h << l << L. \tag{1}$$

The characteristic size h of the heterogeneities is significantly smaller than the characteristic size l of the RVEs, and l is significantly smaller than a characteristic structural size L. The inequalities (1) may be treated as being satisfied provided that h and l are separated by a factor of 2 to 3, and l and L are separated by a factor of 5 to 10.

Cementitious materials, such as cement pastes, mortars, and concretes, are hierarchically organized. The characteristic sizes of their elementary constituents span across several orders of magnitude from the nanometer-sized gel pores and building blocks made of calcium-silicate-hydrates (C-S-H) to centimeter-sized aggregates.

Upscaling methods of continuum micromechanics account for four key features of the microstructure of microheterogeneous materials. The latter are conceptually subdivided in quasi-homogeneous constituents, called material phases. Quantitative key features of the material phases include their volume fractions and their mechanical properties in terms of their elastic stiffness, creep behavior, strength, etc. Qualitative key features of the material phases include their characteristic shape and the type of their mechanical interaction.

The most popular upscaling methods are based on matrix-inclusion problems in which one ellipsoidal inclusion is embedded in an infinite three-dimensional matrix. The latter is subjected, at its infinitely remote boundary, to uniform strain boundary conditions. While stresses and strains exhibit fluctuations inside the infinite matrix, spatially uniform stress and strain states prevail inside the inclusion. Analytic tensorial formulae are available for the

* Corresponding author: Bernhard.Pichler@tuwien.ac.at

computation of the inclusion strains as a function of the remote loading, the stiffness of the infinite matrix, as well as the stiffness, shape, and spatial orientation of the inclusion.

As for modeling of microheterogeneous materials, one auxiliary matrix-inclusion problem is considered for each of the constituents of the real microheterogeneous material of interest. Thereby, the material phases of the real RVE are represented as inclusions with identical stiffness, ellipsoidal shape, and spatial orientation. The stiffness of the surrounding infinite matrices and their remote loading are linked to the stiffness and the loading of the real RVE.

The link regarding the loading is established such that the strain states inside the auxiliary inclusions are equal to the average strains of the real phases of the microheterogeneous material, under consideration that these average phase strains must fulfill the strain average rule.

The link regarding the stiffness accounts for the interaction of the constituents of the microheterogeneous material. In case of a matrix-inclusion composite, the stiffness of the auxiliary infinite matrices is set equal to the stiffness of the matrix of the real microheterogeneous material. This leads to Mori-Tanaka-Benveniste schemes. In case of a highly disordered arrangement of the constituents, with direct phase-to-phase interaction (polycrystalline arrangement of the microstructure), the stiffness of the auxiliary infinite matrices is set equal to the homogenized stiffness of real microheterogeneous material. This leads to self-consistent schemes.

3 Multiscale modelling of cementitious materials

3.1 Early-age evolution of compressive strength

The two-step homogenization scheme illustrated in Fig. 1, was introduced by Pichler and Hellmich [1]. The hydrate foam is a polycrystalline composite consisting of spherical water

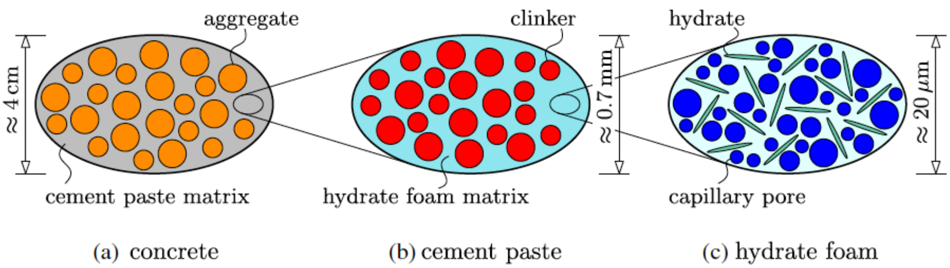

Figure 1. Three-scale representation illustrating qualitative properties of concrete developed by Pichler and Hellmich (2011); the 2D sketches refer to 3D representative volume elements.

and air phases, as well as needle-shaped hydrate-gel phases oriented isotropically in all space directions (homogenization based on the self-consistent scheme). Cement paste is a matrix-inclusion composite consisting of a hydrate foam matrix and spherical unhydrated cement clinker inclusions (homogenization based on the Mori-Tanaka-Benvensite scheme). As for the experimental validation of the strength model at the level of cement paste see [2]. As for the extension to strength-upscaling to the scales of mortar and concrete see [3]: the loading imposed on a specimen of concrete (or mortar), is first downscaled to maximum stresses inside the interfacial transition zones (ITZ) covering the aggregates. These maximum stresses are further downscaled to the micron-sized hydrate-gel needles, in terms of deviatoric and volumetric strain-energy-density-related stress averages. The latter enter a Drucker-Prager failure criterion with material constants derived from nanoindentation tests: cohesion = 50 MPa and angle of internal friction = 12°. The model was successfully validated across the hydrate-to-concrete scales. Polynomial functions were developed which reproduce the performance of the multiscale strength model reliably [3]. This renders the model accessible, without raising the need of implementing the tensorial details.

3.2 Early-age evolution of nonaging creep behavior

The evolution of nonaging creep properties of cement pastes at early ages was modeled in [4]. Creep of cementitious materials was envisaged to result from the viscoelastic behavior of the hydrate-gel needles. An isochoric tensorial creep function of hydrate-gel needles was identified by means of downscaling of 500 different nonaging creep functions of macroscopic cement paste, derived from three-minute-long tests on differently young cement pastes with three different initial water-to-cement mass ratios. In this context, the material representation illustrated in Fig. 1 was used. Homogenization of viscoelastic properties was based on the correspondence principle. Water, air, and clinker were considered to exhibit time-independent linear elastic behavior. It was shown that one single power-law-type creep behavior of hydrate gel needles allows for explaining hundreds of macroscopic three-minutes creep tests carried out in the first week after material production [4]. The general validity of the identified hydrate-gel creep properties was checked exemplarily. To this end, the model was used to predict the material behavior of a 30-year-old cement paste subjected to a 30-days creep test. The model predictions agree very well with results from creep experiments published in the open literature. This underlines that the material representation of Fig. 1 allows for developing reliable multiscale models for the early-age evolutions of the compressive strength and the nonaging creep properties of cement pastes.

3.3 Thermal expansion of mature cement paste

The quasi-instantaneous thermal expansion of mature cement pastes is a nonlinear function of the internal relative humidity (RH) prevailing in the pores right before the temperature change, see Fig. 1 of [5]. This goes hand-in-hand with the spontaneous, reversible, and counterintuitive increase/decrease of this internal RH resulting from a temperature increase/decrease, see Fig. 2 of [5]. Both properties were studied in the context of a multiscale porohygrothermomechanical model. The experimental data could be explained based on quasi-instantaneous and reversible uptake/release of water by cement hydrates and a three-scale representation of mature cement pastes. Because of the focus on mature cement pastes, the hydrate foam could be introduced as a matrix-inclusion composite consisting of capillary pores embedded in a matrix made of hydrate gel. The microstructure of the hydrate gel was introduced as another matrix-inclusion composite consisting gel pores embedded in a matrix made of solid hydrates. Partially saturated gel and capillary pores were considered to be connected and spherical, with radii following exponential distributions. Their characteristic pore sizes were identified based on adsorption porosimetry. Surface tension was considered in the interfaces between the pores and the solid. The Mori-Tanaka-Benvensite scheme was used to provide the scale transition from effective pore pressures to eigenstrains at the cement paste level. This modeling approach, together with consideration of conservation of water molecules during the temperature change, allowed for explaining the macroscopic thermal expansion coefficients based on molecular water uptake/release characteristics of the hydrates. Hydrates release water in a reversible and spontaneous fashion when heated up. This results in the increase of the internal relative humidity and in a reduction of the effective pore under pressures. This reduction manifests itself macroscopically in an additional contribution to the swelling of the composite. The molecular water uptake/release characteristics of the hydrates could be shown to be mixture-independent and in agreement with recent 1H NMR relaxometry tests, carried out during temperature changes, see [5] for details.

3.4 Early-age evolution of the poroelastic properties

State-of-the-art multiscale models for the elastic stiffness of cementitious materials typically introduce two types of hydrate-gel made of solid C-S-H blocks and a constant gel porosity in between. These models are used to upscale nanoindentation-derived elastic properties of "low density C-S-H gel" and "high-density C-S-H gel" to the level of cement paste and concrete. Rather recently, the idea of two specific types of hydrates with two specific and constant mass densities has been challenged by proton nuclear magnetic resonance (1H NMR) relaxometry experiments. The test data suggest that hydrates densify continuously during the hydration process. This was considered in the latest developments concerning multiscale modeling of the early-age stiffness evolution of cement pastes [6]. Therein, a comprehensive hierarchical continuum micromechanics framework is described, for a sequence of material volumes with infinitely many, eigenstressed phases oriented isotropically in all directions of scape. The new scheme is closely related to Dvorak's transformation field analysis coupled with eigenstressed matrix-inhomogeneity problems of the Eshelby-Laws type. The new model is based on elastic stiffness properties of solid C-S-H derived from realistic molecular mechanics approaches, and it is based on a new hydration model accounting for the precipitation-space-driven densification of the hydrate gel, which is in agreement with 1H NMR experiments performed at early material ages [7].

References

1. Pichler, B., Hellmich, C. (2011). Upscaling quasi-brittle strength of cement paste and mortar: A multi-scale engineering mechanics model. Cement and Concrete Research, 41(5), 467–476. http://doi.org/cvh9zh
2. Pichler, B., Hellmich, C., Eberhardsteiner, J., Wasserbauer, J., Termkhajornkit, P., Barbarulo, R., Chanvillard, G. (2013). Effect of gel–space ratio and microstructure on strength of hydrating cementitious materials: An engineering micromechanics approach. Cement and Concrete Research, 45, 55–68. http://doi.org/crnh
3. Königsberger, M., Hlobil, M., Delsaute, B., Staquet, S., Hellmich, C., & Pichler, B. (2018). Hydrate failure in ITZ governs concrete strength: A micro-to-macro validated engineering mechanics model. Cement and concrete research, 103, 77–94. http://doi.org/ch9n
4. Königsberger, M., Irfan-ul-Hassan, M., Pichler, B., Hellmich, C. (2016). Downscaling based identification of nonaging power-law creep of cement hydrates. Journal of Engineering Mechanics, 142(12), 04016106. http://doi.org/f9cxv4
5. Wang, H., Hellmich, C., Yuan, Y., Mang, H., Pichler, B. (2018). May reversible water uptake/release by hydrates explain the thermal expansion of cement paste? Arguments from an inverse multiscale analysis. Cement and Concrete Research, 113, 13–26. http://doi.org/csgw
6. Königsberger, M., Pichler, B., Hellmich, C. (2020). Multiscale Poro-Elasticity of Densifying Calcium-Silicate Hydrates in Cement Paste: An Experimentally Validated Continuum Micromechanics Approach"; International Journal of Engineering Science 147. http://doi.org/dhx2
7. Königsberger, M., Hellmich, C., Pichler, B. (2016). Densification of CSH is mainly driven by available precipitation space, as quantified through an analytical cement hydration model based on NMR data. Cement and Concrete Research, 88, 170–183. http://doi.org/f82z6v

Innovative approaches for strengthening existing concrete structures

Norbert Randl[1,*]

[1]CUAS – Carinthia University of Applied Sciences, 9800 Spittal, Austria

1 Aspects of strengthening reinforced concrete structures

In industrial countries, the ever-increasing percentage of existing buildings and structures requires significant efforts in maintenance, retrofitting and rehabilitation of this heritage. The high traffic loads create an increasing demand for low-invasive techniques for structural strengthening that do not lead to significant traffic disturbances and interruptions. Moreover the global challenge of reducing CO_2 – emissions and minimizing the ecological impact of construction activities has to be met also in this context.

Strengthening techniques can be subdivided into local and global interventions with respect to the overall structural impact and the affected parts of the member. RC structures are typically strengthened either by increasing the compression zone or by adding various types of reinforcing materials. Frequently used global techniques are external pre-stressing of the whole structure or the application of bonded concrete overlays. Local strengthening can typically be done by adding bonded or non-bonded reinforcing bars. Some methods require changes of a member's cross section, while others do not really affect the circumference of the cross section. There are different methods to activate the subsequently applied strengthening system already just under the structure's self-weight, typically pre-stressing or in general introducing deformations via external jacking forces are common approaches.

An observed trend is the increasing use of advanced high-strength materials, for example Ultra High Performance Concrete (UHPC) e.g. as subsequently applied bridge deck overlay (*Brühwiler* (2017)) or textile reinforced mortars as durable high-strength top layers in tensile zones (*Koutas et al* (2019)). UHPC may also serve for built-in strengthening solutions in a way that units of precast UHPC-elements are cast-in to overtake compression loads in highly stressed regions (*Ricker et al* (2017)). Some new developments in typical subsequently applied strengthening techniques have recently been investigated in several research projects at CUAS and are addressed in the following sections.

2 High strength concrete overlays

Subsequently applied concrete layers are a common method in repair and strengthening of existing RC structures. High Strength Concretes (HSC) as overlay material may provide several advantages such as increased robustness, extended durability and an increase of the overall structural stiffness. In addition there is evidence that the concrete-concrete bond strength increases with increasing overlay strength (e.g. *Muñoz et al* (2013)). Other parameters involved are the viscosity and the mix proportions of the overlay concrete.

The investigation of the effect of using HSC as overlay material on the adhesive bond has been in the focus of a recently conducted experimental campaign at CUAS (*Randl et al* (2020)). Various series of different small scale bond and interface shear tests have been performed to investigate the adhesive bond resistance between NSC and subsequently applied HSC with

* Corresponding author: n.randl@cuas.at

respect to different interface roughness categories. The surfaces of the substrates were roughened with high pressure water jetting (HPW) before placing the new concrete layer. Fig. 1 displays the produced 3 roughness categories.

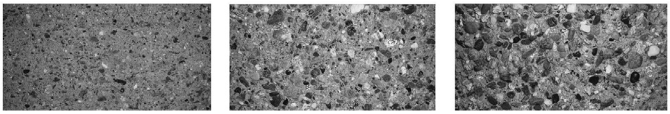

Figure 1. Interface roughness: smooth – rough – very rough.

Push-out and slant shear test setups were chosen to derive the adhesive bond strength (setups see Fig. 2 (left hand side)). In addition pull-off tests were performed on drilled cores to identify the possible linkage to the tensile bond strength. While push-out tests deliver more or less the pure interface shear strength (apart from some normal stresses due to unavoidable load eccentricities, see Fig. 2 (right hand side)), the slant shear setup leads to a superposition of normal and shear forces along the interface.

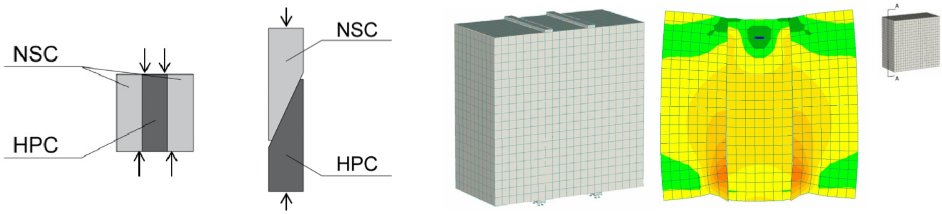

Figure 2. Interface shear test-setups (left) and FE-model of push-out test (right).

It turned out clearly that with an appropriate HPC mixture significantly higher bond strength can be achieved than usually with NSC overlays. Concerning the effect of roughness, shifting from smooth to rough interface leads to a significant bond strength increase while no significant difference occurs from rough to very rough. Strong surface wetting before casting the overlay has a rather unfavourable effect on the adhesive bond in comparison to an only slightly wetted surface (*Randl et al* (2020)).
A numerical simulation of the small-scale tests has been performed with the ATENA software. Based on the finite element analysis, the differences in adhesive bond strength derived from push-out and slant shear setups can be explained. In slant shear tests the shear force is superimposed by a normal force perpendicular to the interface. Therefore the identification of the pure adhesive bond strength $\tau_{j,ad}$ requires the definition of a failure criterion. A simple but still sufficiently accurate and widely used approach to describe the shear resistance along an interface provided by bond and frictional forces is the Mohr-Coulomb hypothesis, a criterion that is also part of the basis for the current MC2010 design approach (*Randl* (2013)). More advanced Mohr-Coulomb envelopes lead to a more accurate judgement of the inherent adhesive bond strength (*Zanotti and Randl* (2019)).

3 Local strengthening in shear

There are few recognized methods for local strengthening of shear deficient RC members (*Adhikary and Mutsuyoshi* (2006)). Basic techniques are the application of externally bonded reinforcement, near surface mounted reinforcement or externally anchored or grouted steel bars inserted into pre-drilled holes. As material for externally bonded or near surface mounted reinforcement, (carbon) fiber reinforced plastics ((C)FRP) are increasingly used due to the strength to weight ratio, durability, and ease of application.

3.1 Addition of reinforcing bars

An already frequently applied method involves bonded reinforcing bars, installed in the existing concrete substrate by drilling holes, injecting them and placing the bars. The efficiency of this method has been verified in a series of beam tests (*Randl and Kunz* (2009)), showing the potential increase in shear resistance. A 45° – inclination of the bars is recommended to provide sufficient end anchorage length. Even though the inclination required some additional efforts in the installation process, it leads to a better utilization of the bars as the shear cracks are crossed nearly perpendicularly. Above that, it was observed in the beam tests that the dowel action effect (*Randl* (2007)) can be mobilized.

Recently, a new type of undercut anchor was designed for subsequent strengthening of RC members in shear (*Randl and Harsanyi* (2018)). The anchor is set vertically into pre-drilled holes and introduces the load at the very end via a self-undercutting expansion sleeve. In a series of member tests (Fig. 3) a significant increase of the beam's shear resistance (+40 to +90%) was observed, even with a number of only 4 to 7 installed anchors ø12 mm.

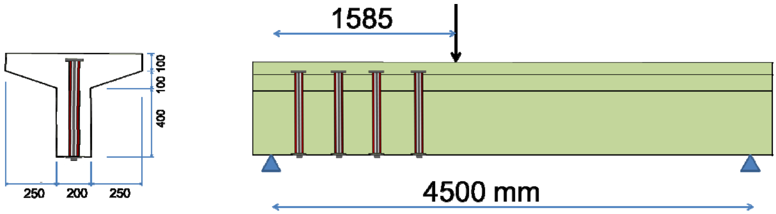

Figure 3. Setup of beam tests strengthened with post-installed undercut anchors.

3.2 Properly anchored CFRP sheets

Numerous researchers have already proven the efficiency and usefulness of applying CFRP sheets to strengthen existing RC structures in shear (see e.g. *Triantafillou* (1998)). If not fully wrapped around, without adequate end anchorage the governing failure mode will be lateral delamination, i.e. de-bonding, of the CFRP ends from the concrete.

Following the before mentioned campaign with undercut anchors, another series of beams with same geometry and reinforcement layout was strengthened with CFRP sheets. In order to avoid premature de-bonding, a simple end-anchorage system has been designed which allows a direct load transfer into the compression zone: A steel plate is fixed to the upper flange of the T-section by means of rapidly curing bonded anchors (details see *Randl and Harsanyi* (2018)). The varied parameters in the tests with CFRP sheets were the number of glued CFRP-layers in one sheet (either one or two layers, one glued upon the other) and the number resp. distance of these sheets. The developed end anchorages prevented debonding of the CFRP and allowed for the formation of a full truss mechanism, utilizing the whole effective depth of the RC member. In addition to traditional measurement techniques for shear tests (*Stoerzel et al* (2013)), a photogrammetric measurement system together with digital image correlation software (DIC) was successfully used (Fig. 4).

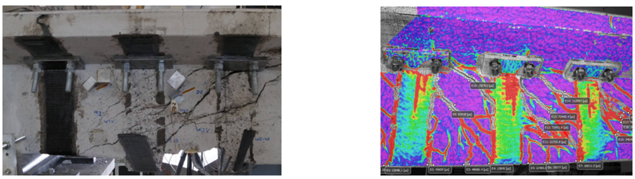

Figure 4. Typical shear failure of CFRP strengthened beam and strain / crack pattern from DIC.

Comparing the two strengthening methods in shear, with the CFRP an even higher shear load gain (+100% to +160%) was achieved than with the before described anchors. However, due to the missing redistribution option with CFRP the load increase is less pronounced with increasing cross section of the strengthening material than in the case of steel rebars or anchors. In both cases a full truss mechanism developed and failure was due to either rupture of a strengthening element or (in the case of the CFRP strengthening) failure of a concrete compression strut. Therefore design can be handled similarly to the standard design procedure for a shear reinforced member, treating the strengthening elements analogously to cast-in shear reinforcement (*Randl and Harsanyi* (2018)).

A part of the herein presented experimental campaigns have been funded by the Austrian Research Promotion Agency FFG (grant no. 866881) and by FFG, ASFINAG and ÖBB Infrastruktur (grant no. 840549) which is gratefully acknowledged. A part of the presented tests with HSC overlays have been funded by the following members of the ÖBV: ASFiNAG, ÖBB-Infrastruktur, PORR, STRABAG und RTB ROHRDORFER Transportbeton. The authors also like to thank the industrial partners Hilti and SIKA Austria for the fruitful cooperation in the project "Querkraftverstärkung".

References

1. Adhikary, B. B., Mutsuyoshi, H. (2006). Shear strengthening of reinforced concrete beams using various techniques. Construction and Building Materials, 20(6), 366–373.
2. Brühwiler, E. (2017): Strengthening of existing structures using R-UHPFRC: Principles and conceptual design. UHPFRC 2017, Montpellier, France, p. 993–1002.
3. Koutas; L.N., Tetta; Z., Bournas; D.A., Triantafillou, T.C. (2019) Strengthening of Concrete Structures with Textile Reinforced Mortars: State-of-the-Art Review, J. Compos. Constr., 23(1), DOI: 10.1061/(ASCE)CC.1943-5614.0000882.
4. Munoz, M., Harris, D., Ahlborn, T., Froster, D. (2013) Bond Performance between Ultrahigh-Performance Concrete and Normal-Strength Concrete, J. Mater. Civ. Eng., DOI: 10.1061/(ASCE)MT.1943-5533.0000890.
5. Randl, N. (2007). Load Bearing Behaviour of Cast-in Shear Dowels, Beton- und Stahlbetonbau, vol. 102, no. 1, pp. 31–37
6. Randl, N., Kunz, J. (2009): Biegeschubversuche an Stahlbetonbalken mit nachträglich eingemörtelter Querkraftbewehrung, Beton- und Stahlbeton, Vol. 104/11 : 728–736
7. Randl N (2013): Design recommendations for interface shear transfer in fib Model Code 2010, Structural Concrete 14(3): 230–241.
8. Randl N., Harsányi, P. (2018): Developing optimized strengthening systems for shear-deficient concrete members, Structural Concrete, vol. 19, no. 1, p. 116–128.
9. Randl, N., Peyerl, M., Steiner, M. (2020): Hochfester Aufbeton zur Tragwerks-verstärkung, Teil 1: Kleinkörperversuche, Beton- und Stahlbetonbau 115/2 106–116.
10. Ricker, M., Häusler, F., Randl, N. (2017): Punching strength of flat plates reinforced with UHPC and doubleheaded studs. Engineering Structures 136: 345–354.
11. Stoerzel, J., Randl, N., Strauss, A. (2015) Monitoring shear-induced degradation of reinforced and pre-tensioned concrete members, IABSE Conference Report, Geneva 2015, pp. 1148–1157.
12. Triantafillou, T. C. (1998). Shear Strengthening of Reinforced Concrete Beams Using Epoxy-Bonded FRP Composites. ACI Structural Journal, 95(2), 107–115.
13. Zanotti, C.; Randl, N. (2019): Are concrete-concrete bond tests comparable? Cement and Concrete Composites, Volume 99: 80–88.

Influence of reinforcement concrete cover to the reliability of slab-column system

Lidia Buda-Ożóg[1,*]

[1]Rzeszow University of Technology, 2 Poznańska, Rzeszów 35-084, Poland

1 Introduction

Reliability of building structures is an important design criterion, while the required level of security depends not only on the function and purpose of the facility, but also from the parameters included in the calculation. Despite numerous studies on safety and reliability, there are factors, with a certain probability, that increase the uncertainty of the parameters assumed in the calculations and as a result the structure fails. It is not uncommon that errors are made during the building process. One of these defects is increased reinforcement concrete cover compared to the designed one. This fact is most often observed in the column strips of slab-column system. Often in the case of such the slab, the question arises whether it is safe or how is the probability of its failure. In this paper, on the example of a selected slab-column system, an attempt the answer of this question was made.

2 Acceptability and target criteria for the reliability index

For the assessment of existing structures, target reliability levels different than those used in the design must be considered [1]. The differences are based on the following considerations:

- economic consideration: the cost between accepting and upgrading an existing structure can be very large, whereas the cost of increasing the safety of a structural design is generally very small; consequently conservative criteria are used in design but should not be used in assessment,
- social considerations, as the consequences of disruption of ongoing activities,
- sustainability considerations: reduction of waste and recycling, which are considerations of lower importance in the design of new structures.

Target values are given in several codes and guidelines. For the definition of the reliability indices various factors are considered as for example consequences of failure (e.g. low, normal, high for EN 1990), reference period, relative cost of safety measures (e.g. small, moderate, great for ISO 13822 [2]), importance of structure (bridges, public structures, residential buildings, etc.) and so on. They vary with the consequences of failure and the reference periods (50 years for design and 1 year for assessment).

3 Case study of the reliability of the slab-column system

The subject of consideration in this paper was the fragment of the RC two-way slab. Failures in such structures are usually the result of exceeding limit states of the punching shear and flexural. In this study, the effects of change of the reinforcement concrete cover for the considered limit states and structural reliability was investigated. For two analysed limit states (shear and flexural) the margin of safety was defined. The margin of safety, G, is the difference

* Corresponding author: lida@prz.edu.pl

between the resistance of the structural member, R, and the effect of the applied loads, E. In the performed analyses, random variables were: loads, compressive strength of concrete, yield strength of steel and effective depth of reinforcement from extreme compressive fibres. During the analysis, the deterministic values of reinforcement diameter and thickness of the slab were adopted; therefore the change in effective depth depends only on the change in reinforcement concrete cover. The random variables were described, by means the mean value, coefficient of variation and type of distribution.

The purpose of this analysis was to estimate the reliability indices β and/or failure probabilities P_f. depending on the different coefficient of variation of effective depth of reinforcement from extreme compressive fibres. The reliability index and failure probability were determined by two methods - the FORM method and the Cornel method. The obtained values of β_c (Cornell´s reliability index) were compared with the corresponding target values of these indices as adopted by international code standards and they are shown in Figure 1.

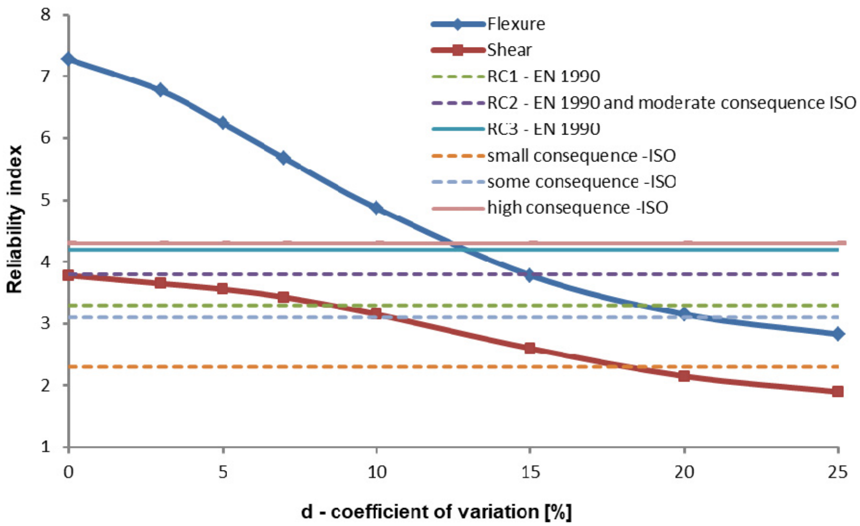

Figure 1. Influence of d-coefficient of variation d for reliability index β_c.

For common material properties and reinforcement ratios, the results of this study showed that there is a wide variation in the reliability index for reinforced concrete members depending on the different coefficient of variation of effective depth. During the assessment of existing structures and considered the consequences of failure, it is possible to accept some change in the depth of concrete cover of reinforcement compared to the design value.

References

1. A.C.W.M Vrouwenvelder, N. Scholten, Assessment Criteria for Existing Structures, *Structural Engineering International*, 20(1), pp. 62–65, (2010)
2. ISO 13822, 2010. Bases for design of structures – Assessment of existing structures. Geneve, Switzerland: ISO TC98/SC2

Bond between concrete and steel reinforcing bars in reinforced concrete elements in the aspect of contemporary experimental research and numerical analysis

Marcin Burdziński[1,*], *Maciej* Niedostatkiewicz[1], and *Patryk* Ziółkowski[1]

[1]Gdańsk University of Technology, Faculty of Civil and Environmental Engineering, Department of Concrete Structures, Gabriela Narutowicza 11/12, 80-233 Gdańsk, Poland

1 Introduction to the issue

The core of reinforced concrete work is the interaction between concrete and reinforcing bars. It is possible due to the adhesion, i.e. the cooperation of concrete and reinforcing bars in the transfer of forces caused by external loads. Bond has a direct impact on the work of the reinforced concrete element, primarily in the Serviceability Limit State (SLS), but also in the Ultimate Limit State (ULS) [1]. Phenomena directly influenced by bond include: the issue of crack formation and development as well as change in the width of their opening, deflection (as a result of the reduction of reinforced concrete element stiffness), issues of development length of reinforcing bars and lap length, analysis of the formation of plastic hinge. Requirements for the safety of realisation as well as the safety of use reinforced concrete structures make that the above issues should be taken into consideration at the stage of their design, execution and subsequent exploitation.

2 Scope of paper

The problem of bond has been the subject for many years of both theoretical analysis, experimental studies conducted on specimen at various levels of observation [2] as well as analysis using numerical calculation methods. The article will present issues related to the theoretical description of the phenomenon of bond between concrete and steel reinforcing ribbed bars and selected methods and elements for studying this phenomenon will be characterized. In addition, the own concept of experimental *pull-out* tests will be presented, discussing the advantages and disadvantages of the proposed experimental model – the so-called small and large specimen.

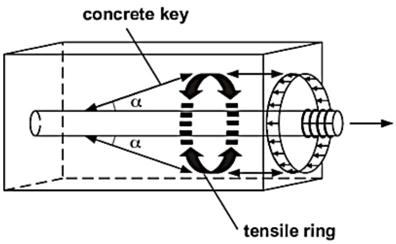

Figure 1. Spatial model of the interaction between concrete and reinforcing ribbed bar – according to Tepfers [3].

* Corresponding author: marcin.burdzinski@pg.edu.pl

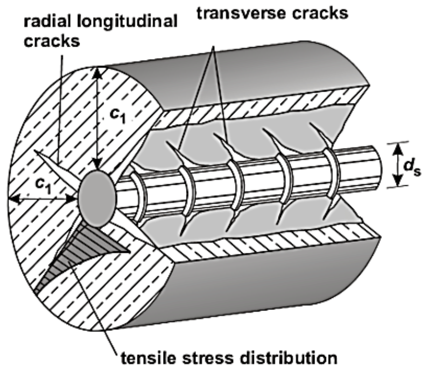

Figure 2. Visualization of the development of cracks and stresses in the specimen as a result of bond – according to Tepfers [3].

References

1. Pędziwiatr J., *Podstawowe zagadnienia przyczepności stali i betonów w elementach żelbetowych*, Oficyna Wydawnicza Politechniki Wrocławskiej, Wrocław 2007
2. Lackner R., Mang H., *Scale Transaction in Steel-Concrete Interaction. I: Model*, Journal of Engineering Mechanics, Vol. 129, No. 4, 2003, pp. 393–402
3. Weiße D., Holschemacher K., Some Aspects about the Bond of Reinforcement in Ultra High Strength Concrete, Leipzig Annual Civil Engineering Report (LACER), 8., 251–263

Assessment of RC elements strengthened with NSM FRP rods by experimental tests

Roberto Capozucca[1,*], and *Erica* Magagnini[1]

[1]DICEA, Polytechnic University of Marche, 60100 Ancona, Italy

1 Introduction

The strengthening of reinforced concrete (RC) beams with damage due to many causes, such as environmental conditions that cause corrosion of steel reinforcement and static not foreseen high loads, is a relevant topic of civil engineering. The use of fiber-reinforced composites has been increased in recent years and, in particular, the near surface method (NSM) with FRP rods inserted inside grooves on concrete cover appears useful to solve many problems [1,2].

The aim of this paper is to analyze the static and dynamic behaviour of RC beams damaged and strengthened by both carbon and glass fiber reinforced polymer (C-GFRP) rods utilizing near surface method. A large investigation both on specimens subjected to pull-out tests with NSM FRP rods and on bending tests of RC beams with and without strengthening [3–5]. Further, the nondestructive method of control based on vibration tests has been adopted during the experiments to assess the response of RC beams at different damage steps due to cracking of concrete [3]. In this paper experimental static and vibration results are discussed and comments on the strengthening bond of NSM C-GFRP rods have been developed.

2 Analysis of bond with pull-out tests

In general, the most dangerous failure mechanism is the loss of bond around the rod at the rod-epoxy interface. An analytical model [4] based on the definition of the system's total potential energy, has been developed to obtain bond stress-slip laws and to estimate the fracture energy value. The differential equation that describes the mechanisms is the following:

$$s''(z) - \xi^2 \cdot s(z) = 0 \tag{1}$$

with: $\xi^2 = K_e / (E_b A_b)$ and stiffness of the epoxy resin equal to: $K_e = (G_e \Sigma_g)/t$ where: A_b = section of rod and E_b = Young's modulus; G_e = shear modulus of the epoxy resin; Σ_g = perimeter of the grooves in contact with the epoxy resin; t = distance between rod and concrete in the groove. For a sufficiently long bond length, having $\tanh(\xi \cdot l_b) \cong 1$, the maximum normal stress for a NSM FRP rod can be obtained [1]:

$$\sigma_{\max} = \sqrt{2E_b \frac{\Sigma_b}{A_b} G_f} \tag{2}$$

In the paper experimental shear stress-slip laws are described by the results using pull-out tests on NSM CFRP and GFRP-rods.

* Corresponding author: r.capozucca@pm.univpm.it

3 Static and vibration tests on RC beams

Static tests were planned for RC beams damaged by bending tests and, successively, strengthened with CFRP circular rods into rectangular grooves measuring 20 mm × 20 mm in section. The dimensions of the beam sections are 150 mm × 220 mm and measure 1700 mm in length. The steel reinforcement used was 4 bars measuring10mm and stirrups at interval of 60 mm having a diameter of 6 mm. Other tests have been foreseen on RC beams damaged and strengthened by NSM GFRP rods.
Finally, experimental free vibration tests were carried out on beams in order to evaluate the influence on the dynamic response of beams of cracking and/or loss of bond of FRP rods.
The experimental dynamic test was carried out using a specific impact hammer using the well-known technique where a mobile accelerometer measures the acceleration of the structural element triggered using a hammer in a fixed point. It was determined that the specimens would be tested dynamically in free-free edge condition.

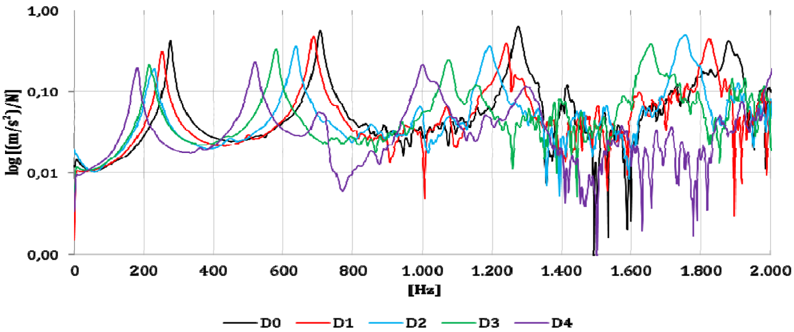

Figure 1. Envelope of FRFs at different damage degree Di, i=1,…,4 due to bending tests for un-strengthened RC beam recorded with accelerometer in one point.

Results of dynamic tests are described in the paper considering envelope of FRFs at different damage degree due to bending tests (Figure 1). Comparison of results obtained with the same technique of near surface mounted has been developed. Comparing the responses to static tests for the un-strengthened beams and strengthened, an increase of bending stiffness of beams can be noted as referred to un-strengthened beam both for strengthening with glass-FRP and carbon-FRP rods. Hence, CFRF NSM rod strengthening brings a noteworthy increase in resistance capacity.

References

1. L. De Lorenzis, J.G. Teng. Near-Surface mounted FRP reinforcement: an emerging technique for strengthening structures. Composites Part B: Eng. **38**, 119–143 (2007)
2. I.A. Sharaky, L. Torres, M. Baena, C. Miàs, An experimental study of different factors affecting the bond of NSM FRP bars in concrete, Composite Structures, **99**, 350–365 (2013)
3. R. Capozucca. Static and dynamic response of damaged RC beams strengthened with NSM CFRP rods. Composite Structures, **91**, 237–248 (2009)
4. R. Capozucca. Analysis of bond-slip in RC beams strengthend with NSM CFRP rods. Composite Structures, **102**,110–123 (2013)
5. R. Capozucca. On the strengthening of RC beams with near surface mounted GFRP rods. Composite Structures, **117**, 143–155 (2014)

Influence of different geometrical and mechanical parameters on confinement effect FRCM-wrapped concrete columns

Dario De Domenico[1,*], *Devid* Falliano[1], *Salvatore* Quattrocchi[1], *Natale* Maugeri[1], *Paolo* Longo[1], and *Giuseppe* Ricciardi[1]

[1]University of Messina, Department of Engineering, 98166 Messina, Italy

Fiber Reinforced Cementitious Matrix (FRCM) systems 1 have been widely used to strengthen or retrofit existing masonry and concrete elements as externally bonded elements. These systems have inherent advantages over alternative Fiber Reinforced Polymer (FRP) systems in terms of better compatibility with the underlying concrete substrate, easier application without careful surface preparation as well as fire resistance.

Flexural and shear strength gain obtained by FRCM systems when applied to reinforced concrete beams have been broadly documented in the literature 2, 3. Moreover, FRCM systems were applied to externally wrapping concrete columns, thus increasing the confinement action in a similar manner to steel stirrups. Axial strength and ultimate deformation of FRCM-wrapped concrete columns can be increased up to 25-30% by one or more layers of FRCM sheets 4. Since the effectiveness of the FRCM system depends on the transfer mechanism of the hoop stresses, critical zones are expected to be concentrated near the corners of prismatic columns. While cylindrical specimens do not suffer from this issue, prismatic columns should be carefully prepared by rounding the corners prior to the FRCM system application.

In this study, an experimental campaign carried out at the University of Messina, Italy, concerning compression tests on FRCM-wrapped concrete columns is documented. Both cylindrical specimens (15 cm diameter and 30 cm height) and prismatic specimens (section of 15 x 15 cm, 30 cm height) are tested in displacement-controlled mode. The parameters investigated in this experimental work are: 1) the number of FRCM layers (1 and 2 layers) applied to the concrete columns; 2) the type of FRCM system (based on PBO fibers and on carbon fibers); 3) the presence of an initial state of damage in the specimens; 4) the corner radius in the prismatic columns. In particular, two corner radii of 0.186 and 0.306 are analyzed, as shown in Figure 1. In addition to the tests performed on the undeformed specimens (no damage), a class of the specimens was previously tested in compression, stopping the test after the attainment of the peak stress value, until a reduction of 15% of the peak load is observed (damaged specimens). In this way, the capability of the FRCM to recover the original strength and deformation capacity of the uncontrolled undamaged specimen is assessed. In this regard, it is well known that in the design earthquake scenario, ordinary structures are expected to undergo significant plastic deformation according to the ultimate limit state principles. Therefore, the aim of the damaged specimens being included in the experimental campaign has been to check whether the FRCM system can be effectively applied to retrofit damaged structures, for instance after an earthquake event, besides the traditional applications for strengthening purposes.

Each specimen is equipped with a series of electrical strain gauges installed on the FRCM fabric (at around the mid-height of the column) to record the hoop strains at different levels of axial load, thereby enabling the calculation of the effective lateral confining pressure for

* Corresponding author: dario.dedomenico@unime.it

different FRCM configurations. The axial strain is recorded with mechanical transducers (placed at around the mid-height of the column) up to the attainment of the peak stress, and then with the stroke of the load actuator of the testing equipment. The concentration of stress in the prismatic columns is also monitored by the digital image correlation (DIC) technique. The results show that both the FRCM fabrics (PBO- and carbon-based) are effective in increasing the axial strength and ductility of the columns. However, only in few cases the FRCM system was also able to recover the axial strength of the damaged columns. The influence of the corner radius is significant in terms of ultimate strain rather than axial strength.

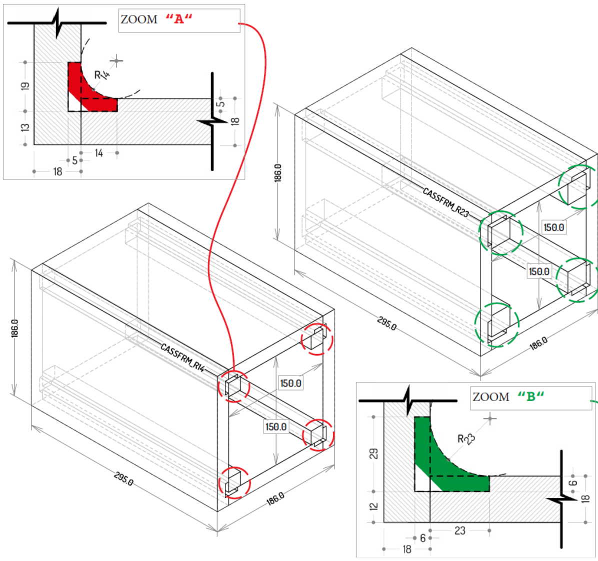

Figure 1. Configurations of prismatic column specimens with two corner radii.

References

1. De Felice, G., Aiello, M. A., Caggegi, C., Ceroni, F., De Santis, S., Garbin, E., Gattesco, N., Hojdys L., Krajewski, P., Kwiecień, A., Leone, M., Lignola G.P., Mazzotti, C., Oliveira, D., Papanicolaou C., Poggi, C., Triantafillou, T., Valluzzi, M.R., Viskovic, A. (2018). Recommendation of RILEM Technical Committee 250-CSM: Test method for Textile Reinforced Mortar to substrate bond characterization. Materials and Structures, 51(4), 95
2. Ombres, L. (2011). Flexural analysis of reinforced concrete beams strengthened with a cement based high strength composite material. Composite Structures, 94(1), 143–155.
3. Gonzalez-Libreros, J. H., Sneed, L. H., D'Antino, T., & Pellegrino, C. (2017). Behavior of RC beams strengthened in shear with FRP and FRCM composites. Engineering Structures, 150, 830–842
4. Gonzalez-Libreros, J., Zanini, M. A., Faleschini, F., & Pellegrino, C. (2019). Confinement of low-strength concrete with fiber reinforced cementitious matrix (FRCM) composites. *Composites Part B: Engineering*, *177*, 107407

The influence of shear span-to-depth ratio on the capacity of the posttensioned crane beams

Wit Derkowski[1,*], and *Rafał* Walczak[1]

[1]Cracow University of Technology, Poland

1 Definition of the research problem

Since the early development of concrete structure design, a consistent approach has been sought for the design of members subjected to shear without transverse reinforcement or with a low ratio of transverse reinforcement. Research on shear members are carried out continuously in numerous research centres around the world because the issue of the assessment of shear capacity of elements without shear reinforcement or with a low ratio of shear reinforcement is a very complex issue and depends on a variety of parameters. The issue of shear capacity of RC members with a low amount of transverse reinforcement has been discussed by numerous research centers, however, the number of scientific works related to prestressed members with a low transversal reinforcement ratio is very limited.

2 The factors affecting the shear capacity

The basic mechanisms involved in the transmission of shear forces are as follows:
– aggregate interlock – occurs after the inclined crack has been formed and is strongly dependent on aggregate grain size [1]. The aggregate friction is also dependent on the crack width and decreases as the crack width increases. In the UHSC, where the crack cuts through aggregate grains, the phenomenon of aggregate interlock occurs to a limited extent;
– dowel action of the reinforcement – becomes visible when the inclined crack reaches the level of longitudinal reinforcement and the rebars take over part of the lateral force [2];
– strain-softening, which occurs in the inclined crack tip – a mechanism associated with the phenomenon of concrete weakening in the micro-cracking zone [3];
– work of uncracked concrete in the compression zone.
Shear span-to-effective depth ratio has the most significant influence on the shear capacity of concrete members and determines the failure mode. Shuaib and Lue [4] have demonstrated that beams with a shear index a/d = 1.0 and 2.0 obtain a much higher shear capacity compared to members with greater shear span-to-effective depth ratio, i.e. $a/d > 2.3$.

3 Experimental tests

The subject of the experimental tests are precast prestressed concrete crane beams disassembled after more than fifty years of being used in an industrial plant. During their service life, they served as a track for overhead cranes with a lifting capacity of 12.5 tons. These are typical I-section prefabricated post-tensioned concrete crane beams, with the height of 800 mm and modular span of 6.0 m (theoretical span – 5.6 m). Each beam was prestressed with five bonded cables with steel cone anchorages.
Although the transverse reinforcement in the crane beam's web were designed at a spacing of 15 cm, the concrete cover exposure of tested beams showed that stirrups are spaced irregularly, at different spacing from 14 to 30 cm.

* Corresponding author: derkowski@pk.edu.pl

Smooth steel transverse reinforcement with a ϕ8 mm diameter had been used. The actual ratio of transverse reinforcement is smaller than assumed in the design, and according to the Eurocode and Model Code 2010 standards the girders does not meet the required minimum level of $\rho_{w,min}$ = 0,21%. The failure mode, the failure load and the corresponding maximum cross-sectional forces for all tested beams are shown in Table 1. Table 2 summarises the design shear capacities of the tested elements determined using the calculation models given in Eurocode 2 and Model Code 2010, assuming the mean values of the material properties. This table also gives the shear capacity determined from V_{Rd} formula even though the minimum transverse reinforcement condition was not met.

Table 1. The failure load and the corresponding maximum cross-sectional forces.

Beam denotation	**Failure load** [kN]	M_{max} [kNm]	V_{max} [kN]	***a/d***	**Failure mode**
KBP-01	1234.7	1177.1	983.9	1.57	Shear-compression
KBP-02	886.4	1157.4	583.6	2.61	Shear-tension
KBP-03	837.7	1192.1	432.6	3.66	Bending-shear

Table 2. Shear capacity of the beam calculated with different models.

$V_{Rd,c}$ EC2 - cracked sections	$V_{Rd,c}$ EC2 - uncracked sections	$V_{Rd,c}$ Model Code 2010	V_{Rd} Model Code 2010	$V_{Rd,max}$ EC2
158.4 kN	674.1 kN	234.6 kN	355.0 kN	1546.7 kN

4 Conclusions

The research showed that despite the low shear reinforcement ratio, the elements does not failure in a brittle mode but clearly indicate future destruction. The experimental shear capacity of KBP-02, KBP-03 elements is significantly higher than the one calculated by means of basic standard models. The best convergence was achieved using the model given in Model Code 2010, which takes into account the interaction of concrete and stirrup in the total design shear resistance. In the case of testing the KBP-01 element, the shear capacity was exhausted with the crushing of the compressed concrete strut. Assuming its actual slope of the strut, its calculated capacity is 1546.7 kN and it is higher than the value obtained in the test. This can be explained by the higher strut's stress intensity when it transfers loads directly to the support.

References

1. Walraven J.: *Fundamental analysis of aggregate interlock* (Journal of the structural Division, ASCE, v.107, no.ST11, 1981, pp. 2245–2270)
2. Kobayashi K.: *Effect of bond and dowel action on shear capacity of RC beams. Earthquake Engineering* (Tenth Word Conf, Balkema, 1992, pp. 3101–3108)
3. Hillerborg A. et al.: *Analysis of crack formation growth in concrete by means of fracture mechanics and finite elements* (Cement and concrete research, v. 6, 1976, pp. 773–782)
4. Shuaib A. H. Lue D.M.: *Flexural-shear interaction of reinforced high-strength concrete beams* (ACI Structural Journal, v. 84, no. 4, 1987, pp. 330–341)

Experimental confirmation of computational method for composite "slim floor" system

Jerzy Derysz[2], and *Paweł* Lewiński[1,*]

[1]Instytut Techniki Budowlanej, 1 Filtrowa Str., 00-611 Warszawa, Poland
[2]PFEIFER Steel Production Poland Sp. z o. o., 68 Wrocławska Str., Krępice, Poland

1 Introduction

Hybrid beams are fully prefabricated, load-bearing structural elements, which due to their high rigidity for bending and torsion are the supports for various floor slab systems (Derysz *at al.* [1]). The composite BHM beam can be described as the structural member with components of concrete and structural steel, interconnected by horizontal shear studs (see Fig. 1). Their main advantage is that they are within the floor slab height, which allows minimization of the floor slab structural thickness (the so-called *slim floor* system).

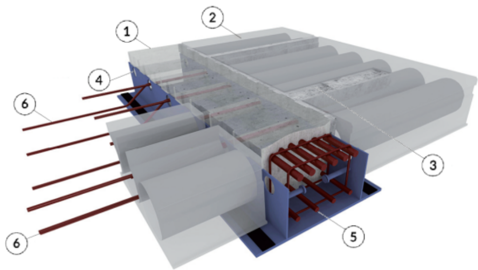

Figure 1. Structural systems of BHM beam and HC slabs. Symbols: 1 – BHM beam, 2 – HC slab, 3 – cast concrete, 4 – opening, 5 – longitudinal rebar, 6 – stitching reinforcement.

Important issues related to the slim-floor composite structures were recently the subject of the Stahlbau-Kalender-Tag 2018 seminar in Stuttgart (see Stahlbau Kalender 2018).

The research project includes both laboratory testing of separate beams and field tests of entire systems, the purpose of which is to determine a full description of their mechanical behavior, because their ultimate load capacity has not been reached in hitherto tests despite the application of very high loads [1, 2].

2 Schedule and layouts of research program

The test load method was developed. The field tests were prepared for the floor systems on BH 20-300 hybrid beams (2 test fields) and BH 27-350 hybrid beams (2 test fields) interconnected with HC pre-tensioned slabs. A series of field full-scale short-term tests was carried out on the premises of PFEIFER SPP, as a result of which, load-bearing capacities of the slab-beam systems, and the deflections and strains in selected areas were determined. Schedule and layouts of the tests of slab-beam systems together with the set-ups of strain gages in order to determine an effective flange width were prepared. The scheme of the research set and the arrangement of

* Corresponding author: p.lewinski@itb.pl

loads is shown in Fig. 2. Electronic measurements were carried out by a team from Wrocław University of Science and Technology.

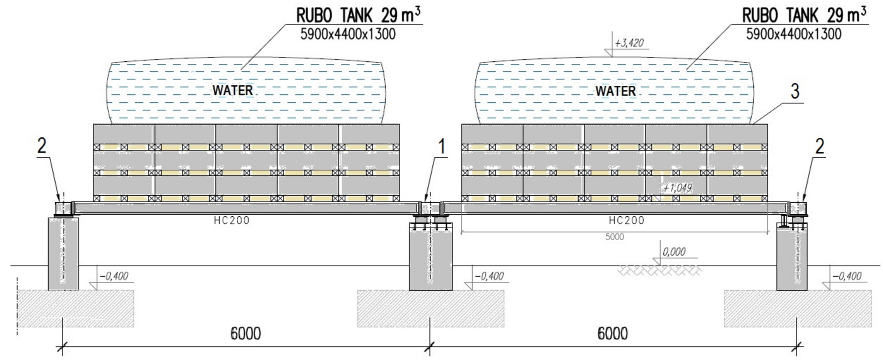

Figure 2. The research set and the arrangement of loads. Notations: 1 – middle beam: BHM 20-300-600 type, 2 – edge beam: BHR 20-250-600 type, 3 – leveling layer of OSB boards on stacking palettes.

3 Analysis of test results and conclusions

The results of laboratory tests on representative BHM 20-300 and BHM 27-350 hybrid beams, and then field testing the beams of the same type, but interconnected with pre-tensioned HC200 and HC265 slabs, respectively, their load-bearing capacity in both cases was compared. Comparison of the magnitude of these loads showed a two-fold increase in the load-bearing capacity of beams due to the interconnection of beams with HC slabs, compared to the load capacity of the beams themselves. Since the separated beams were damaged due to crushing of the compression zone, it was initially assumed (without experimental evidence) that the destruction of the entire hybrid beam-plate system would occur as a result of shearing joints between the HC slabs and BH beam, which would entail the separation of BHM beam and its final damage due to the failure of compression zone. In addition, the load-bearing capacity of the hybrid beam-slab system is determined by the effective width of the slabs interconnected with the beam. Due to the appropriate parameterization of the equilibrium equations of the analyzed cross-sections of the beams in the ultimate limit state, an additional calibration of the calculation methods used so far was made. Test results will be supplemented with non-linear analyses of the hybrid system supported on BHM beams which will allow for accurate determination of the behavior of the hybrid system supported on BHM beams. The results obtained from the conducted tests indicate high repeatability of recorded critical load values. The performed tests allowed accurate determination of the ultimate capacity of the research elements, and thus – confirmation of the legitimacy of the calculation methods used.

References

1. Derysz J., Lewiński P.M., Więch P.P., New concept of composite steel-reinforced concrete floor slab in the light of computational model and experimental research, Procedia Engineering, **193** (2017)
2. Lewiński P. M., Derysz J., Dudziak S., Więch P., Newly designed structural solutions for the "slim floor" composite system, Proc. *fib* Symp., Kraków (27–29 May 2019)

Analysis of confined masonry with Strut and Tie models

Łukasz Drobiec[1,*], *Wojciech* Mazur[1], and *Tomasz* Rybarczyk[2]

[1]Silesian University of Technology, Department of Building Structures, 44-100 Gliwice, Poland
[2]Solbet Spółka z o.o., 86-050 Solec Kujawski, Poland

1 Introduction

Strut & Tie (S-T) models are commonly used for the analysis of confined wall subject to seismic results [1-3]. Such models can be, however, used to analyse monotonically loaded walls [4]. Paper presents the concept of building Strut & Tie models for confined masonry made of autoclaved aerated concrete. Calculations were performed for natural-scale research models of walls in compression. The analysis of cracks in research models and results of numerical models were used to assume the geometry of S-T models. Values of load capacity were compared with results from testing confined solid walls in compression, walls with an opening and additional confining cores at the opening.

2 Concept of building the S-T model of the confined masonry

Preparing the strut-and-tie model of the confined masonry is different from preparing such models for reinforced concrete or traditional masonry. The analysis should include different stiffness of concrete and wall. Therefore, reinforced concrete spandrel beams and confining cores were replaced with rebars. They formed a frame into which jointly supported rebars representing changes in stress in the masonry were placed. The tensile strength of the masonry was negligibly low, so ties cannot be prepared from that material.

3 Description of analysed models

Research models were built from blocks of autoclaved aerated concrete, with a thickness of 180 mm, laid in the thin-layer mortar. Compressive strength of the wall was f_{test}= 2.97 N/mm^2 in walls with unfilled vertical joints and $f_{test,2}$ = 2.61 N/mm^2 in walls with filled vertical joints. Modulus of elasticity was E = 2040 N/mm^2 and E = 2447 N/mm^2, respectively and Poisson's ratio equal to ν = 0.18. Models were built from concrete of class C20/25 and steel with yield strength of 500 N/mm^2. Tests were scheduled and conducted on 12 confined walls. They included four confined walls without openings, four walls confined along their perimeter and with openings, and four walls confined along their perimeter and with additional cores at an opening. Models were 4.43 m long and 2.49 m high.

4 Numerical analysis and assumed geometry of S-T model

Calculations based on the finite element method were performed to adopt the structure of compressed rods in S-T models representing masonry. One half of the wall model was built using the symmetry of research models. An elastic-plastic model on Menétrey-Willam surface

* Corresponding author: lukasz.drobiec@polsl.pl

was used to describe the material behaviour under compression. Behaviour of the material under tension was described using Rankine criterion, the model of smeared cracks developing in uniform directions, and the exponential function of fatigue. ATENA 2D software was used for computations. Contact elements were applied at the interface between masonry units. Parameters of the material and contact elements were determined on the basis of our own material tests [5]. Cracks in models and the distribution of stress in numerical models were analysed. Those analyses were the base to assume the geometry of rod models for the S-T method (Fig. 1).

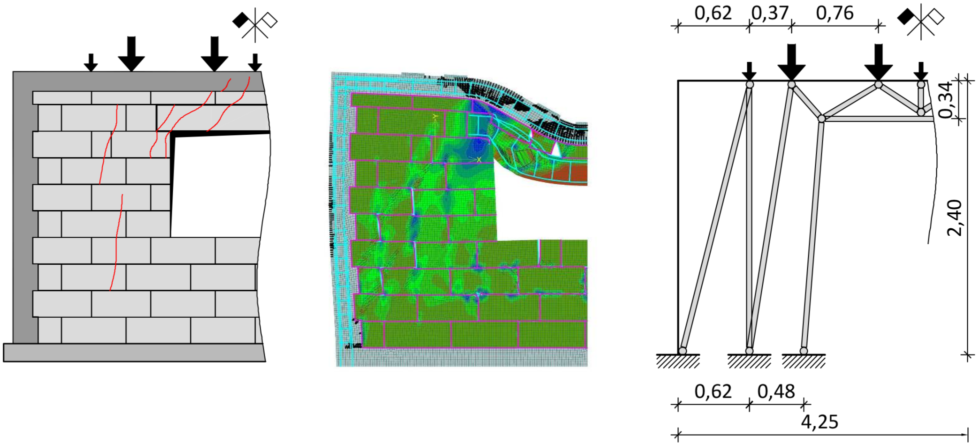

Fig. 1. Arrangement of cracks, main stress in FEM and recommended rod model of confined masonry with opening.

5 Results of calculations using S-T models

Results from tests and S-T method were compatible. Depending on the analysed model, computed loading contributed to 82÷92% of values obtained from tests. The highest level of compliance was observed for the model with additional inner cores.

6 Conclusions

Binding standards do not contain recommendations on determining the load capacity of confined masonry. Computational analyses conducted on Strut & Tie models demonstrated that such models can be successfully used for computational analyses of confined masonry. The compliance of S-T method results with test results was acceptable.

References

1. Brzev S., Perez-Gavilán J.J:, *Proc.of the 16th Intern. Brick and Block Masonry Conf.*, Padova, Italy, (2016)
2. Ghaisas K.V., Basu D., Brzev S., Perez-Gavilán J.J., Constr. a. Build. Mat., **147**, pp. 677–700 (2017)
3. Liberatore L., Noto F., Mollaioli F., Franchin P., Eng. Struct., **167**, pp. 533–548, (2018)
4. Jasiński R., IOP *Conf. Series: Materials Science and Engineering* **245**, (2017).
5. Drobiec Ł.: Mauerwerk, Heft 1, **24**, pp. (2020)

Comparison of tension stiffening models in non-linear FEM analysis of RC structures

Sławomir Dudziak[1,*], and *Paweł M.* Lewiński[1]

[1]Building Research Institute (ITB), Filtrowa 1, 00-611 Warszawa, Poland

1 Introduction

The experimental results show that the cracked concrete in tensile zones can have significant influence on the overall stiffness of the whole RC element due to the bond of rebars to concrete. This phenomenon is well-known as the "tension stiffening" effect (TS). According to standards, its range depends mostly on: reinforcement ratio and reinforcement bars type. Neglecting the TS effect may result in serious overestimation of element deflection. On the other hand, the TS effect usually does not affect load capacity because bond properties between steel and concrete vanish at the stage of rebar yielding. Therefore, the TS effect is important in the assessment of serviceability limit states and often can be neglected during evaluation of ultimate limit state [1].

There are two main ways of including the TS effect in the non-linear FEM analysis: by enhancement of steel constitutive law or by modification of concrete constitutive model (softening branch after crack formation).

Due to negligible influence on load capacity, it is often not included in analyses, e.g. in Kotsovos material model which recently gained in popularity for the analysis of large RC structures [2]. In the present paper, the generalized constitutive law for steel reinforcement is proposed. It provides a possibility for including the TS effect in "Kotsovos type" material models. The two approaches to modelling the TS effect are compared below in the simulation of WT3 deep beam behaviour which was tested by Leonhardt and Walther [3].

2 Constitutive models and WT3 deep beam

The proposed approach consists of generalized concrete and steel material models. In case of concrete in tension, the material behaviour is modelled as fully brittle, whereas in compression regime the hypoelasticity constitutive law is used for concrete. The reinforcement steel is modelled with multilinear relation based on Model Code 2010 [4] in which 4 phases can be distinguish: an elastic stage, a phase of crack formation, a stabilized cracking phase and a plastic stage (see Fig. 1). The proposed models were implemented in the Abaqus code by UMAT user's procedure. In the comparative analysis the quasi-brittle-elasto-plastic "smeared crack" (SC) material model was examined which is standard available in the Abaqus code. In this material model the TS effect is described by descending branch of concrete stresses after cracking. Material parameters in the simulation of the WT3 deep beam behaviour were assumed according to the report [3].

The results of two simulations are compared in Fig. 2. In "smeared crack" approach with descending branch, two values of crack strain at which stresses in crack tend to zero, were adopted in the analysis. The results show that numerical stability of non-linear procedure is ruled by this parameter.

* Corresponding author: s.dudziak@itb.pl

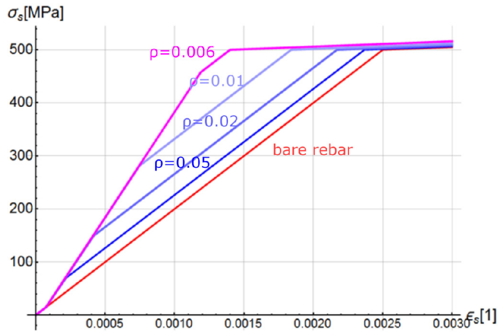

Fig. 1. The stress – strain relationship for the proposed generalised constitutive steel model.

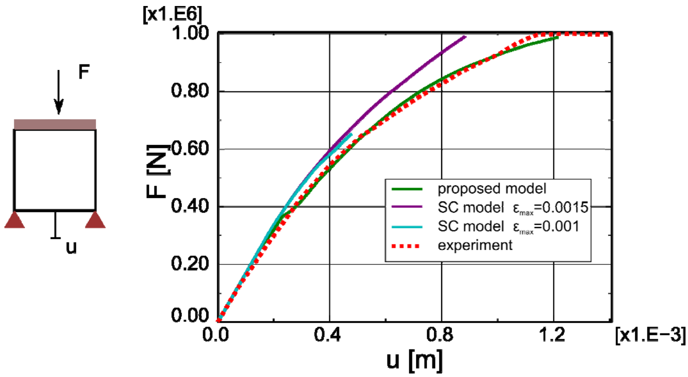

Fig. 2. The results of the WT3 deep beam behaviour simulation using two approaches.

3 Summary

In "smeared crack" approach in which the TS effect is modelled by descending branch after cracking in concrete material model, it is hard to calibrate its parameters according to standards (like [4]) due to the problems with iteration convergence. Moreover, the model response is very sensitive to changes in descending branch shape.

The proposed model is based on the provisions of codes and the TS effect parameters do not affect the stability of non-linear procedure or the load capacity prediction. Consequently, it promises to be useful in the assessment of serviceability limit states using FEM.

References

1. *CEB Bulletin 237. Concrete Tension and Size Effects* (Comité Euro-International du Béton, 1997)
2. M. Engen, M. A. N. Hendriks, J. A. Øverli, E. Åldstedt, European Journal of Environmental and Civil Engineering, **23**, 11 (2019)
3. F. Leonhardt, R. Walther, *Wandartige Träger* (Deutscher Ausschuss für Stahlbeton 178, 1966)
4. *fib Model Code for Concrete Structures 2010*. (International Federation for Structural Concrete fib, 2013)
5. Dassault Systèmes. Manual Abaqus 6.14 (2014)

Bond load-slip behaviour for FRP bars in recycled concrete

Ahmed Godat[1,*], *Ebtesam* Alghafri[1], *Noura* AlTamimi[1], *Hamda* Aljaberi[1], and *Shaima* Aldaweela[1]

[1]United Arab Emirates University, Civil and Environmental Engineering Department, Al-Ain, UAE

1 Introduction

This research aims at investigating the bond behaviour of FRP bars in recycled aggregates that can expand the life service of structures and reduce their cost of rehabilitation or replacement. The study compares between the bond behaviour of carbon, glass and basalt FRP bars in recycled concrete to the ones in normal concrete. The experimental program contains thirty six specimens that are tested using the direct pull-out test. The FRP bars are casted in different recycled concrete strengths. The impact of the various concrete strengths considered is identified based on the gain in the bond load. The results of the study is prepared in terms of bond load-slip relations that can assist practical engineers with a clear conclusion of the bond performance of FRP bars in recycled concrete.

2 Experimental program

The test specimens were prepared using recycled aggregates for three concrete strengths with an average of 32, 46 and 63 MPa. The concrete strength was selected to be a parameter for study in order to investigate the bond behaviour for high strength concrete. The concrete mixes had maximum nominal aggregate size of 20 mm. In this study, a concrete strength of 37 MPa with normal aggregate was prepared as a benchmark for the study. Pultruded CFRP, GFRP and BFRP bars were utilized in this study with a nominal diameter of 12 mm.

Cubic wooden moulds with 200 mm side were used to prepare he pull-out tests. FRP bars with 1,000 mm length were concentrically positioned in the mould. Prior to casting, FRP bars were plastic wrapped to ensure the desired embedded length, 5d, where is d is the bar diameter. The embedded length was located at the middle third of the cube that was opposite to the pull-out direction. The other side of the FRP bar was inserted in a steel sleeve to avoid the crushing of the bar in the grip of the testing machine.

The test matrix is presented in Table 1. For each set of parameter, three specimens were prepared in order to ensure the reliability of the test results. The specimens were labelled as follows: the first term indicates the bar material type (B for basalt, G for glass and C for carbon) followed by the bar diameter. The second term marks the concrete type (RC for recycled concrete, and N for normal concrete) along with the concrete strength.

All specimens were subjected to pull-out testing following the standard procedure. The tests were carried out in displacement control of 1.2 mm/min. The slip at the free end of the FRP bar was measured using linear variable displacement transducer (LVDT). The applied pull-out load and the bar slippage were recorded automatically throughout the test.

* Corresponding author: Ahmed.Godat@uaeu.ac.ae

Table 1. Pull-out test matrix.

Specimen	Concrete type	Concrete strength (MPa)	FRP type	Maximum bond load
B12-RC30	Recycled concrete	32	BFRP	52.0
B12-RC45	Recycled concrete	47	BFRP	61.6
B12-RC60	Recycled concrete	63	BFRP	64.7
C12-RC30	Recycled concrete	32	CFRP	49.2
C12-RC45	Recycled concrete	47	CFRP	43.7
C12-RC60	Recycled concrete	63	CFRP	67.8
G12-RC30	Recycled concrete	32	GFRP	58.5
G12-RC45	Recycled concrete	47	GFRP	64.6
G12-RC60	Recycled concrete	63	GFRP	56.1
B12-NC30	Normal concrete	37	BFRP	52.9
C12-NC30	Normal concrete	37	CFRP	48.6
G12-NC30	Normal concrete	37	GFRP	49.6

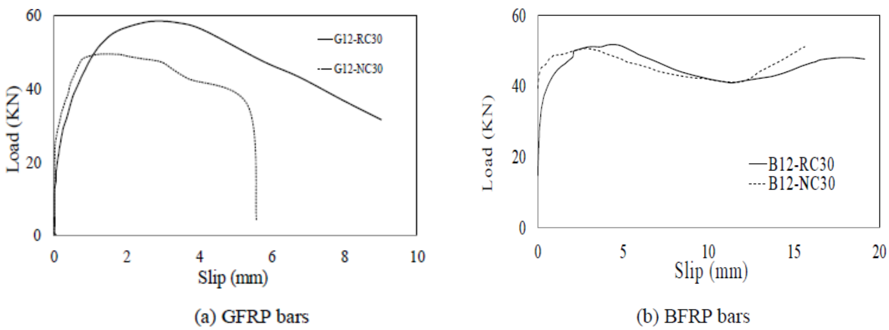

Figure 1. Comparison of bond load-slip behaviour for FRP bars in recycled and normal concrete.

3 Experimental results and discussion

The maximum bond load of the tested specimens are presented in Table 1. The maximum bond load is the average value for the three specimens of the specific group. As can be seen in the table, the maximum bond load for the FRP bars in recycled concrete are similar to the ones in normal concrete. This indicates that the FRP/concrete bond behaviour remained unchanged when recycled aggregates are used to cast the concrete. The bond load-slip relation for the FRP bars indicates that both the normal and recycled concrete experienced similar curves, as depicted in Fig. 1. The bond load-slip curves for GFRP bars (Fig. 1a) showed initial ascending branch up to the maximum bond load followed by softening branch. For the BFRP bars, fluctuating branch was observed after the maximum bond load was attained, as shown in Fig. 1b. All the FRP bars in the recycled concrete exhibited a typical pull-out failure mode, which was identical to the one observed for the FRP bars in normal concrete.

Simulation of three-point beam bending test using the X-FEM method

Jakub Gontarz[1,*], and *Jerzy* Podgórski[1]

[1]Lublin University of Technology, Faculty of Civil Engineering and Architecture, Lublin, Poland

1 Introduction

This paper presents an attempt to simulate a three-point bending test on a notched beam in the Abaqus FEA system using X-FEM method. X-FEM (extended Finite Element Method) is a method of simulating the fracture independent of the finite element mesh. In each increment, the program leads the crack to the next element, modifying the displacements in the element nodes with the appropriate shape function. The authors attempted to simulate the fracture of the beam shown in Fig. 1a to determine whether it is possible to predict or simulate the destructive force and crack path obtained in laboratory tests.

2 Description of the model

The analyzed model is a beam in the plane stress state, dimensions 10×40 cm with a notch 3.5 cm. Load and notch are shifted in opposite directions by 5 cm. The material parameters required by Abaqus FEA were taken from the literature [1]. The parameters were set: Young's modulus $E = 31.915$ GPa, Poisson's ratio $\nu = 0.2$, tensile strength $f_t = 3.13$ MPa, critical stress intensity factor $K_{Ic} = 1.15$ MN/m$^{1.5}$, which means that critical strain energy release rate equals $G_{Ic} = K_{Ic}^2/E = 41.438$ N/m.

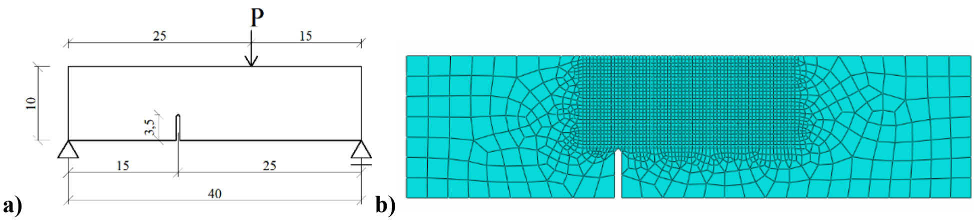

Figure 1. a) Scheme of the task, b) FE mesh of the model.

The finite element mesh is shown in Fig. 1b. The criterion of maximum principal stress was chosen for the initiation and propagation of the crack [3]. The direction of the crack is the direction of rotation of the stress in the element to the principal stresses. Unfortunately, this method is underdeveloped, because Abaqus calculates the arithmetic mean determined from stresses at four integration points in the analyzed element. The result of the analysis is shown in Fig. 2a. Of course, this is an incorrect result, the crack should actually go towards the force P, and not turn back.

Getting the correct result, however, is possible using own Abaqus user subroutine. Figure 2b presents a field of principal stresses at the moment when the crack begins to return. From this drawing, it can be seen that the largest stress drop from the crack tip is to the right up, not down, as the simulation showed.

* Corresponding author: j.gontarz@pollub.pl

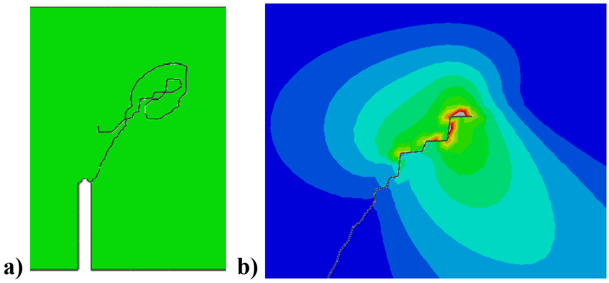

Figure 2. a) Crack obtained in the simulation, b) Field of maximum principal stresses before changing direction.

3 Own crack propagation criterium

The authors are currently at the stage of implementing their own failure criterion, which could be called "the displacement symmetry criterion". The Griffith crack and it's Westergaard solution [2] were used. The formulas for horizontal and vertical displacements relative to the Griffith crack tip at the point in polar coordinates are given below, where θ is the angle (angle 0 is along the crack) and r is the distance from the crack tip:

$$u_x = c\sqrt{r}\left[(\kappa-1)\cos\frac{\theta}{2}+\sin\theta\sin\frac{\theta}{2}\right],\; u_y = c\sqrt{r}\left[(\kappa+1)\sin\frac{\theta}{2}-\sin\theta\cos\frac{\theta}{2}\right], \tag{1}$$

where $\kappa = (3-\nu)/(1+\nu)$, and c is the vertical adjustment coefficient. These graphs were transformed into polar coordinates (u_r – displacements along the radius, u_θ – displacements perpendicular to the radius) and are shown in Figure 3a. It can be concluded that the crack will occur where u_r reaches the extreme value, and u_θ takes the value 0. The displacements on a certain radius around the crack tip in the discussed model were read and they are presented in Figure 3b (angle 0 is the vertical direction). As can be seen, according to the above hypothesis, the crack will occur to the right at an angle 20 degrees to the vertical direction. This is a very realistic result. Therefore, the next step is to adjust the Westergaard's field to the displacements in four nodes of the analyzed element during every increment and implement it to Abaqus FEA.

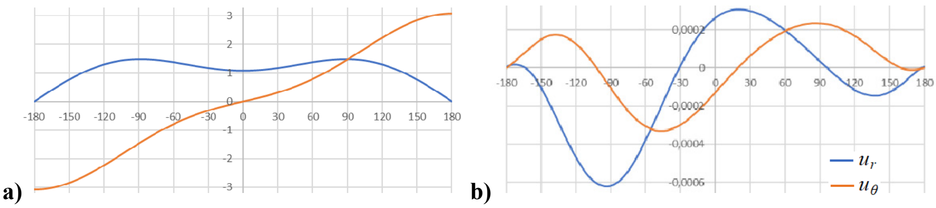

Figure 3. a) Westergaard solution for displacements around the crack tip for $r = 1$, b) displacements around the crack tip for exemplary simulation's increment.

This research was sponsored by the Lublin University of Technology Research Fund 2019.

References

1. J. G. M. van Mier, *Fracture Processes of Concrete* (CRC Press Inc., 1996)
2. H. M. Westergaard, J. Appl. Mech., **61** (1939)
3. Abaqus V 6.14.2 User's Manual, (2014)

Computational analysis of displacement of the rectified building

Krzysztof Gromysz[1,*]

[1]Silesian University of Technology, Faculty of Civil Engineering, 44-100 Gliwice, ul. Akademicka 5, Poland

1 Introduction

The renovation, the purpose of which is to remove the deflection of the building, consists of several stages. First, piston hydraulic jacks are placed in the walls of the lowest storey and then the structure is torn apart horizontally by them. The basic stage is rectification, which consists in uneven lifting of the object by forced extensions of jack pistons. Due to the limited range of extension of these pistons, it is necessary to install a stack of parallelepiped elements under the jacks. In this way, temporary supports are formed, the stiffness of which depends mainly on the length of the stack [1].

During rectification, the building is divided into two parts: an unevenly elevated part situated above the detachment plane and the part remaining in the ground situated below the detachment plane. The part situated above the detachment plane is displaced upwards and the deflection of this part is removed (fig. 1). The part situated below the detachment plane is also slightly displaced due to subsoil deformations. In addition, the temporary supports are subject to deformations and the values of the forces occurring in the supports are changing.

a) b)

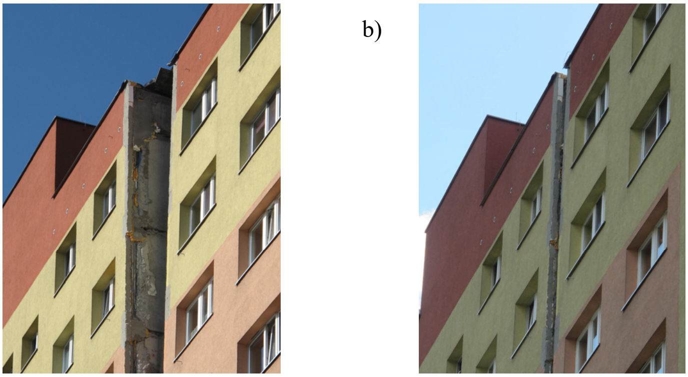

Figure 1. Building which was subjected to rectification: a) expansion joint before the process, b) expansion joint after the process.

2 Analysed model

The subject of computational analysis is a model of a building. The structure provided with basement is made using the precast technology and has five aboveground storeys. The building plan is a rectangle with dimensions of 18.59 m and 10.38 m (Fig. 2a). The thickness of the load-bearing layers of walls is 0.15 m, the ceiling thickness is 0.24 m and the height of all stories is 2.8 m.

* Corresponding author: krzysztof.gromysz@polsl.pl

A constant cross-section of foundation footings (*b/h*) of 1 m /0.5 m has been adopted. The modulus of elasticity of the material of walls, ceilings and footings was assumed to be equal to 29 GPa and the Poisson coefficient equal to 0.2. The system was loaded with its own weight. 52 temporary supports were installed between the elevated part of the building and the part remaining in the ground, the position of which is shown in Figure 2b. The calculations were carried out for two values of stiffness of all supports equal to 160 MN/m and 50 MN/m. These values correspond to two situations: the first one, where the supports are formed by the jacks themselves, and the second one, where the jacks are placed on the stacks of parallelepiped elements which increase their working range. Moreover, two values of subsoil stiffness were assumed in the calculations of 100 MN/m^3 and 10 MN/m^3. These values correspond to soils with high rigidity and low rigidity, accordingly.

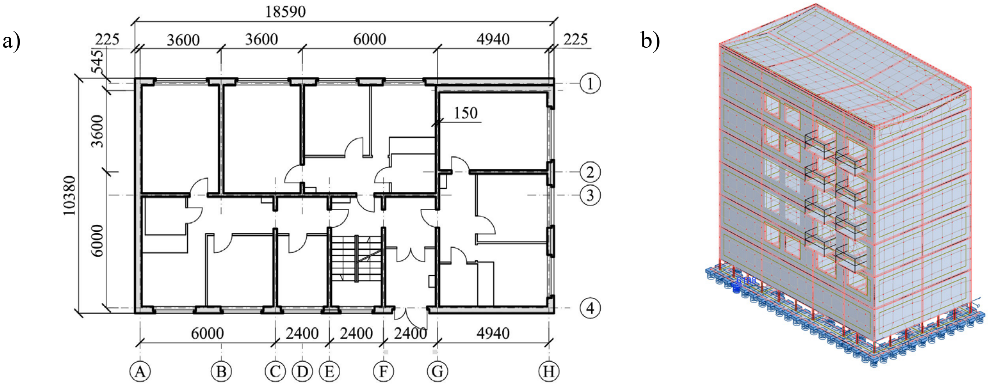

Figure 2. The analysed building with basement and five aboveground storeys: a) ground floor view, b) view of the model.

3 Conclusions

The analyses carried out reveal that the stiffness of temporary supports has a decisive influence on the parameters of the building being rectified. Similarly, the stiffness of these supports has the greatest influence on the values of displacement of the elevated part of the building and changes in the value of forces in supports with forced extension of jack pistons. Major changes in subsoil stiffness do not significantly affect the value of displacements of the elevated part of the building and the value of forces in temporary supports.

The equations derived set the basis for experimental determination of the parameters of straightened buildings, control of the complex process of deflection removal and optimisation of the position of temporary supports for the planning of rectification.

References

1. K. Gromysz, Deformations of temporary wooden supports used to reduce building deflections in mining areas. E3S Web of Conferences 36, 03002 (2018) https://doi.org/10.1051/e3sconf/20183603002, BIG 2018

Thermal deformations of reinforced concrete floors in multi-storey building garages

Marcin Górecki[1], and *Jerzy* Szerafin[1,*]

[1]Lublin University of Technology, Civil Engineering and Architecture Faculty, 20-618 Lublin, 36 Nadbystrzycka Str., Poland

1 Issues described in the article

In the garage part of the multi-storey building, numerous damages to the structural elements occurred, in particular cracks and chipping of concrete fragments in the column corbels on which reinforced concrete inter-floor slabs were based. On the basis of the damage inventory and analysis of the static work of the building structure, it was determined that the reason for the defects observed were the thermal deformations of the ceilings, resulting from the intense impact of external temperature on the elements of the structure inside the building. Garages in the building are intensively used, which is associated with frequent inflow of outside air through wide entrance gates, which are opened and closed many times a day, and even left open for a few hours.

The article shows the damages of the brackets, indicates structural errors that directly contributed to the damage and presents the method and implementation of the repair. Measurements of thermal deformations of concrete slabs at four selected measurement locations, together with measurements of external and internal temperature, are also presented. The measurements were carried out for the period of one year.

1.1 Damages to the structure

The article will show the damage to the building structure in the form of photographs with their location on the building plan. Examples of damage are shown in Fig. 1 and Fig. 2.

Fig. 1. Damage of the corbel surface.

Fig. 2. Crack on the corbel edge.

[*] Corresponding author: j.szerafin@pollub.pl

1.2 Presentation of the results of measurements of thermal deformation of concrete slabs

The concrete slabs thermal deformation was measured at four measuring locations, located directly at the dilatation of the ceiling, two on each garage floor. Measurements were made using metal indicators with a Vernier scale (Fig. 3).

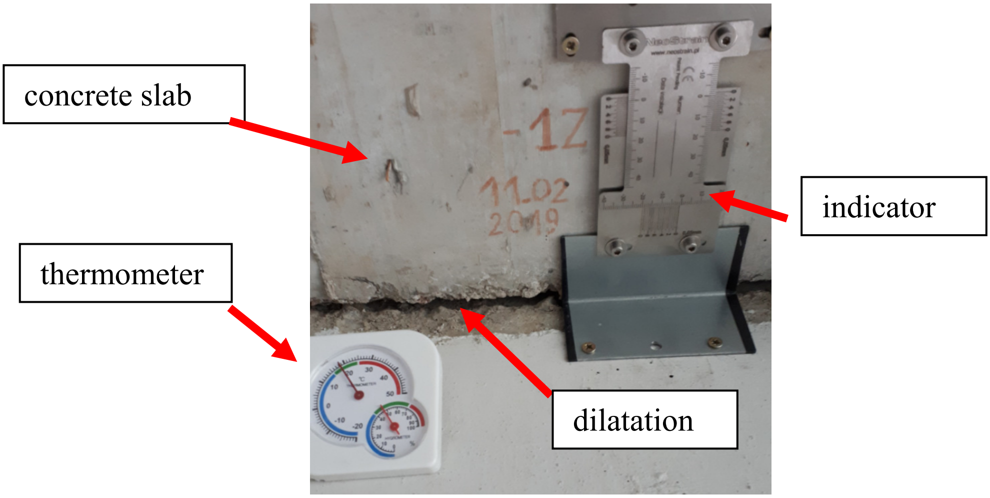

Fig. 3. Measurements of floor slab deformations.

The measurement results are shown in tables and in graphic form, as exemplified in Fig. 4.

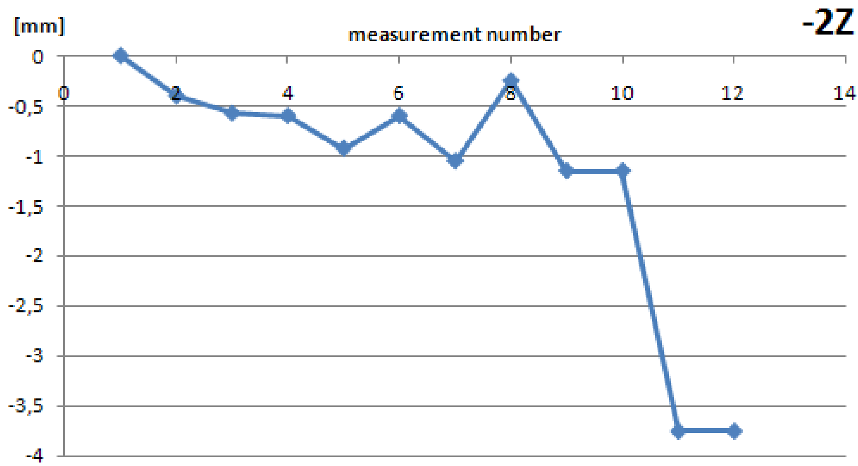

Fig. 4. Change of the dilatation width at the measuring location -2Z.

The article will also present an analysis of thermal deformations of ceilings depending on the external and internal temperature in individual locations.

Strengthening of RC plates with mineral-bonded composite layers for enhanced impact safety

Marcus Hering*,[1], *Tino* Kühn[1], *Franz* Bracklow[1], and *Manfred* Curbach[1]

[1]Technische Universität Dresden, Faculty of Civil Engineering, Institute of Concrete Structures, 01062 Dresden, Germany

The presented research paper deals with a series of impact experiments conducted in the drop tower facility of the Otto Mohr Laboratory (OML) at the Technische Universität Dresden. The presented research results were generated in three research projects.
A number of reinforced concrete (RC) plates and subsequently on the not impacted side strengthened RC plates were produced and tested. As basic materials for the RC plates, a normal strength C40 concrete reinforced with conventional BST500 reinforcement steel were used. Different material combinations are possible for the subsequently applied strengthening layer. However, only cement-bonded strengthening layers were applied. The paper deals with the experimental program, the used experimental setup, and the results of the experiments and their interpretation.

1 Specimen and experimental setup

Samples with a geometry of 1.5 m × 1.5 m× 0.3 m were examined. For the first part of the investigations, five specimens were produced. These plates were conventional RC plates. Furthermore, additional four RC plates were prepared during production in such a way that a washed concrete surface was created on the bottom side of the plates. Different strengthening layers were subsequently applied to this plate side. The thickness of these layers was 2 cm consisting of matrix material and optional fibre reinforcement.
The accelerated mode of the drop tower facility available at the OML was used for the experimental investigations. Technical details are summarized in [1]. For the experiments, impactor velocities from 54 m/s to 68 m/s were chosen. The kind of impactor remained equal for all experiments. It was 380 mm long, had a flat nose and weighed 21.66 kg. With these parameters, a large number of different types of damage could be provoked to the plates.
After the experimental investigations, the plates were cut in the middle with a concrete saw. So it was possible to get a direct look at the damage inside the specimen.

2 Exemplary experimental results

Figure 1 shows a collection of saw cuts. In the left half of the picture, the saw cuts through the 30 cm thick reinforced concrete plates are displayed. The impact velocities and specimen labels used in each case were supplemented in the picture. Here it is very easy to see how the local damage, which is characterized by a punching cone failure, increases steadily with increasing impact velocity.
The right half of the picture shows the RC plates strengthened with an additional layer of material. The strengthening layers consisted of fine grained concrete as matrix, which was reinforced by four layers of different fabric materials each.

* Corresponding author: marcus.hering@tu-dresden.de

The considered configurations of the strengthening layer were summarized in Table 1.

Table 1. Used strengthening layers.

specimen label	matrix material	reinforcing material
PL145	fine concrete	carbon fabric 1
PL147		glass fabric
PL148		none
PL149		carbon fabric 2

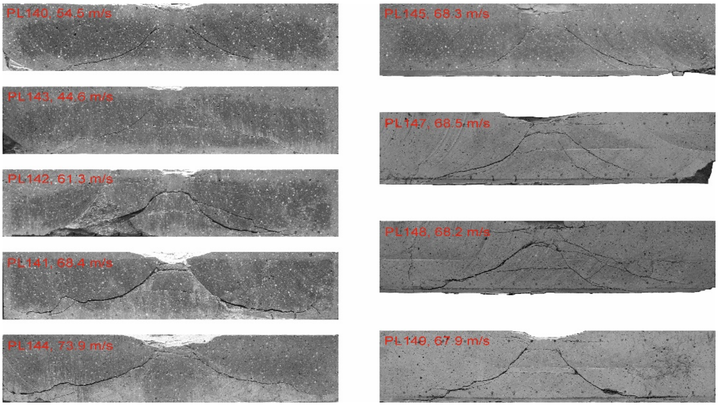

Fig. 1. Saw cuts of the tested plates (30 cm thickness); PL140–144, see [2]; PL145 see [3]; PL147–149, picture: M. Hering.

The impact velocity was approximately 68 m/s for all tested strengthened RC plates. Depending on the strengthening layer used, different stages of damage could be observed. The characteristic of the cone was visible in all experiments, but there were sometimes significantly differences. The investigations carried out provided an overview of the performance of different strengthening layers.

Parts of the presented paper were funded by the German Federal Ministry of Economic Affairs and Energy (BMWi, project no. 1501541) on basis of a decision by the German Bundestag.
The authors express their great acknowledgement to the German Research Foundation (Deutsche Forschungsgemeinschaft, DFG) for the financial support offered within the framework of the Research Training Group GRK 2250.
Further thanks go to the research association 'Forschungskuratorium Textil e.V.'for founding the project IGF 19009 BG. This is a joint project of the Institute of Concrete Structures and the Institute of Textile Machinery and High Performance Material Technology, TU Dresden, and was funded by the 'Arbeitsgemeinschaft industrieller Forschungsvereinigungen "Otto von Guericke" e.V.' (AiF) as part of the program for the promotion of industrial joint research (IGF) by the Federal Ministry for Economic Affairs and Energy (BMWi) based on a resolution of the Deutscher Bundestag.

References

1. https://tu-dresden.de/bu/bauingenieurwesen/imb/labor/ausstattung/falltum; Retrieved 14.10.2019
2. M. Hering, T. Kühn, F. Bracklow, M. Curbach, *Impact experiments with reinforced concrete plates of different thicknesses*, Structural Concrete. (2019), DOI: 10.1002/suco.201900195
3. C. Cherif, Zierold, K., M. Curbach, M. Hering, *Textilverstärkte Betonkonstruktionen für Impaktbeanspruchungen* (final report : IGF 19009 BG, Dresden, 2019)

Effect of load level of corner columns on punching shear resistance of flat slabs

Michał Gołdyn[1,*], and *Tadeusz* Urban[1]

[1]Lodz University of Technology, Department of Concrete Structures, al. Politechniki 6, Łódź, Poland

1 Introduction

A crucial area in the slab-and-column structural systems is usually a support zone, where the slab, due to concentration of internal forces, is exposed to punching shear failure. In the real structures the effects acting on the support zones results not only from the load transferred from the floor slab, but also from the transmission of forces between columns of subsequent floors. Therefore, a justified question arises about the effect of the load interaction on the load carrying capacity of columns and slabs of multi-storey buildings.

Previous experimental investigations conducted at the Department of Concrete Structures at the Lodz University of Technology (i.e. [1,2]) concerning the connections of high-strength concrete columns with ordinary or lightweight aggregate concrete slabs have shown a significant effect of the slab on load carrying capacity of columns intersected by concrete of lower strength. This resulted from the limitation of lateral deformation of the joint concrete by the surrounding slab. As a result of confinement, the effective strength was increased by up to above $200 \div 300\%$ with respect to uniaxial stress state. It should be emphasized that the beneficial effect of confinement of joint concrete was also observed in case of external columns – edge and corner column-and-slab connection joints.

Observations made during the tests [1] prompted the authors to consider the effect of column load on the resistance of the slab. On the one hand, lateral deformations of the joint concrete will lead to the formation of normal (compressive) stresses in the cross-section of the slab. On the other hand, they will cause additional tensile forces in the longitudinal reinforcement and thus lead to its yielding at lower slab load levels. Therefore, an important question arises about the effect of the column load on the punching shear resistance of the slab. Despite the significance of the issue, it has not yet been fully explained. An analysis of the available literature demonstrated that such a problem was considered only by *Guidotti* et al. [3]. However, these studies covered only internal connections, when an increase in the punching shear resistance due to the membrane action should be expected.

2 Experimental investigations

The need to supplement the current state of the art was the premise for the authors to undertake experimental investigations on the effect of external columns load on the punching shear resistance of flat slabs. As part of the first research series, three models of corner column-and-slab connection joints, made on a scale, were casted. They constituted 140 mm thick slabs connected with columns of 200 × 200 mm cross-section and a height of 1340 mm. The slabs were made from ordinary concrete with compressive strength $f_{cm} = 28.9$ MPa, while the columns of concrete with $f_{cm} = 45.5 \div 55.0$ MPa. The elements were tested in a test setup specially designed for this purpose, enabling independent loading of the column and the slab. The only variable parameter was the column load (F_{col}), which was equal to 500 kN

* Corresponding author: michal.goldyn@p.lodz.pl

(MN/1.25/L), 1000 kN (MN/1.25/M) and 1500 kN (MN/1.25/H). The load was applied on the slab by means of a transverse beam, with a constant eccentricity of $e = 1.25c$ (where c is the side length of the column).

In the initial phase of the test, only column was loaded. The increase in column load resulted in lateral deformation of the joint concrete and the occurrence of tensile forces in the longitudinal reinforcement – see Fig. 1. The average strains of the reinforcement passing within the column contour were proportional to the column load and equal to ε_{init} = -0.01, 0.08 and 0.26 ‰, respectively.

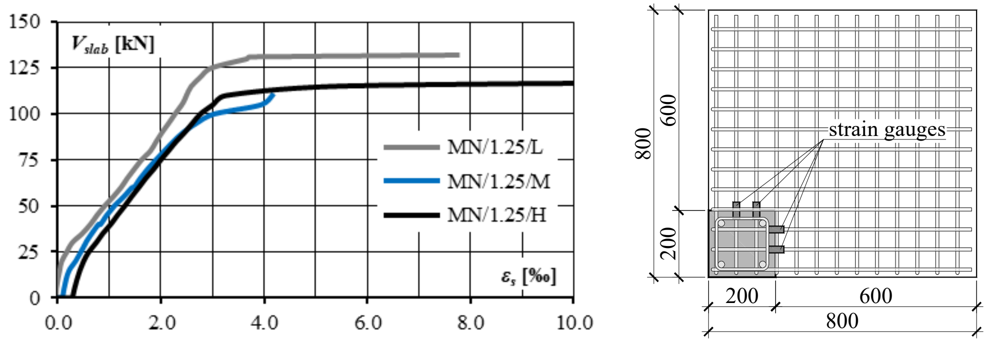

Fig. 1. Mean strains of the slab longitudinal reinforcement and location of the strain gauges.

In the next phase of the test, the load applied on the column remained unchanged, while only the slab load was increased. Considering Fig. 1, it can be seen that the initial load of the column did not affect the intensity of the strain increase rate in the reinforcement, however, it determined the moment of its yielding. In case of MN/1.25/L specimen, the reinforcement yielded at a load of about V_{slab} = 125 kN, which was about 20 ÷ 25% higher compared to the other two elements. This also translated into differences in the destructive forces, which were equal to 130, 120 and 118 kN, in the case of the elements MN/1.25/L, MN/1.25/M and MN/1.25/H, respectively.

3 Conclusions

The results of the first series of the experimental investigations demonstrated that column load level can affect the punching shear resistance of flat slabs also within external support zones. This results from lateral deformation of joint concrete, which causes additional tensile forces in the slab reinforcement. In the presented study, however, the effect of the column load was not significant and resulted in a reduction of punching shear resistance of the slabs by about 9% when increasing the column load from 500 to 1000 kN.

References

1. T. Urban, M. Gołdyn, *Behaviour of Eccentrically Loaded High Strength Concrete Columns Intersected by Lower Strength Concrete Slabs*, Structural Concrete, **4** (2015)
2. M. Gołdyn, Ł. Krawczyk, T. Urban, *Carrying Capacity of Axially Loaded HSC Concrete Columns Intersected by NSC Slab*, ACEE Journal, **3** (2015)
3. R. Guidotti, M. Fernández Ruiz, A. Muttoni, *Crushing and flexural strength of slab–column joints*, Engineering Structures, **3** (2011)

Influence of the interface reinforcement in the support zone on static performance of concrete composite T-shaped beams

Łukasz Jabłoński[1,*], and *Anna* Halicka[1]

[1]Lublin University of Technology, Faculty of Civil Engineering and Architecture, Nadbystrzycka 40, Lublin 20-618, Poland

1 Introduction

Authors have already conducted research on T-shaped composite beams, in which they analyzed the interface location on the performance of such beams. This paper describes the next stage of the mentioned research, which involves enlargement the test variants of the beams with the interface between the web and the flange. Initially 3 series of tests were carried out (Jabłoński, Halicka 2015). The current extension of the study involves the construction of two subseries of the (S2) beams with joining stirrups, and with removed adhesion (chemical and mechanical) at the interface. On the basis of the results and the fib Model Code 2010 methodology, the parametric study is carried out.

2 Elements investigated and tests

Elements were prepared in two stages. In the first stage the web was prepared and after 14 days a top slab was cast. The interface surface was prepared by vibrating the concrete mixture during the molding process, then was modified by a chemical agent breaking the adhesion or a PVE membrane. In the subsequent series, the joining reinforcement ratio ρ_i was varied.

The arrangement of interface in particular series was as follows:

- BZ/P+S – reinforced interface (ρ_i= 0.21%) with adhesion,
- BZ/P – nonreinforced interface with adhesion,
- BZ/S1 – reinforced interface (ρ_i =0.21%) with limited adhesion (chemical agent),
- BZ/S2 – reinforced interface (series BZ/S2/A ρ_i =0.21%, series BZ/S2/B ρ_i =0.42%) with completely broken adhesion using utilization of PVE membrane.

The beams were tested as simply supported in four-point test.

3 Results

The cracks morphology was investigated by documenting the cracks appearance on two beams of each series. Characteristic crack patterns for representative beams from various series after destruction were documented.

Measurement of deflection was carried out using the LVTD gauges. Figure 1 shows a load-deflection curve for the representative beams of each series.

Strain of reinforcement bars was measured by the electric strain gauges arranged on the stirrups and main bar. The increase in the strain of the main reinforcement along with the increase of the load was shown and similar charts for the stirrups were shown. Only the BZ/S2/B series (no adhesion, higher reinforcement ratio) have reached the yield stress, which

* Corresponding author: l.jablonski@pollub.pl

has a direct effect on the mixed nature of the destruction (shear with bending). With a lower degree of reinforcement, under the same adhesion conditions (BZ/S2/A series), the yield stress was not reached; the beam was destroyed by shear. Characteristic for the BZ/S2/B series is also the activation of the stirrups in the constant momentum zone Stirrups in the other beams achieved little strain values in this zone.

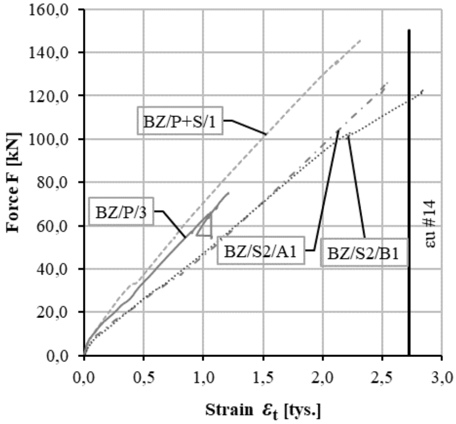

Figure 1. Representative strain values of the main reinforcement from each series tested.

4 Analysis of results

The results were compared with the theoretical forces calculated according to fib Model Code 2010, at which cracking and load bearing capacity occurs. Moreover, dependence on the reinforcement ratio in the interface was compared to the theoretical one.

5 Conclusions

Based on the studies and analyzes carried out, it can be stated that:

1. Interface without adhesion component activate the static performance of the stirrups along all interface length, even in the constant moment zone of beam.
2. Increasing the reinforcement ratio increase the load bearing capacity of the composite beams in case of the interface crack also. In spite of the eliminated adhesion in the interface of the BZ/S2/B series (with higher stirrups ratio), the destructive forces were achieved similar to the values obtained by the beams with adhesion in the interface.

References

1. Jabłoński Ł. 2014. Budownictwo i Architektura **13(3)**, 95–102 (2014)
2. Jabłoński Ł., Halicka A., Inżynieria i Budownictwo **7**, 362–365 (2015)
3. Halicka A., Jabłoński Ł., Proceedings of the Institution of Civil Engineers – Structures and Buildings **169**, 67–75 (2016)

The importance of shaping the length of buildings in the context of stresses in the structure caused by mining substrate deformations

Łukasz Kapusta[1], and *Leszek* Szojda[2,*]

[1]Department of Geotechnics and Roads, Silesian University of Technology 44-100 Gliwice, Poland
[2]Department of Structural Engineering, Silesian University of Technology 44-100 Gliwice, Poland

1 Introduction

The urban buildings of the agglomeration of Upper Silesia have developed over the centuries and at present a large part of residential buildings date back to the beginning of the 20th century. The significant increase in housing construction dating back to this period was connected with the dynamically developing heavy industry, in particular mining. The buildings erected at that time were usually maladapted and protected against the influence of ground deformations caused by the settling area after mining exploitation. One of the few methods that were used at that time was the division of a structure into smaller segments, which allowed for limiting the increase of internal forces in the event of ground deformations.

2 Background

Substrate deformations caused by mineral exploitation were classified as continuous and discontinuous [1]. Continuous deformations occurring in the majority of cases were described by the relationships given in Budryk-Knothe theory [2]. The theoretical basis for the behavior of building structures under these influences was given by Budzianowski [3]. Determining the actual values of the impact directly on a structure is no longer unambiguous and depends on many factors, which include the rigidity of the structure and the properties of the ground at the place of foundation. This provided the basis for measuring the deformed ground and the responses of the deformed buildings. The location of the structures subjected to measurements in this case was such that the direction of the revealed deformations was parallel to the longer axes of the buildings.
Because the operating period of the coal-bed exploitation was known and the surrounding area as well as the objects themselves were measured, the benchmarks were stabilized in the ground directly at the building and on the longitudinal walls above the ground level. The measurements were being carried out as the deformations were revealed, which allowed for determining horizontal deformations of the ground and the curvature of the terrain, as well as the curvature of the building structures. Figure 1 shows the location of the measuring points on one of the buildings and the adjacent measuring line. An inventory of the damage to the structures was also made before and after the appearance of all the influences. This became the basis for confirming the validity of the results of the numerical analysis.

* Corresponding author: leszek.szojda@polsl.pl

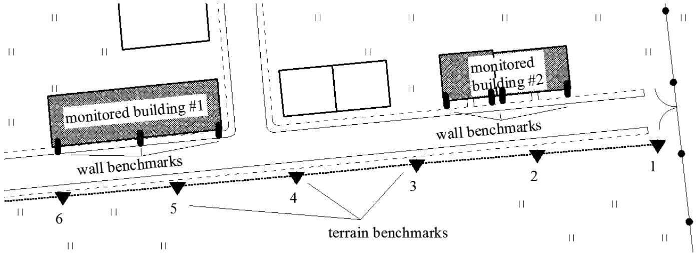

Fig. 1. Location of field points.

3 Assumptions made for the numerical analysis

Two buildings were subjected to the numerical analysis. The first of the buildings consisted of one segment and had projection dimensions 44.3 x 11.8 m, while the other was a two-segment one with projection dimensions respectively 12.7 x 10.7 m and 17.4 x 10.1 m. Both buildings had similar wall construction material (brick wall) with a wooden structure of the above-ground floor and roof. A schematic projection of repetitive floors is shown in Fig. 2.

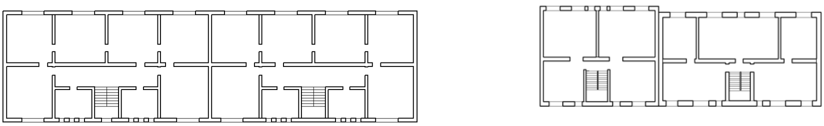

Fig. 2. Projection of the repetitive stories for monitored buildings.

Strains of objects caused by deformations of the ground were applied to the lower parts of building structures not directly, but through elements enabling the real behavior of the building to be taken into account. The magnitude of the impacts, i.e. the horizontal deformation e and the curvature of the terrain K, was assumed on the basis of own field measurements. The numerical calculations were carried out in the commercial Athena Science software package.

4 The results of the numerical analyzes

The results of the numerical analyzes were presented in the form of colored stress maps in the walls. Due to the nature of terrain deformation strains, an increase in horizontal normal stresses s has been found. The increase in these stresses depends on the length of the structure and is located in the upper parts of the wall. The highest stresses occur in a longer structure in the event of convex curvature of the terrain and horizontal terrain deformations of a stretch nature. The obtained results were confirmed by finding wall damage in places of the highest concentration.

References

1. Popiołek E., *Ochrona terenów górniczych*, Wydawnictwo AGH, Kraków 2009
2. Knothe S., *Równanie profilu ostatecznie wykształconej niecki osiadania,* Archiwum Górnictwa i Hutnictwa, 1953, t.1, z.1
3. Budzianowski Z., *Działanie wygiętego podłoża na sztywną budowlę znajdującą się w obszarze eksploatacji górniczej*, Inżynieria i Budownictwo, nr 6 i 7, 1964

Evaluation of seismic performance measures for MDOF RC structures subjected to simulated and real ground motions

Shaghayegh Karimzadeh[1], and *Ahmet* Yakut[1,*]

[1]Civil Engineering Department, Middle East Technical University, Ankara, Turkey

1 Introduction

Nonlinear time history analyses of structures require full time series of ground motion records. For regions with sparse seismic networks or potential large earthquakes, ground motion simulation techniques have gained more attention in recent years. Simulated records are required to be generated using regional input dataset and then verified against existing recorded ground motions corresponding to past events. To use simulated ground motions in engineering applications, estimation of reliable structural seismic demand parameters is essential. Since different characteristics of input excitations influence alternative structural performance measures, it seems necessary to examine their efficiency in estimating the structural demand parameters. To accomplish this, as a case study, the real and simulated records of the 2009 L'Aquila, Italy earthquake with moment magnitude of 6.3 are investigated herein employing two alternative simulation methods (i.e.: Stochastic and Hybrid). In the first step, misfits are evaluated for alternative seismological measures (e.g.: peak values, duration and frequency as well as energy content of the time histories). Next, varying multi-degree-of-freedom reinforced concrete structures with different number of stories are selected. Numerical models of the structures are generated in OpenSees platform. As the seismic performance measure, inter-story drift ratio of the selected structures is assessed through nonlinear time history analyses for both the real and simulated ground motions. Then, the misfits are estimated in terms of structural demand parameters. Results of this case study reveal a good agreement between the seismological and engineering demand misfits for the selected ground motion simulation approaches.

2 Methodology

In this study, the observed and simulated time histories from the hybrid integral composite (HIC) and stochastic finite fault (SFF) approaches corresponding to the 2009 L'Aquila earthquake with Mw = 6.3 are employed (Gallovic and Brokesova, 2007; Motazedian and Atkinson, 2005). To check the efficiency of simulations in estimating the real seismic performance measures, a total of nine symmetric RC frame structures with varying fundamental periods are considered. All frames are modeled in OpenSees platform using nonlinear fiber-based beam-column elements along with Kent-Scott-Park concrete and steel with strain hardening ratio of 0.005. The selected frames, F1, F2, F3, F4, F5, F6, F7, F8, and F9 have, respectively, the fundamental period of 0.47, 0.72, 0.53, 0.69, 0.49, 0.78, 0.52, 1.05, and 1.3 seconds. As the seismic performance measure, maximum interstory drift ratios are calculated for all frames subjected to the ground motions.

* Corresponding author: ayakut@metu.edu.tr

3 Results

For evaluation of the observed and simulated ground motion record sets, in this study, logarithmic misfits are defined in terms of both seismological and structural demand measures. For this purpose, misfits are first evaluated in terms of different seismological parameters: Fourier Amplitude Spectrum (FAS), PGA, Peak Ground Velocity (PGV), PGV to PGA ratio (PGV/PGA), Arias Intensity (I_a), Cumulative Absolute Velocity (CAV), and Significant Duration (t_{eff}) defined as the time interval of 5% – 95% of the accumulated I_a. Next, misfits are investigated for the maximum inter-story drift ratios of the selected buildings. The misfits are calculated using the following formula:

$$Misfit=log(Simulated\ Value/Real\ Value) \quad (1)$$

The results in terms of logarithmic misfits for some selected seismological parameters and frame structures are provided in Fig. 1. From this study it can be seen that there is generally consistency between the structural logarithmic misfits and seismological logarithmic misfits.

(a)

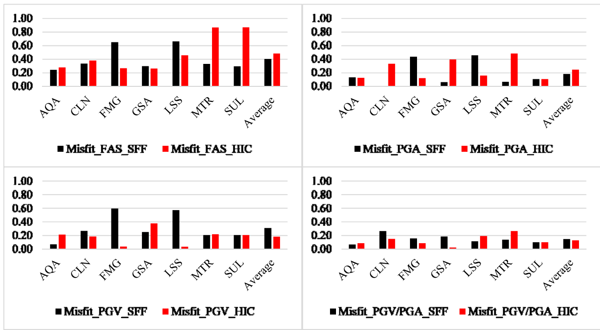

(b)

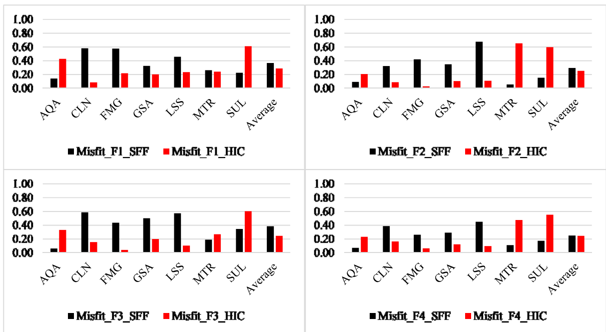

Figure 1. (a) Seismological, (b) structural logarithmic misfits.

References

1. F. Galloviç, and J. Brokešová. Phy.s Earth Planet, **160**, 34–50 (2007)
2. D. Motazedian, and G.M. Atkinson. B. Seismological Soc. Am., **95**, 995–1010 (2005)

Critical stress regarding to buckling of cylindrical concrete tanks due to prestressing

Bartosz Kawecki[1,*], *Anna* Halicka[1], and *Jerzy* Podgórski[1]

[1]Faculty of Civil Engineering and Architecture, Lublin University of Technology, Poland

1 Introduction

For the stability analysis of concrete structures two approaches are possible. The precise one constitutes the non-linear second-order analysis based on standard "σ_c-ε_c" relationship with tangent concrete modulus. The simplified methods based on the mean value of secant concrete modulus are also used.

In the Eurocode 2-1-1 buckling is defined as the failure of a member or structure due to instability under perfectly axial compression and without transverse load. "Pure buckling" understood in such a way is not a relevant limit state in real structures, because of imperfections and transverse loads. Therefore the use of simplified methods recommended by EC2-1-1 – nominal stiffness method and nominal curvature method, are reasonable only for structural elements under uniaxial load (e.g. columns and walls). In the case of 3D structures under biaxial or triaxial load the simplified methods are inappropriate.

Concrete cylindrical tanks and silos are the 3D structures. The possibility of their buckling arise mainly due to prestressing. The question is which simply procedure may be used by designers for buckling possibility assessment.

The expressions dedicated for calculation of the meridional critical stress in axially loaded cylinders and the critical values of external perpendicular stress (without axial force) causing the ovalization of circular cross-section can be found in the theory of elasticity.

The expressions were compiled and numerically verified by authors [1] for cylinders of geometrical parameters and boundary conditions typical for concrete tanks. They cannot be directly introduced for concrete tanks analyses because of biaxial load in the one hand and changes in modulus of elasticity along with load increase in other hand.

The concrete tanks and silos are prestressed in order to avoid vertical cracks due to pressure of liquid or solid material by relatively thin concrete walls. The hoop prestress value is established on the basis of balance of internal pressure and external prestress. This is treated as the persistent design situation. Nevertheless before filling the stored material, the transient design situation takes place and the biaxial compression arise. The walls are compressed meridionally (vertically) by self-weight and roof reaction (including roof weight and technological devices located on it), whereas the hoop (horizontal) compression is caused by prestressing.

Hoop prestress alone is not a reason of the stability loss and buckling because the tendons route follows the ovalization of cross section. It influence however the value of meridional critical force. The higher prestress – the lower meridional critical force.

The authors executed and presented below the numerical analysis of the hoop compression influence on the tank stability, assuming that compression is caused by prestressing. The Simulia Abaqus software [2] was used and the nonlinear constitutive relation for concrete with

* Corresponding author: b.kawecki@pollub.pl

Concrete Damaged Plasticity model [3]. An incremental approach was applied to searching for critical forces values causing loss of structural stability [4].

2 The results of calculation

The results of calculation are compiled in the form of relationship between two parameters. The first parameter constitute the ratio of the lateral pressure q (value of uniform prestress distribution or maximum value of linear distribution) to the vertical pressure σ exerted onto the upper edge. This ratio may also be expressed use of unitary vertical force P_v applied to the wall of t thickness:

$$\omega = \frac{q}{\sigma} = \frac{q\,t}{P_v}; \qquad\qquad P_{\text{crit}} = \mu_{\text{crit}} \frac{\mathrm{E}_t\, t}{r\sqrt{3(1-\nu^2)}} \cdot 10^{-3}$$

The second parameter constitute coefficient μ_{crit} describing the critical vertical pressure exerted to the upper edge of tank. This form may be used in design process: knowing the ω ratio one can find the critical value of vertical stress easily.

The concrete tank of the dimensions typical for cement silos was modeled: 15 m in diameter, 30 m in height and wall thickness of 20 cm. Concrete of C25/30 was considered therefore the E_{cm} = 30 GPa and f_{cm} = 28 MPa.

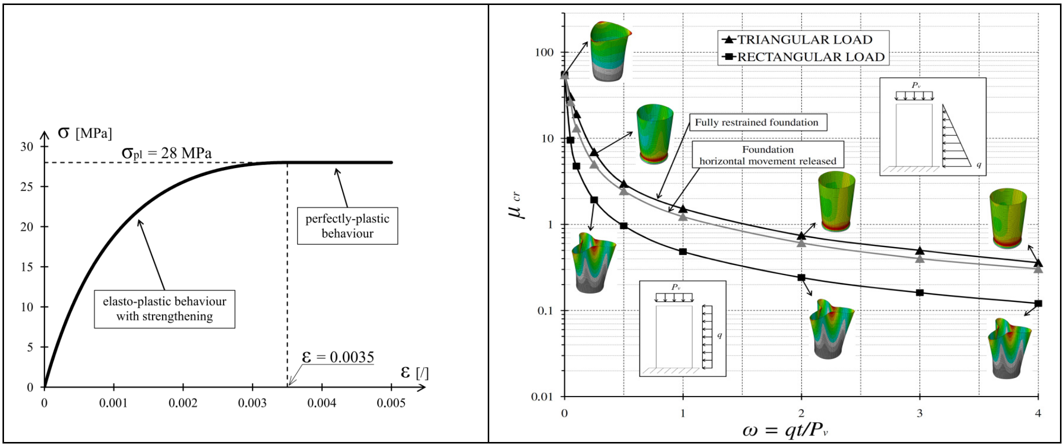

Fig. 1. The "$\omega - \mu_{\text{crit}}$" relationship of the 1st buckling modes for the wall fixed in foundation (without regard of self-weight under the uniform (rectangular) and linearly changing (triangular) prestress.

References

1. A. Halicka, J. Podgorski, "Designing of cylindrical concrete tanks with regard to buckling and second order effects", Procedia Engineering, Elsevier, 2017, vol. 193, pp. 50–57
2. Simulia Abaqus 2018 (https://www.3ds.com/products services/ simulia/products/ abaqus/latest-release/)
3. Lubliner J., Oliver J., Oller S, Ońate E.: A plastic-damage model for concrete, International Journal of Solids and Structures, Vol. 25, 1989, pp. 299–329.
4. Riks E. (1979), "An incremental approach to the solution of buckling and snapping problems", Int. J. Solids Struct., 15:524–551

Nonlinear analysis of lightweight aggregate concrete columns

Ewelina Kołodziejczyk[1,*], and *Tomasz* Waśniewski[1]

[1]Lodz University of Technology, Department of Concrete Structures, Lodz, Poland

1 Introduction

Lightweight aggregate concrete (LWAC) in structural applications is usually identified with its brittle behaviour that is an unfavourable feature in reinforced concrete structures. It is also connected with low elastic modulus causing high deformations. All these parameters play an important role in the performance of slender elements subjected to bending and axial force. However, experimental data concerning the problem of second-order effects in LWAC columns are rare in literature and concerns the narrow scope of the issue [1–3]. In this paper, numerical analysis of deformability and load-bearing capacity of this kind of elements, led in line with Eurocode 2 [4] requirements, is presented. Parametric study focused on the influence of assumed concrete density on its material properties acc. to EC2 and as a result, structural behaviour considering different values of concrete strength, slenderness and eccentricity of force.

2 Modelling assumptions

The parametric analysis was conducted in OpenSees, an open-source finite element software for simulating the nonlinear response of structural elements.

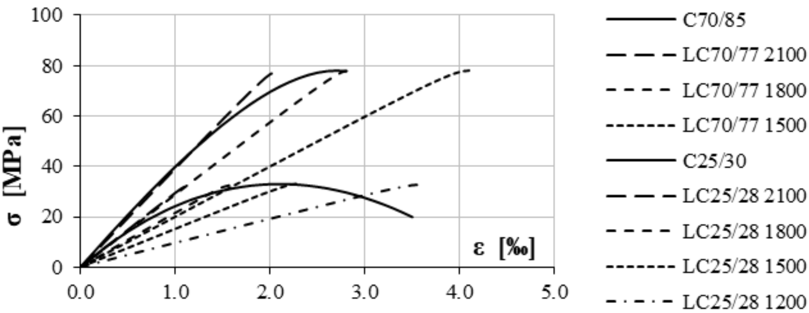

Figure 1. Concrete stress-strain law.

Nonlinear stress-strain model depicted in Figure 1 was assumed for concrete. Two different concrete strength f_{cm} values of 33 MPa and 78 MPa and several different oven-dry densities were considered in the simulations. ElasticMultiLinear material was used as the stress-strain law for concrete. The nonlinear stress-strain relationship is given by a multi-linear curve that is defined by a set of points which were calculated acc. to EC2 nonlinear model. Steel01 bilinear steel material without hardening was applied in relation to the main reinforcement. Square cross-section of the column was analysed as fiber section. Reinforced concrete members were

* Corresponding author: ewelina.kolodziejczyk@p.lodz.pl

modelled by *nonlinearBeamColumn* elements. The static scheme of a cantilever column under eccentric loading is studied. Corotational coordinate transformation is used to consider geometric non-linearity of the model. Two different column slenderness cases and two eccentricities ware assumed.

3 Results and conclusions

First part of the analysis concerns the load-bearing capacity of the cross-section. The results are presented in the form of interaction *N-M* curves in relation to different concrete strength. Significant impact of limit strain of concrete on obtained values of maximum force and moment is visible. The example results are presented in Figure 2.

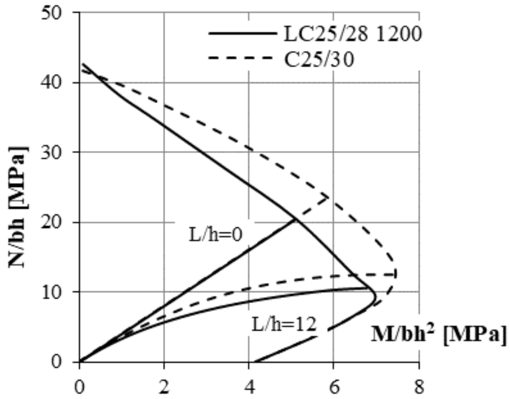

Figure 2. Interaction diagrams for C25/30 and LC25/28 1200 concrete section, *M-N* diagrams for columns with slenderness L/h = 12 and without second-order effect (e/h = 0.25, ρ_L = 2%, f_{cm} = 33 MPa).

In the second part of the parametric study, we focused on the second-order response of the elements. Diagrams of axial force to the displacement of the end of the column showed that LWAC columns reach higher displacement which leads to the decrease in maximum force. The effect is more significant as the density decreases and the slenderness of the columns increases.

References

1. M. Tawfik, S. Elwan, H. Seleem, i A. Abdelrahman, „Behavior of lightweight concrete columns under eccentric loads (Parametric study)", *Al-Azhar University Civil Engineering Research Magazine (CERM)*, vol. 40, no 1, p. 67–81 (2018)
2. M. Tawfik, S. Elwan, H. Seleem, i A. Abdelrahman, „Behavior of lightweight concrete under uniaxial eccentric compressive stresses", *International Journal of Engineering Research and Development*, vol. 13, no 9, p. 15–27 (2017)
3. D. Galeota, M. M. Giammatteo, i A. Gregori, „Ductility and strength in high-performance lightweigth concrete columns", *13th World Conference on Earthquake Engineering*, Vancouver, no 3414 (2004)
4. European Committee for Standarization. EN 1992-1-1, Eurocode 2: Design of concrete structures – Part 1-1 : General rules and rules for buildings, t. 1. Brussels (2004)

Analysis of selected shear strength models based on research of beams without stirrups

Renata Kotynia[1], and *Monika* Kaszubska[1*]

[1]Faculty of Civil Engineering, Architecture and Environmental Engineering, Lodz University of Technology, Lodz, Poland

1 Introduction

The analysis was performed for two different models (Zhang, Oehlers, and Visintin 2014) and (Yang 2014). The undoubted advantage of the first model (Zhang, Oehlers, and Visintin 2014) is its universality and possibility using for elements without transversal reinforcement with steel and FRP longitudinal reinforcement. The basic assumption of the model is initiation on shear, which begins with a diagonal cracking of the beam. After cracking, the crack width increase and diagonal crack develops towards the upper edge of the beam. Failure occurs when the slope of this crack will reach the limit angle at which both edges of the diagonal crack slip. The basis of the second model by (Yang 2014) is an analysis of the diagonal crack development. The vertical displacement of the crack edge caused by its opening does not activate the aggregate interlock mechanism to transfer shear force. The additional vertical displacement resulted by the secondary horizontal branch of the crack development is considered in this analysis. The load increase causes development of cracks at the reinforcement level and proceeds sudden and uncontrolled increase in the crack width and loss of the shear capacity provided by the aggregate interlock. The shear capacity according to the Yang's model is ae sum of shear forces transferred by the uncracked compression chord, across web cracks and by the dowel action in the longitudinal reinforcement.

2 Experimental program and analysis

The experimental program was composed of 29 T-section single span and simply supported RC beams reinforced with steel and GFRP bars, which in part was reported in (Kaszubska, Kotynia, and Barros 2017; Kaszubska et al. 2018). The computational models discussed in this paper was applied to elements without stirrups failed in typical shear – tension. To assess the agreement between calculated and experimental results the coefficient $\eta = V_{max}/V_{cal}$, where V_{max} – the maximum shear force from experimental test and V_{cal} – the shear force calculated according to analysed models. The results corresponding to values $\eta < 1$ indicated the overestimation of the shear strength, because they overstate the experimental results. Results corresponding to $\eta > 1$ means low values of shear load capacity, which confirms conservative approach of verified model (Fig.1).

[*] Corresponding author: monika.dymecka@p.lodz.pl

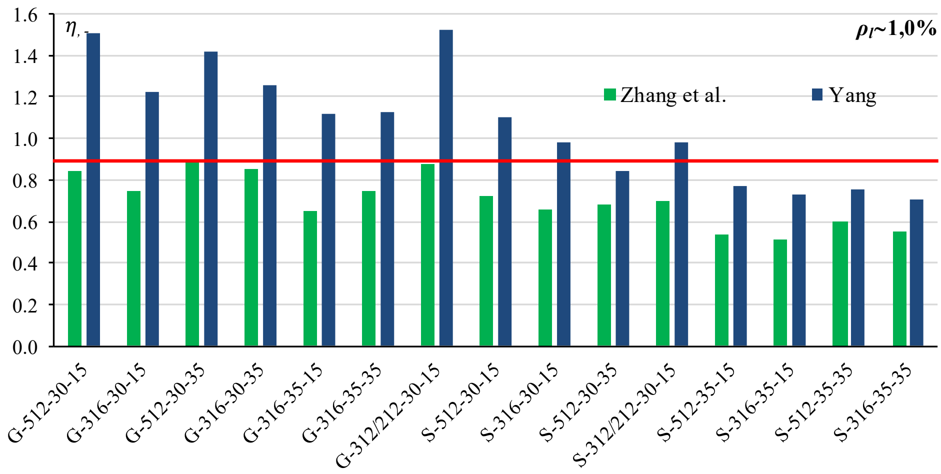

Fig. 1. The coefficient η for beams with ρ_l~1.0%.

3 Results

In the generalized assessment of shear models without division into a type of longitudinal reinforcement, the model by (Yang 2014) turned out more conservative in contrast to the model by (Zhang, Oehlers, and Visintin 2014). The average value of the coefficient for first mentioned model is η_m = 1.09, while for second model η_m = 0.70. Application of these calculation models to the beams reinforced with GFRP bars did not reduce the theoretical values of shear capacity, unlike, the η coefficient was usually higher in the GFRP reinforced beams than in the corresponding RC beams.

References

1. M. Kaszubska, R. Kotynia, J.A.O. Barros. Influence of Longitudinal GFRP Reinforcement Ratio on Shear Capacity of Concrete Beams without Stirrups. Procedia Engineering. 193 (2017)
2. M. Kaszubska, R. Kotynia, J.A.O. Barros, H. Baghi. Shear Behavior of Concrete Beams Reinforced Exclusively with Longitudinal Glass Fiber Reinforced Polymer Bars: Experimental Research, Structural Concrete 19, 1, 152–61 (2017)
3. Y. Yang, Shear Behaviour of Reinforced Concrete Members without Shear Reinforcement, a New Look at an Old Problem. PhD Thesis. Delft University of Technology (2014)
4. T. Zhang, D. J. Oehlers, P. Visintin. Shear Strength of FRP RC Beams and One-Way Slabs without Stirrups, Journal of Composites for Construction 18, 5 (2014)

Example of modelling concrete corbel using Finite Elements Method

Łukasz Krawczyk[1,*], and *Tadeusz* Urban[1]

[1]Department of Concrete Structures, Lodz University of Technology, 90-924 Łódź, Poland

1 Introduction

In the paper results of concrete corbel numerical calculation are presented. The geometry of the element refers to corbel which was experimentally investigated in Lodz University of Technology [1–3]. In the paper comparison between results obtained during element testing and modelling is made.

2 Corbel geometry and calculation model

The height of element was equal 450 mm and the width was 250 mm. Two bars 16 mm diameter were used as a main reinforcement and stirrups were made of 6 mm bars. In the column four bars 20 mm diameter and seven stirrups were used. The compressive strength of concrete was 47.3 MPa. The calculation model represents a half of described corbel, see Fig. 1. Models with different size of finite elements are used. Comparison between different models of concrete and bonding of steel reinforcement is presented.

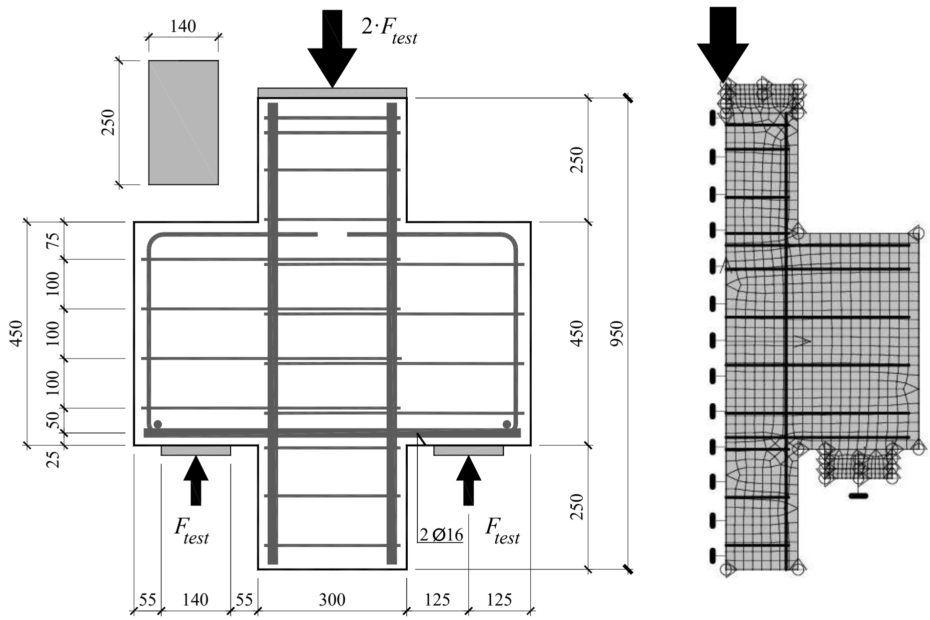

a) b)

Fig. 1. E – 0 corbel a) geometry and reinforcement, b) calculation model.

* Corresponding author: lukasz.krawczyk@p.lodz.pl

3 Results

During experimental test surface of the corbel was registered by Digital Image Correlation (DIC), so it is possible present results connected with displacement and strain of concrete surface [4]. Similar results can be generated by FEM calculation. Comparison between principal maximum strain of E – 0 corbel obtained by DIC and FEM is shown in Fig. 2.
Some comments refer to the other numerical calculation [5–7] are included in the paper.

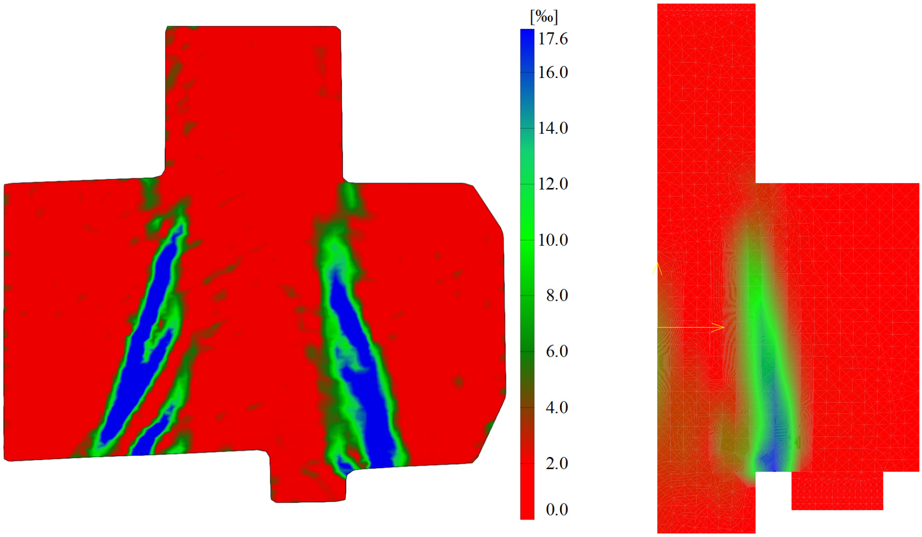

a) b)

Fig. 2. Principal maximum strain of E – 0 corbel a) Digital Image Correlation (DIC), b) Finite Elements Method (FEM).

References

1. Krawczyk Ł. Strengthening of short corbels with embedded through-section reinforcement, (in Polish) PhD thesis, Technical University of Lodz, Poland, (2017).
2. Urban T., Krawczyk Ł. Strengthening corbels using post-installed threaded rods, Structural Concrete, 304–315 (2017)
3. Urban T., Krawczyk Ł., Gołdyn M. Experimental investigations of strengthening of very short reinforced concrete corbels (2016)
4. Krawczyk Ł., Gołdyn M., Urban T. Digital Image Correlation Systems in the Experimental Investigations: Capabilities and Limitations, Archives of Civil Engineering 65, 171–180 (2019)
5. El-Maaddawy T.A., Sherif E.S.I. Response of Concrete Corbels Reinforced with Internal Steel Rebars and External Composite Sheets: Experimental Testing and Finite Element Modeling. Journal of Composites for Construction, 18
6. Canha R.M.F., Kuchma D.A., El Debs M.K., de Souza R.A., de Souza R.A. Numerical analysis of reinforced high strength concrete corbels. Engineering Structures, 74, 130–144
7. Syroka E., Bobiński J., Tejchman J. FE analysis of reinforced concrete corbels with enhanced continuum models. Finite Elements in Analysis and Design, 47, 9, 1066–1078, 2011

Experimental issues on concrete at high loading velocities

Tino Kühn[1,*], *Marcus* Hering[1], and *Franz* Bracklow[1]

[1]TU Dresden, Institut für Massivbau, Germany

The presented work analyses questions of speed effects in the high dynamic determination of concretes properties. The original idea of a cross-scaled numerical analysis of velocity effects and the integration of these findings into a meso- and macroscopic FEM model has been abandoned in favour of a detailed experimental study of the so called strain rate influence. It became quite clear that the causes of many of these velocity effects can be found in the experimental environment and the underlying assumptions, rather than in the reaction of the material. For this reason, the author provides parameters and a detailed analysis of possible causes that may lead to the misinterpretation of those material reactions. He assumes that the classical strain-rate effect is a purely structural property that has nothing to do with a reaction on the material level.

1 Can we trust Split Hopkinson Bar tests on a brittle concrete?

This question is the guiding principle for more than 3000 experiments on different concrete crates, which were carried out in the context of a dissertation within the last years. Rising loading speeds causes increasing strain rates in concrete. As a rule, areas of lower and higher strain rates are distinguished. For both areas different physical reasons are assumed. For smaller strain rates up to approximately 1 1/s, viscous effects in the concrete matrix or moisture redistribution in the pores lead to increased load capacity. At higher strain rates of approximately 100 1/s, inertia effects come to the foreground. The cracks open delayed and thus cause a seemingly higher load capacity. This main hypothesis are based on a large number of highly dynamic studies from the last decades assuming the validity of the experiment. But can we really trust them? Within the presentation we will discuss several aspects on this topic.

2 Logarithmic or linear scaling the DIF results?

In his approach, the author consciously decides to look beyond the box and critically scrutinizes established methods such as the biaxial course of the strength in the famous DIF-diagram as recommended by the CEB. A logarithmic representation of the DIFs with respect to strain-rates should be consciously avoided. The linear representation of the data leads to a straight monotonic increasing line without any steps. The bilinear assumption instead leads to misinterpretations due to the unequal data weighting. The bilinear curves shape also show unphysical behaviour at their boundaries which cannot explained by any theory.

* Corresponding author: tino.kuehn@iban-engineering.de

3 Considering inertia effects in SHB tests

The author compared existing and developed a new inertia correction method on a deeper level which, in the example experiments, leads to the entire cancelation of a strain-rate dependency of the strength. Most methods considering the strain acceleration in the specimen as driving parameter. The authors method considers the activated mass by time which is accelerated by the incident bar (Fig. 1). It leads to a straight horizontal course of the data in the following figure (Kuehn2).

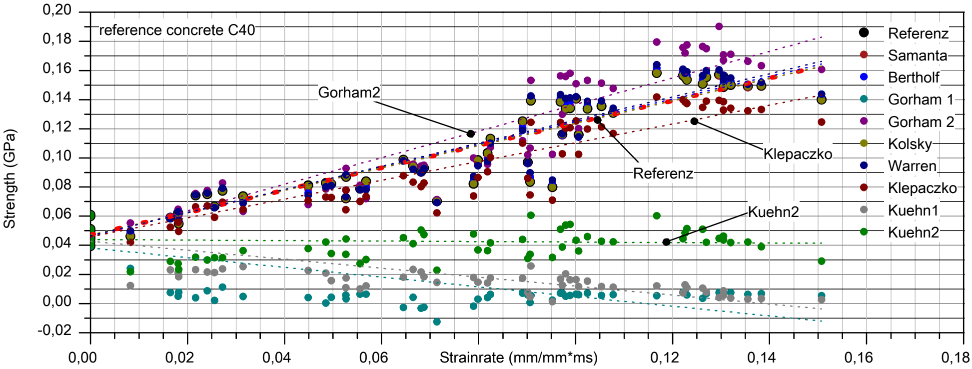

Fig. 1. Effects of several inertia correction methods applied to data of a C40 concrete type.

4 Discovering energetic overloaded specimens

An alternative testing methodology was developed which allows improved statistical evaluation of results. It resembles a fatigue testing method and it prevents the inclusion of a certain surplus of energy in the assessment of strengths. A consistent energy balances involves the kinetic energy of the resulting fragments in this evaluation. At the same time, the resulting fracture surfaces were determined and used in the evaluation of a real specific strengths and fracture energies in tension and in the quantification of damage in the compressive domain. With this method a trust worthier strength can be declared at zero damage of the specimen (Fig. 2).

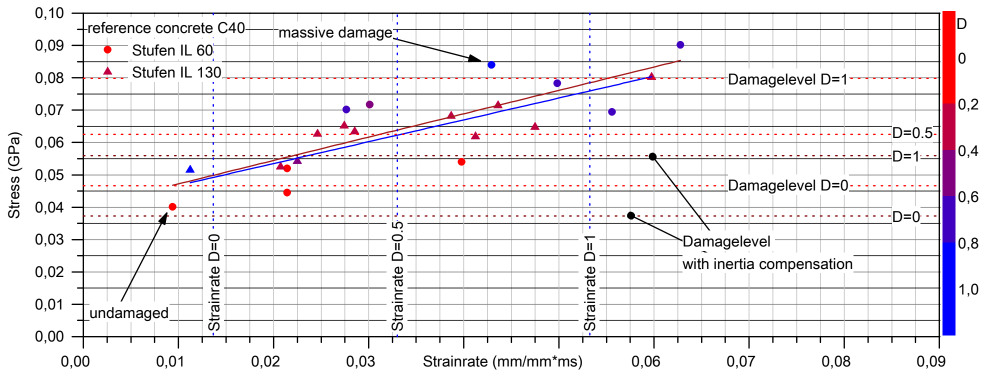

Fig. 2. Methodology to define a real specimen strength at different damage levels.

Analytical solution for the resistance of composite beams subjected to bending

Marek Lechman[1,*]

[1]Instytut Techniki Budowlanej, Department of Building Structures, Geotechnics and Concrete, 00-611 Warsaw, ul. Filtrowa 1, Poland

1 Introduction

Newly designed floor slab systems are in the recent years the subject of particular interest of many researchers due to their importance in engineering practice. The system under consideration consists of steel and concrete composite beam, named BH beam, structurally connected with prefabricated or cast *in situ* slabs [1]. The considerations of this paper are focused on the analytical solution for determining the resistance of composite beams subjected to bending. The beams under consideration consist of reinforced concrete (RC) rectangular core placed inside a reversed TT welded steel profile with the cross-section shown in Fig. 1, as an example.

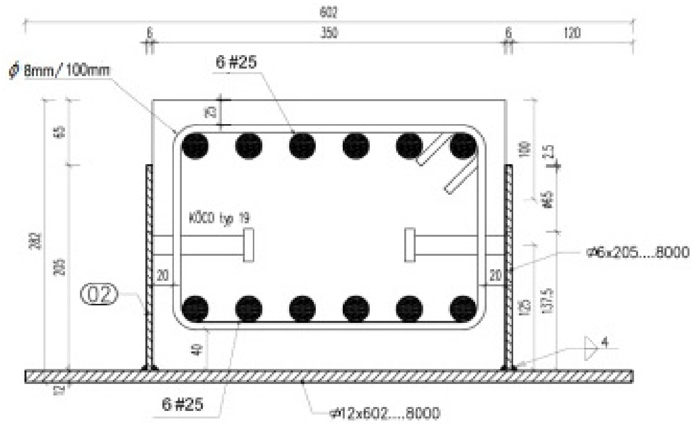

Fig. 1. The cross-section of the composite beam under consideration.

2 Derivation of formulas

The stress-strain relationship for concrete σ_c - ε_c in compression uniaxially loaded is assumed for nonlinear structural analysis according to Eurocode 2

$$\sigma_c = (k\eta - \eta^2)/(1+(k-2)\eta) f_{cm} \, , \tag{1}$$

where: $\eta = \varepsilon_c/\varepsilon_{c1}$, ε_{c1} – the strain at peak stress on the σ_c - ε_c diagram, f_{cm} – the mean compressive strength of concrete, $k = 1{,}05\, E_{cm} \left| \varepsilon_{c1} \right| / f_{cm}$, E_{cm} – secant modulus of elasticity of concrete. This stress-strain relation adequately represents the behavior of concrete by

* Corresponding author: m.lechman@itb.pl

introducing four parameters: f_{cm}, ε_{c1}, ε_{cu} and E_{cm}. For reinforcing and profile steels, characterized by yield stresses f_{yk}, f_{Hyk} , respectively, linear elastic – ideal plastic model is applied. In the presented derivation it is assumed that plane sections remain plane and the tensile strength of concrete is ignored. The resistance of the composite cross-section is reached when either ultimate compressive strain in concrete ε_{cu} or ultimate tensile strain in steel ε_{su}, or ultimate tensile strain in steel profile ε_{Hsu} is reached anywhere in that section. The normalized ultimate bending moment m_{HRm} determining the resistance of the BH beam is derived by integrating the equilibrium equation of the bending moments about the symmetry axis of the section, taking account of the physical and geometrical relationships:

$$m_{HRm} = 0,5(1+\xi_f)\, \rho_f f_{Hyk} / f_{cm}\, [\delta_{k2} + \delta_{k2+1}\, (1- 1/\xi)\, \varepsilon'/\varepsilon_{ss}\,] + \rho_s f_{Hyk} / f_{cm}\, [-0,5(1-\xi_0)+ (1-\xi_0^2)\, (0,5/\xi +1) - 1/(3\xi)(1-\xi_0^3)] + m_{Rm} \qquad (2)$$

where: $m_{HRm} = M_{HRm} / (b\, t^2 f_{cm})$, M_{HRm} – the ultimate bending moment, b, t – dimensions of the RC rectangular core, ε' – maximum compressive strain in concrete, ξ – coordinate describing the location of neutral axis, F_{Hf}, t_f – area and thickness of the lower flange, F_{Hs}, t_s – area and thickness of the web, x_0 – coordinate of the upper edge of web, $\xi_0 = x_0 / t$, $\xi_f = t_f / t$, $\rho_f = F_{Hf} / bt$, $\rho_s = F_{Hs} / bt$, $\varepsilon_{ss} = f_{Hyk} / E_s$, E_s – modulus of elasticity of profile steel, $\delta_i = ((-1)_i +1)$. The term m_{Rm} refers to the rectangular RC core and is derived in [2].

3 Comparison with experimental results

For verifying the obtained analytical solution the test was carried out on the BH beam subjected to bending, with the cross-section presented in Fig. 1. The beam of the length of 8 m was made of concrete grade C50/60, reinforcement f_{yk} = 500 MPa and profile steel f_{Hyk} = 460 MPa. It was loaded up to failure. The failure mechanism of the BH beam occurred in the form of crushing of the concrete. The partial test results are given in Table 1. According to formula (2) M_{HRm} = 634.7 kNm has been calculated. This shows good agreement between the analytical solution and the test results in ultimate bending moment.

Table 1. Strains and failure bending moment in the cross-section of the tested BH beam.

Concrete	Compressive reinforcing steel	Tensile reinforcing steel	Steel profile	Failure bending moment
ε_c [‰]	ε_{s1} [‰]	ε_{s2} [‰]	ε_{Hf} [‰]	M_u [kNm]
-3.5	-2.6	0.629	2.03	635

References

1. J. Derysz, P. Lewiński, P. Więch, Procedia Engineering 193 (2017)
2. M. Lechman, Transportation Research Procedia 14 (2016)

Complex multilevel fracture tests of concrete

David Lehký[1], *Hana* Šimonová[1,*], *Barbara* Kucharczyková[1], and *Petr* Daněk[1]

[1]Brno University of Technology, Faculty of Civil Engineering, Brno, Czech Republic

1 Introduction

The theory of concrete fracture, despite all the efforts of numerous researchers, still did not provide a clear answer to the problem of the fracture processes in concrete. Fracture energy is a fundamental fracture parameter, representing cracking resistance and ductility of concrete, and is generally considered as a material property in concrete fracture mechanics and cracking analyses. The most commonly used method for measuring the fracture energy is the work-of-fracture method recommended by RILEM (1985). However, the values determined by this method are dependent on the size and shape of the test specimen. Several researchers have analyzed this size effect on fracture energy measurements according to RILEM procedure, and they have proposed modifications to obtain size-independent specific fracture energy of concrete. Abdalla and Karihaloo (2003) showed that the same size-independent specific fracture energy can be obtained by testing only two specimens of the same size but with notches that are well separated.

When simulating the tensile cracking of concrete a softening curve is representing the relationship between the crack opening displacement and the gradual stress drop after the tensile strength. The crack band model (Bažant and Oh, 1983) and the cohesive crack model (Hillerborg, 1976) are representative approaches in practical finite element analyses for cracking. It was shown that parameters of softening models can be unambiguously identified neither from the standard size effect tests nor from the tests of complete load-deflection curve of specimens of one size. A combination of both types of tests is required. Therefore, a comprehensive test program including tests of both types made with one and the same concrete was carried out (Fig. 1).

The aim of the current research is to develop a complex multilevel approach for experimental–computational determination of mechanical fracture parameters of concrete as a typical quasi-brittle material. This includes testing, advanced evaluation and soft computing-based identification of specimens of multiple sizes in multiple test configurations and analyses of fracture processes using multiscale modeling approaches. This paper introduces the first experimental part of the whole procedure.

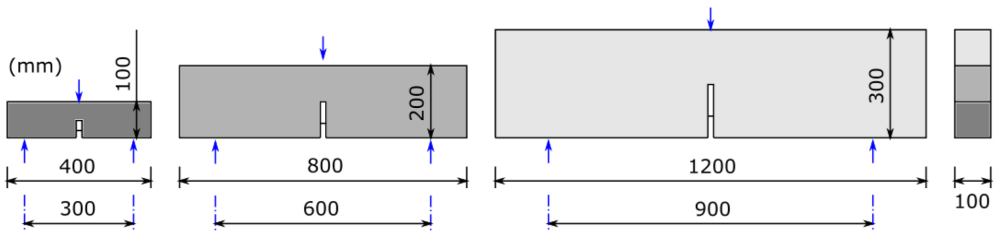

Figure 1. Specimen of three different sizes each with shallow and deep notch tested in three-point bending configuration.

* Corresponding author: simonova.h@fce.vutbr.cz

2 Fracture experiments and determination of mechanical fracture parameters

In order to more clearly verify the effect of specimen size and geometry on the fracture energy and other mechanical fracture parameters, three-point bending, and wedge splitting tests were performed simultaneously using different specimen sizes and initial notch depths. Regarding the size effect, three different specimen sizes in the ratio 1:3 were tested, see three-point bending specimens in Fig. 1. In order to follow the procedure of Abdalla and Karihaloo, specimens with two well-separated depths of notches were tested for each size and test configuration. The shallow starter notches have a relative notch depth $a/D = 0.2$, where a is the notch depth and D is the overall depth of the specimen. The value for the deep notches was 0.5. Three specimens were tested for each testing case. In total, forty-two fracture tests were performed. The outcome of each test is a load–deflection diagram, which is subsequently used for mechanical fracture parameter determination.

In order to extend the knowledge of mechanical and fracture behavior of tested concrete, compression tests, splitting tensile tests and non-destructive tests based on the resonance method for determination of dynamic modulus of elasticity were also carried out in different ages of hardening. Tested material was concrete of C30/37 strength class which is widely used in engineering practice. The maximum aggregate grain size was 16 mm. Evaluation of mechanical fracture parameters was carried out using the double-K fracture model, the effective crack model, and the work-of-fracture method. The obtained parameters are compared and discussed in relation to the identification of size-independent mechanical fracture parameters.

3 Conclusions

A comprehensive test program was performed as the first step of the development of an advanced experimental–numerical procedure in order to gain “true” fracture energy and other material parameters, which will be independent on testing configuration and specimen size. Such a set of parameters together with an appropriate numerical model can be then utilized for modeling of real size concrete structures.

This work has been supported by project MUFRAS No. 19-09491S, awarded by the Czech Science Foundation (GACR).

References

1. H.M. Abdalla, B.L. Karihaloo, Determination of size-independent specific fracture energy of concrete from three-point bend and wedge splitting tests, Mag. Concr. Res. **55** (2004), 133–41
2. Z.P. Bažant, B.H. Oh, Crack band theory for fracture of concrete, Mater. Struct. **16**, 3 (1983), 155–77
3. A. Hillerborg, M. Modéer, P.E. Petersson, Analysis of crack formation and crack growth in concrete by means of fracture mechanics and finite elements, Cem Concr. Res. **6**, 6 (1976), 773–82
4. RILEM TC-50 FM, Determination of the fracture energy of mortar and concrete by means of three-point bend tests on notched beams, Mater. Struct. **18**, 107 (1985), 287–90

Evaluation of bond properties from drop tower beam tests

Lena Leicht[1,*] *Franz* Bracklow[1], *Marcus* Hering[1], and *Manfred* Curbach[1]

[1]TU Dresden, Institute of Concrete Structures, Germany

Drop tower tests help to gain understanding about the general behavior of reinforced concrete members under impact loading and to especially investigate the bond properties. For this purpose, beam and slab specimens are usually employed. The main advantage of beams compared to slabs is that they are less complex due to the almost two-dimensional instead of three-dimensional wave propagation within them.
After the impact, shear and longitudinal waves start propagating within the beam. The longitudinal waves are the most relevant ones as for this type of wave, the direction of the wave propagation is equal to the direction of particle movement leading to stresses and strains within the specimen [1]. These waves are responsible for the typical cone failure at the bottom of the beam as the firstly compressive wave is reflected as a tensile wave on the free bottom surface.

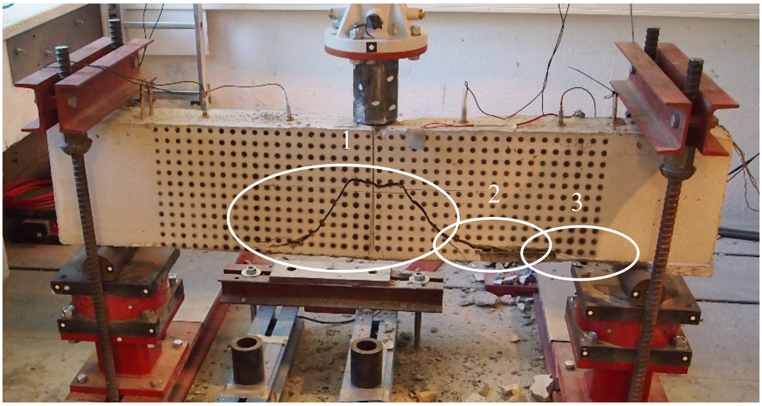

Figure 1. Test with 0.1 bar loading pressure and punching cone (Photo: F. Bracklow).

Figure 1 shows the three critical areas in beam tests. No. 1 is the mentioned punching cone which is limited to a height of approximately two thirds of the beam's height. However, the higher the velocity becomes, the more damage happens on the top surface leading to a smeared damage consisting of the shear failure on the bottom surface and lateral spalling off of the concrete on the upper side of the beam (see Fig. 2). Area number 2 is characterized by spalling off of the concrete cover due to the untying of the cone. Lastly, area 3 is marked by the end anchorage of the reinforcement bars, which is uncritical for small cones which guarantee large anchorage lengths but can become critical for large cones with small anchorage lengths.

* Corresponding author: lena.leicht@tu-dresden.de

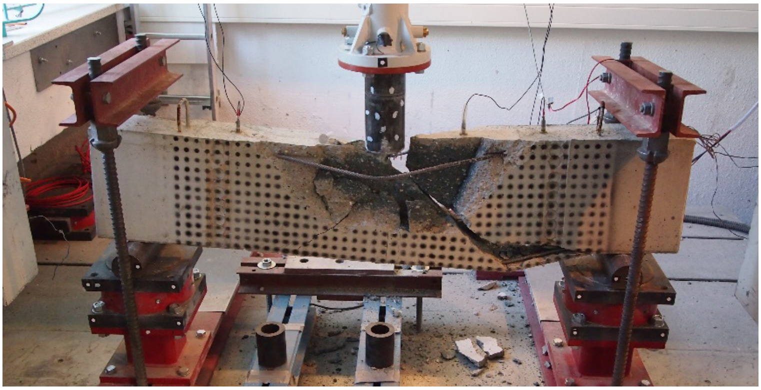

Figure 2. Test with 1 bar loading pressure and extensive damage (Photo: F. Bracklow).

To investigate the bond properties, impact tests under various loading rates were performed. The reinforcement bars were instrumented with strain gauges. The measured data suggest that strains and strain rates in beam tests are independent of the loading velocity. In fact, they seem to decrease with increasing loading velocity. The reason is the increasing concrete damage due to crushing under the impactor (comp. Fig. 1 and 2) which reduces the energy that is transferred into the reinforcement. The strains in the reinforcement bars result from the deflection coming from the impact itself, the spreading of longitudinal waves in horizontal direction, and the cracking of the concrete leading to strain concentrations within the steel. To increase the knowledge about the behaviour of different types of reinforcement bars under different loading velocities, multiple beam tests were carried out.

References

1. M. A. Meyers, *Dynamic behavior of materials*, (University of California, San Diego, 1994)

Effect of fine recycled aggregates on the properties of non-cement blended materials

Wei-Ting Lin[1,*], *Lukáš* Fiala[2], *An* Cheng[1], and *Michaela* Petříková[2]

[1]Department of Civil Engineering, National Ilan University, No.1, Sec. 1, Shennong Rd., I-Lan 260, Taiwan
[2]Department of Materials Engineering and Chemistry, Faculty of Civil Engineering, Czech Technical University in Prague, Thákurova 7, 166 29 Prague 6, Czech Republic

1 Introduction

Concrete is a mixture of cementitious materials, aggregate, and water. Aggregate occupies over half of the concrete volume, which means that the quality of the aggregate largely determines many of the properties of the resulting concrete. Most of the sand and gravel in Taiwan is obtained via river dredging, sand and gravel mining, and importation. Approximately 90 million tons of sand and gravel is consumed in Taiwan every year. Continuing efforts to improve the infrastructure of the country means that the demand for ready-mixed concrete is also growing swiftly, further increasing the consumption of aggregate to levels that cannot be maintained indefinitely. Replacing some of the natural aggregate with RCA can have economic benefits and help to protect the environment.
For Civil Engineering, most buildings are built using cement, the production of which creates massive amounts of CO_2, the leading culprit of the greenhouse effect [1, 2]. To mitigate the greenhouse effect, governments should focus on devising effective measures to reduce greenhouse gas emissions. Cutting down on cement use would not only reduce CO_2 emissions and slow down the greenhouse effect but also promote energy conservation. Portland cement is one of the primary materials used in construction. An investigation report in 2000 [3] revealed that an average of 0.87 kg of CO_2 is emitted for every kilogram of cement produced and that the cement manufacturing industry contributes to 7% of global CO_2 emissions [4]. Development of the fully replacement of cement using effective fly ash or slag formulas enables a decrease in the production costs of concrete as well as in environmental impact. This is achieved through energy conservation, carbon reduction, and optimization of waste recycling [5]. This study is aimed to conduct the effect of fine recycled aggregates on the properties of non-cement blended materials without using alkali activator. Green non-cement mortar specimens with water-quenched blast-furnace slag and co-fired fly ash from circulating fluidized bed combustion were mixed to compare to the compressive strength, absorption and scanning electron microscopes (SEM) observation.

2 Materials and test procedures

Co-fired fly ash used in this study had a fineness of 2800 cm^2/g and specific gravity of 2.73. Its chemical composition was 29.47% SiO_2, 35.54% CaO, 19.27% Al_2O_3 and 3.49% Fe_2O_3. Slag had a fineness of 5860 cm^2/g and specific gravity of 2.88. Its chemical composition was 33.68% SiO_2, 40.24% CaO, 14.37% Al_2O_3 and 0.29% Fe_2O_3. The specific gravity, water absorption rate, and fineness modulus of the fine recycled aggregates were 2.61, 4.45%, and 1.13, respectively. Control mix design (water/blended ratio is 0.45) was consisted of water

* Corresponding author: wtlin@niu.edu.tw

(211.9 kg/m^3), slag (197.1 kg/m^3), fly ash (295.7 kg/m^3), fine aggregates (1355.2 kg/m^3) and superplasticizer (9.9 kg/m^3), respectively. The substitution ratio for recycled fine aggregates to natural fine aggregates was used as 10%, 20%, 30%, 40% and 50%. Compressive strength was measured in accordance with ASTM C109. Absorption was conducted in accordance with ASTM C642 and SEM observations were conducted in accordance with ASTM C1723.

3 Results and conclusions

Figures 1 and 2 display the compressive strength and absorption results of the non-cement blended mortar. For the same flowability (210 mm), the compressive strength decreased and absorption increased as the replacement ratio of fine aggregates increased. Compressive strength of non-cement blended materials containing 20% recycled fine aggregates can reach to the target strength of 37 MPa, which is the 95% of control non-cement blended specimens. SEM micrographs were verified the development in compressive strength originated from the C-S-H and C-A-S-H gel produced by $Ca(OH)_2$, SiO_2, and Al_2O_3, the hydrations made the structure denser and had a greater strength development significantly. Using this new green non-cement blended composites without alkali activator in construction materials can be regarded as an innovation material to save natural resources.

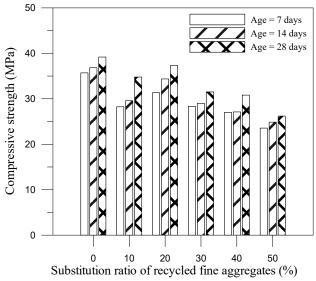

Fig. 1. Strength histograms.

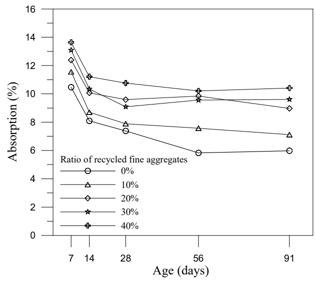

Fig. 2. Absorption curves.

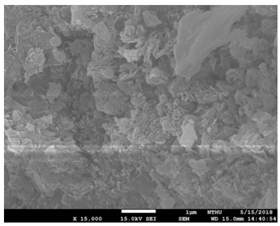

Fig. 3. SEM photo.

This support of the Ministry of Science and Technology (MOST) under the Grant MOST 108-2221-E-197-006 in Taiwan and the Czech Science Foundation under project No. 19-11516S is gratefully acknowledged.

References

1. B.L. de Sena Costa, J.C. de Oliveira Freitas, P.H.S. Santos, D.M. de Araújo Melo, R.G. da Silva Araujo, Y.H. de Oliveira, Constr. Build. Mater. **159**, 252 (2018)
2. R. Bouma, F. Vercauteren, P. van Os, E.Goetheer, D. Berstad, R. Anantharaman, Energy Procedia **114**, 72 (2017)
3. J. Damtoft, J. Lukasik, D. Herfort, D. Sorrentino, E. Gartner, Cem. Concr. Res. **38**, 115 (2008)
4. M. Ali, R. Saidur, M. Hossain, Sust. Energ. Rev. **15**, 2252 (2011)
5. K.L. Lin, K.W. Lo, M.J. Hung, C.L. Hwang, T.W. Cheng, Y.M. Chang, T.P. Huynh, Environ. Prog. Sustainable Energy **36**, 1466 (2017)

Mechanical fracture parameters of fine-grained alkali-activated slag-based composites

Martin Lipowczan[1,*], *David* Lehký[1], *Hana* Šimonová[1], and *Barbara* Kucharczyková[1]

[1]Brno University of Technology, Faculty of Civil Engineering, Veveří 331/95, 602 00 Brno, Czech Republic

1 Introduction

The paper deals with the experimental and numerical determination of mechanical fracture parameters of fine-grained composites based on the alkali-activated slag (AAS) at different ages of hardening. The main aim of the performed experimental investigation was to verify the effect of the addition of shrinkage reducing admixture (SRA) on the overall progress of length changes and mechanical fracture properties during AAS composites ageing.

Two AAS composites, which differed only in the presence of SRA, were studied. The composites were prepared using ground-granulated blast-furnace slag which was activated by water glass with silicate modulus of 2.0, standardized CEN siliceous sand with the particle grain size distribution of 0−2 mm, and water. Commercially produced SRA was added into the second mixture in amount of 2% by weight of slag. The test specimens were not protected from drying during the whole time interval and were stored in laboratory at ambient temperature of 21 ± 2 °C and relative humidity of 60 ± 10%. The prism specimens made of the above-mentioned composites with nominal dimensions of 40 × 40 × 160 mm and initial central edge notch were subjected to fracture tests in three-point bending configuration. The load F and displacement d (deflection in the middle of the span length) were continuously recorded during the fracture tests. Furthermore, the length changes of bigger specimens with dimensions of 100 × 60 × 1000 mm were continuously measured for approximately 90 days. After measurement, the big specimens were cut to make an additional set of specimens with dimension 40 × 40 × 160 mm for fracture tests. The specimens obtained in this manner are designated as “cut”.

2 Methods

The obtained $F-d$ diagrams and specimen dimensions were used as input data for the identification of parameters via the inverse analysis based on the artificial neural network (Novák and Lehký 2006, Lehký et al. 2014). The aim of identification is to determine the mechanical fracture parameters and to feed material models for the deterministic and stochastic simulation of the quasi-brittle/ductile response of structural elements made of studied materials.

In this paper, the values of modulus of elasticity E_{ID}, tensile strength $f_{t,\,\mathrm{ID}}$ and fracture energy $G_{\mathrm{F,\,ID}}$ were identified and subsequently compared with values obtained based on the direct fracture test evaluation using the effective crack model (Karihaloo 1995) and the work-of-fracture method (RILEM Recommendation 1985): modulus of elasticity E, effective fracture toughness K_{Ice}, and specific fracture energy G_{F}.

* Corresponding author: lipowczan.m@fce.vutbr.cz

3 Results

The mean values and coefficient of variations (CoV) of the selected mechanical fracture parameters obtained from direct evaluation of fracture tests records using the effective crack model and the work-of-fracture method of both studied composites tested at 3, 28, 90 days and 2 years of hardening are presented in Table 1 (AAS – composite without SRA, SRA – composite with SRA). The statistical characteristics obtained from identification can be found in the full paper.

Table 1. Mean values (CoV in %) of selected mechanical fracture parameters of studied composites tested in different age of hardening.

Parameter	Unit	Set	Age of specimens 3 days	28 days	90 days	90 days (cut)	2 years	2 years (cut)
E	GPa	AAS	12.0 (15.4)	0.9 (13.0)	14.3 (5.3)	12.7 (22.3)	14.1 (5.1)	17.8 (6.6)
		SRA	11.6 (13.9)	3.1 (29.0)	6.9 (8.0)	6.1 (5.8)	16.2 (3.8)	16.5 (10.6)
K_{Ice}	$MPa{\cdot}m^{1/2}$	AAS	0.541 (12.1)	0.052 (9.2)	0.717 (10.2)	0.643 (25.1)	0.678 (11.5)	0.790 (10.6)
		SRA	0.418 (7.4)	0.108 (20.2)	0.279 (12.3)	0.283 (6.5)	0.696 (5.7)	0.778 (7.1)
G_F	J/m^2	AAS	69.7 (19.2)	5.4 (7.2)	116.4 (7.3)	114.4 (2.5)	94.3 (8.7)	130.9 (14.8)
		SRA	47.6 (9.3)	18.3 (23.4)	52.0 (38.3)	77.7 (43.0)	118.4 (5.6)	129.4 (7.4)

Both techniques provided comparable results (a similar trend of parameters development during the ageing). The differences in mean values of fracture energy correspond to their different physical meanings – the identified values are primarily related to the material point, whereas the values obtained from the work-of-fracture method are related to the tested specimen, the size and shape of fracture process zone and represent the average fracture energy.

This work has been supported by projects MUFRAS No. 19-09491S and No. 18-12289Y, awarded by the Czech Science Foundation (GACR).

References

1. D. Novák, D. Lehký, ANN Inverse Analysis Based on Stochastic Small-Sample Training Set Simulation, Eng. Appl. Artif. Intel. **19** (2006)
2. B. L. Karihaloo, *Fracture Mechanics and Structural Concrete* (Longman Scientific & Technical, New York, 1995)
3. D. Lehký, Z. Keršner, D. Novák, FraMePID-3PB Software for Material Parameters Identification Using Fracture Test and Inverse Analysis, Adv. in Eng. Soft. **72** (2014).
4. RILEM TC – 50 FMC (Recommendation), Mater. Struct **18**, 4 (1985)

The efficiency of reinforcing masonry bridges with the use of corrugated steel sheets

Czesław Machelski[1,*], *Jan B.* Michalski[2], and *Krystyna* Szcześniak[1]

[1]Wroclaw University of Science and Technology, Faculty of Civil Engineering, Wyb. Wyspiańskiego 27, 50 370 Wrocław, Poland
[2]PIW Ekspert, Production Department, Nowa Ruda 91944, Poland

1 Introduction

The strengthening of masonry bridges using corrugated metal sheets is an effective way of revitalizing old building structures made of brick or stone. The advantage of such vault strengthening is the small reduction of space under the bridge, and at the same time a significant increase in the bridge's load bearing capacity. The reinforcement technology involves the introduction of corrugated metal sheets under the structure and fixing them in the support of the operated object. The next step includes the filling with concrete of the empty area between the reinforced structure and the coating. The filling layer in this system acts as an element of the structure. Due to the principle of operation of masonry vaults and corrugated steel coatings, no fasteners are required to force the cooperation of these structural elements.

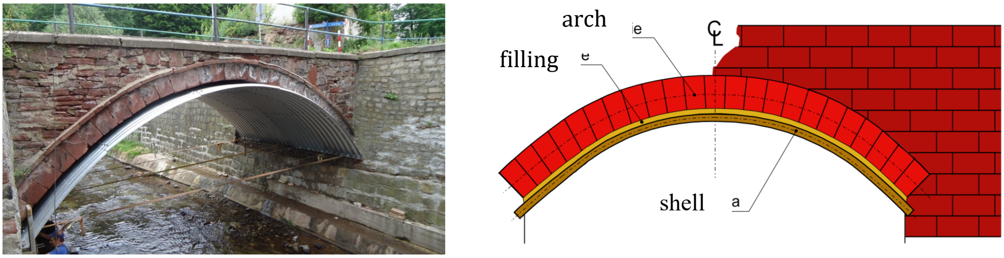

Figure 1. View of the structure and scheme of reinforcement vaults.

2 Model of the object after strengthening

After strengthening the vault with the use of corrugated steel, as in Fig. 1, a three-layer system with various material parameters is created. Due to the much greater Young's modulus of corrugated steel over the other elements, the coating becomes the dominant element in the system. The considerable thickness of the vault (with reinforcement) and the distribution of concentrated loads from the wheels of vehicles in the ground above the structure cause almost complete reduction of the bending of the coating. Also the axial forces from service loads are small compared to the effect of the constant weight of the structure and equipment. For these reasons, the main strength problem in the reinforced object is the stress resulting from the deformation of the corrugated metal arising during the filling of the space between the vault and the coating.

* Corresponding author: czeslaw.machelski@pwr.edu.pl

3 Construction fase

During the construction phase of the structure, the primary part with the vault and surge is distinguished, as well as an independent coating of corrugated metal, as in Fig. 1. Thus, in the geometry model, the structure of the structure is divided into two subsystems with the joint hydrostatic interaction of the filling *p*(s). In general [1] this interaction is related to the distribution of axial force *n*(s) and bending moment *m*(s) along the peripheral band of the coating as in the equation:

$$p(s) = \frac{n}{R} + \frac{d^2m}{ds^2} \quad . \tag{1}$$

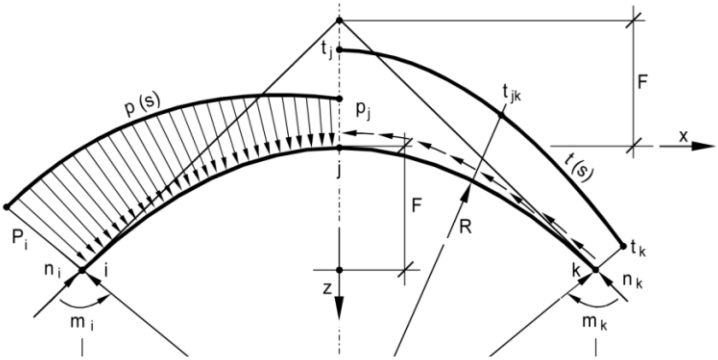

Figure 2. Distribution of interaction between the coating and the vault.

The deformation of the coating during the filling of the space between the vault and the coating, as in Fig. 1 is by nature a random phenomenon. The hydrostatic pressure resulting from different filling levels on both sides of the coating is not symmetrical. In addition, as a result of working breaks, a different degree of binding (compaction) of the filling mix occurs. The paper analyzes the deformation process of the flaccid corrugated sheet coating. In the construction phase, it is very similar to the situation of laying backfill in soil and coating structures [1].

To measure internal forces in the corrugated coating sheet, measuring strain gauges are used [2]. Due to significant displacements of the flaccid coating, geodetic measurements are also carried out, as at work. With regular placement of measuring points, the functions of internal forces and filling effects from the relationship (1) are convenient to bind in differential terms [1, 2].

References

1. C. Machelski, Effects of surrounding earth on shell during construction of flexible bridge structure. (Studia Geotechnica et Mechanica, No 2 2019)
2. C. Machelski, Soil-steel structure shell displacements functions based on tensometric measurements. (Studia Geotechnica et Mechanica, No 2 2018)

Analysis of AAC precast lintels behavior in walls confined with reinforced concrete and reinforced lightweight concrete

Wojciech Mazur[1,*], *Łukasz* Drobiec[1], *Radosław* Jasiński[1], and *Tomasz* Rybarczyk[2]

[1]Silesian University of Technology, Department of Building Structure, Gliwice, Poland
[2]SOLBET Sp. z o.o., Kujawski, Poland

1 General

Currently, considerable emphasis is placed on the design of environmentally friendly buildings and low energy demand. Therefore, walls with the lowest heat transfer coefficient are designed. In extreme cases, reinforced concrete core located inside the wall causes the occurrence of a thermal bridge, which significantly deteriorates the thermal parameters of the building partition. An alternative solution combining the advantages of concrete and good thermal insulation parameters may be the implementation of rims and cores made of lightweight concrete. The window opening is a weakening of each wall and requires the use of a suitable lintel [4]. The use of a reinforced concrete rim makes it possible to increase the lintel load capacity. In extreme cases, the rim stiffness is so high that it transfers the load from the floor and masonry above, and the lintel is only the filling and covering of the opening [2]. Strength parameters of lightweight concrete are not as favorable as ordinary concrete, so the lintel plays a more important role by taking on a greater load. The impact of changing strength parameters and rim stiffness on lintel behavior was verified during tests of confined walls made on a natural scale.

2 Experimental tests and results

The research program included testing of eight confined walls made of autoclaved aerated concrete (AAC) with a window opening covered by reinforced system precast lintel made of AAC [1, 3].

a)

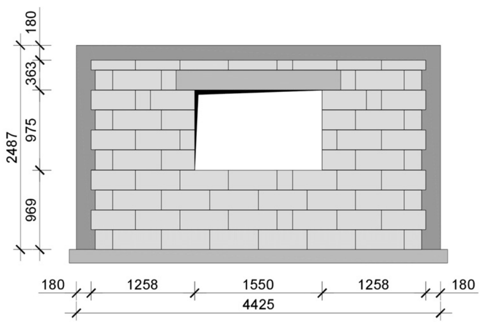

b)

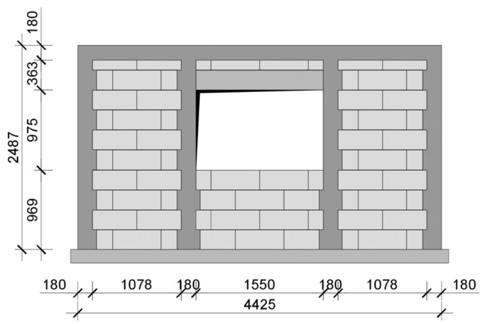

Figure 1. Models of series: a) MSOL and MSO, b) M2SOL and M2SO.

* Corresponding author: wojciech.mazur@polsl.pl

Two models of walls confined with lightweight concrete (MSOL-Z series) and ordinary concrete (MSO-Z series) in accordance with Fig. 1a were made, as well as two models of walls confined with lightweight concrete (M2SOL-Z series) and ordinary concrete (M2SO-Z series) with additional cores in accordance with fig. 1b. The research consisted in the analysis of deflection, maximum load and method of destruction of research models. This article focuses on the analysis of the wall zone above the window opening. The tests were monitored by Digital Image Correlation system Aramis.

a) b)

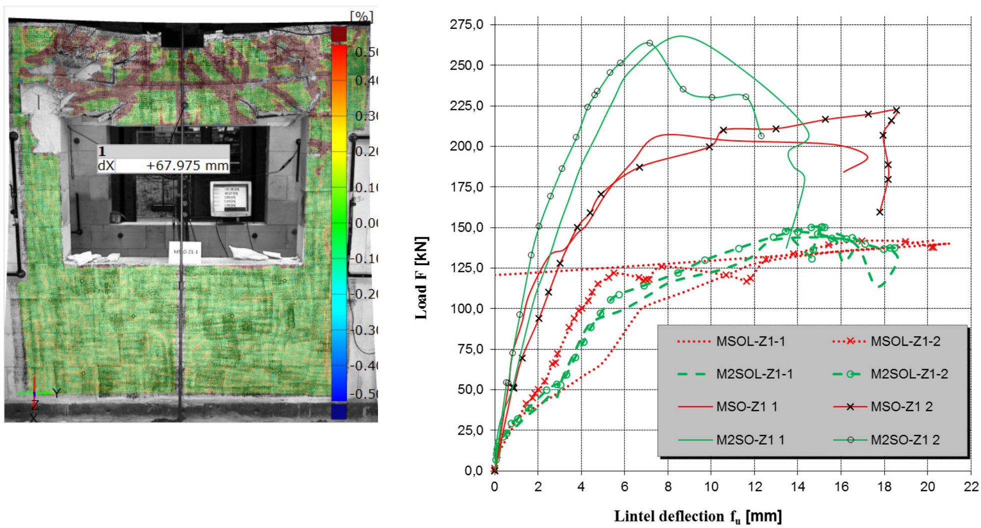

Figure 2. a) Crack development in the model MSO-Z1 gained from Aramis system, b) Relationships of load and lintel deflection of all tests.

The models were cracked and destroyed in an analogous manner regardless of the type of concrete used. The view of the cracks of the MSO-Z1 model obtained through the Aramis system is shown in Fig. 2a. Models confined with lightweight concrete were cracked and destroyed at a lower load level than models confined with ordinary concrete, which confirms the graph of the relationship load – deflection of the lintel shown in Fig. 2b.

References

1. 845-2:2013-10 PN-EN: Specification for ancillary components for masonry. Part 2: Lintels
2. PN EN 1996-1-1: Eurocode 6: Design of masonry structures – Part 1-1: General rules for reinforced and unreinforced masonry structures
3. W. Mazur, Ł. Drobiec, R. Jasiński, Research of Light Concrete Precast Lintels. Procedia Engineering 161/2016, 611–617
4. W. Mazur, Ł. Drobiec, R. Jasiński, Research and numerical investigation of masonry – AAC precast lintels interaction. Procedia Engineering 193/2017, 385–392

Study of the effects of strengthening compressed walls of autoclaved aerated concrete by the FRCM system

Wojciech Mazur[1,*], *Łukasz* Drobiec[1], and *Remigiusz* Jokiel[2]

[1]Silesian University of Technology, Department of Building Structure, Gliwice, Poland
[2]BudInż Sp. z o.o., Rybnik, Poland

1 General

The article presents the results of research aimed at determining the effect of surface reinforcement of autoclaved aerated concrete walls by the FRCM system. Walls without reinforcements reinforced on one and two side surfaces were examined.

2 Experimental tests and results

Compression masonry tests were carried out in accordance with PN-EN 1052-1 [1]. Walls made of SOLBET OPTIMAL blocks of dimensions were tested l×w×h = 590×180×240 mm. The masonry units density class declared by the Manufacturer is ρ = 600 kg/m^3, average compressive strength f_b =4 N/mm^2, and production category I. The models use SOLBET masonry mortar for thin joints on white cement – marked with symbol 0.1 of the nominal class M5.
Individual series have been designated with the letter S, Arabic numeral denoting the type of mortar used (1 – wall with thin joints and unfilled butt joints), the letter N denoting the unreinforced wall and the next serial number. In the case of surface reinforced walls, instead of the letter N, the letter F and a number indicating the number of reinforced surfaces were placed. In reinforced models, the PBO-MX GOLD MURATURA system mortar was applied to the side surfaces and the PBO-MESH GOLD 70/18 mesh was applied to it, followed by the top layer of the PBO-MX GOLD MURATURA system mortar (Fig. 1a). During the tests, the compressive force was measured using a 0.001 kN force gauge and vertical and horizontal displacements using inductive sensors with an accuracy of 0.002 mm. In addition, displacement was measured using an Aramis contactless optical system. This required painting the samples in irregular patterns (Fig. 1.b). The dimensions of the base for measuring wall displacements were determined according to the recommendations contained in the PN-EN 1052-1 standard. This standard assumes a base equal to 1/3 of the height of the element and a width of 1/2 of the test element. With the elements arrangement as in Fig. 5.1 1/2 the element length falls on the vertical joints. The previous experience of the authors showed that such a system can lead to disturbances in the conducted measurement, therefore it was decided to increase the horizontal base by 20 mm compared to the base assumed by the standard. The measurement of vertical deformations was used to determine the graph of the relationship vertical stress σ_y – vertical deformation ε_y, while the measurement of horizontal deformations was used to determine the Poisson's ratio ν of the wall.

* Corresponding author: wojciech.mazur@polsl.pl

a) b)

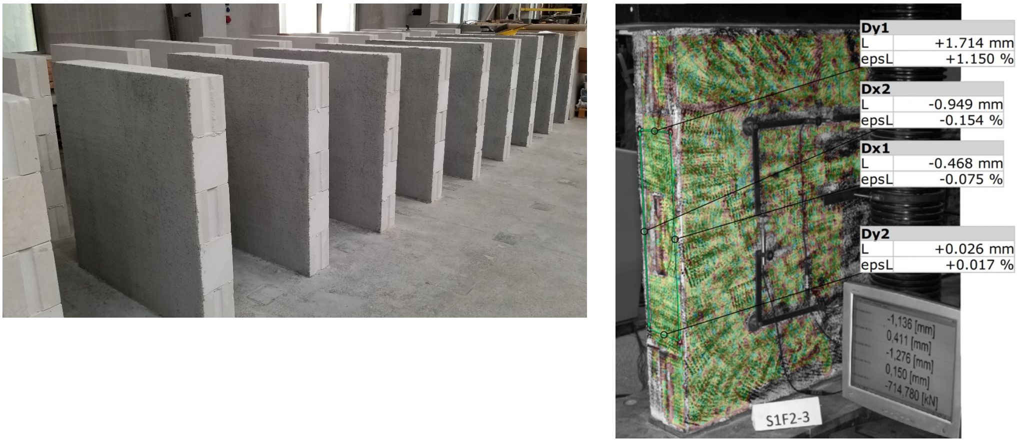

Figure 1. View of model: a) all series, b) S1F1 series during the test.

Test results indicate the lack of clear effects of wall reinforcement on the one side on compressive strength in relation to walls without reinforcement. With two-sided reinforcement, an increase in compressive strength of the models by more than 15% was observed compared to walls without reinforcement.

References

1. PN-EN 1502-1: Methods of test for masonry – Part 1: Determination of compressive strength

Application of non-metallic composite reinforcement for contact line supports

Valery Nikolaev[1], *Valentina* Stepanova[2], and *Vyacheslav* Falikman[3,*]

[1]Composite building materials Assoc., 109428 Moscow, Russia
[2]Scientific Research Institute for Concrete and Reinforced Concrete, 109428 Moscow, Russia
[3]Structural Concrete Assoc., 109428 Moscow, Russia

1 Introduction

In recent years, many types of composite polymer reinforcement have been appeared on the construction market, but the volumes of used concrete structures made with its application are growing very slowly. One of the reasons is the lack of completed testing of experimental structural concrete for real operating conditions [1]. Noting the positive properties of reinforcement, its disadvantage is often indicated, viz. low modulus of elasticity compared to steel reinforcement [2]. This property and distinctive feature of composite reinforcement could be took advantage to the greatest possible extent in prestressed structures.
The supporting structures for overhead line conductors are various types of poles and towers called line support. In general, the line supports should have the following properties: high mechanical strength to withstand the weight of conductors and wind loads etc.; light in weight without the loss of mechanical strength; cheap in cost and economical to maintain, and longer life.
The reinforced concrete poles have become very popular as line support in recent years. They have greater mechanical strength, longer life and permit longer spans than steel. Moreover, they give good outlook, require little maintenance and have good insulating properties. Nevertheless, it is known that reinforced concrete line supports are subject to electrochemical corrosion caused by stray currents. In this regard, the lighter diamagnetic composite reinforcement, which is a dielectric and effectively works in structures under the influence of aggressive environments, is extremely attractive.

2 Experimental

Within the framework of the RUSNANO project, supporting poles with rod reinforcement by prestressed composite basalt fiber polymer reinforcement (BFPR) were developed and manufactured under production conditions (Table 1).

Table 1. Characteristics of the tested prototypes of contact line supports.

Supports No.	Reinforcement	Prestressing conditions
1-6	Prestressed composite bars, 12 rods Ø 15.7 mm	1080 kN
7	Prestressed steel bars, steel A-IV (A600), 12 rods Ø 14 mm 1080	1080 kN
8	Non-stressed steel bars, steel A-III (A400), 8 rods Ø 14 mm	-

* Corresponding author: vfalikman@yandex.ru

For prestressing of composite reinforcement, special anchoring devices were used that enable to reliably anchor rebar with more than 40% rupture load and provide its quick replacement [3].
Poles bench tests by loading to evaluate their strength, stiffness and crack resistance were carried out with determining of the deflection magnitude of the support in the plane of the control load application with an accuracy of 1 mm for every stage of the design loads at the level of the contact wire.
Life (resource) tests were carried out by vibration loading of poles. During vibration loading, the load was applied to the console, the working length of which was 2.5 m, installed at a height of 8 m from the base of the support. The static load was 2, 25 kN, dynamic one was 6 kN, the oscillation frequency was 0.5 – 0.7 Hz. The number of loading cycles was 1000000.
The test results showed that the vibration loading did not have a significant impact on the properties of the supports reinforced with composite reinforcement. During vibration loading, no visible damages of poles were detected; the deflection of a pole at the level of a contact wire from application of the standard bending moment was in admissible limits. Poles reinforced with BFRPR, without vibration loading and undergoing vibration loading, comply with the GOST 19330 requirements for crack resistance. After vibratory loading and application of verificatory load, they restore their straightness. The straightness of the poles meets the requirements of the standards also.
The deflection under the normative bending moment application before and after vibration loading for the poles with BFRPR also satisfies to requirements of standards. All tested poles provide the safety factor on structural failure before and after vibration loading established by the norms.

3 Conclusions

Thus, the technology of prestressing and anchoring of composite polymer reinforcement of the high performance contact line supports, which have a number of advantageous characteristics in comparison with ordinary reinforced concrete structures, has been developed and tested. The obtained results confirmed the possibility to use concrete poles reinforced with prestressed BFRP bars for the contact lines of Russian Railways.
For the further development of the project, working drawings would be developed on the replacing of steel reinforcement with composite polymer reinforcement, and also technical specifications for perspective supports of the Russian Railways contact lines, as well as technological regulations for their production.

References

1. V.F. Stepanova, A.Yu. Stepanov, E.P. Zhirkov, *Polymer composite reinforcement* (ASV Publ., Moscow, 2013)
2. V.R. Falikman, V.F. Stepanova, Proceedings of the 4th International Conference on Service Life Design for Infrastructures (SLD4). Delft, the Netherlands. Publ. by RILEM Publications S.A.R.L. 1104 p., pp. 1016–1025 (2018)
3. V.N. Nikolaev, Patent 2203372 RU (2011)

Numerical modelling of concrete structures through a MPMM approach

Francesco Pesavento[1,*], *Dariusz* Gawin[2] , *Bernhard* Schrefler[1] , and *Giuseppe* Sciumé[3]

[1]Dept. of Civil, Environmental and Architectural Engineering, University of Padua, Padova, Italy
[2]Dept. of Building Physics and Building Materials, Lodz University of Technology, Łodz, Poland
[3]Institut de Mécanique et d'Ingénierie I2M – Dép. TREFLE, Université de Bordeaux, Bordeaux, France

1 Introduction

A realistic prediction of the behavior of concrete structures during their service life is crucial in many applications in civil, industrial, environmental and nuclear engineering especially if they are under severe conditions (e.g. aggressive environment, fire, etc.).

In most of these cases, numerical tools available in the market do not provide a sufficiently accurate and reliable response, so it is needed to use more sophisticated approaches. In this work, a general mathematical/numerical model for the simulation of the non-linear behavior of concrete is described together with some relevant applications. It is based on the Multiphase Porous Media Mechanics (MPMM). The mathematical model is developed by formulating an appropriate set of balance equations for the constituents at the local level, i.e. at micro-scale. Then, according to the Thermodynamic Constrained Averaging Theory (TCAT), these governing equations are up-scaled to the macro level, taking into account at the same time some thermodynamic constraints. This special procedure allows for a complete upscale of the thermodynamics from the micro level to the macroscopic one, in a proper way. This means that with the adopted averaging procedure all physical quantities are correctly defined and no unwanted dissipations are fictitiously generated.

The final form of the mathematical model is discretized directly at the macroscale by means of Finite Element Method in the domain of space and Finite Difference Method in the domain of time.

2 Applications of the general framework

The resulting model can be successfully applied to several practical cases: evaluation of concrete's performance at early stages of maturing massive structures, structural repair works, concrete exposed to high temperature, e.g. during fire, cementitious materials subject to freezing/thawing cycles, etc. As typical application of the model we first show the results of the numerical simulation of a massive concrete beam cracking. The analysed test is a large beam specimen built for ConCrack (2011), see Fig. 1, and subject to variable environmental conditions in terms of temperature and relative humidity (Fig. 2).

A second relevant example is the case of concrete structure exposed to high temperature. Figure 3 shows the geometry of a cross section of a pillar under fire (Standard ISO-Fire curve) and some results in terms of total damage distribution at the end of the calculation (82 minutes), which considers also a fast cooling phase (2 minutes long).

* Corresponding author: francesco.pesavento@dicea.unipd.it

The reader can find more details in [1-3].

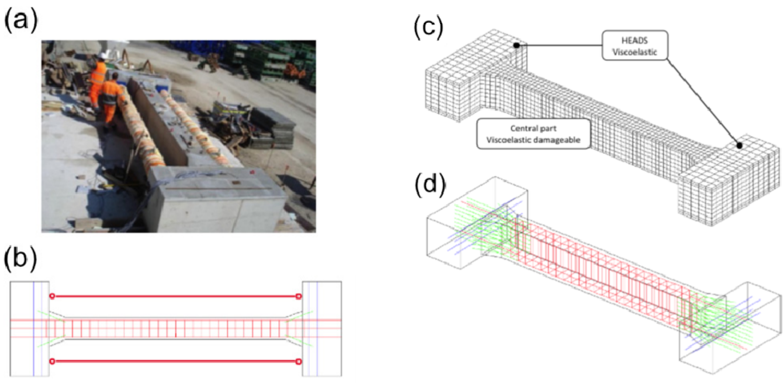

Figure 1. Experimental specimen (a), upper view of steel reinforcements and metallic struts contrasting longitudinal expansion/shrinkage (b), finite elements mesh of concrete for the modeled case (c), mesh of steel reinforcements (d).

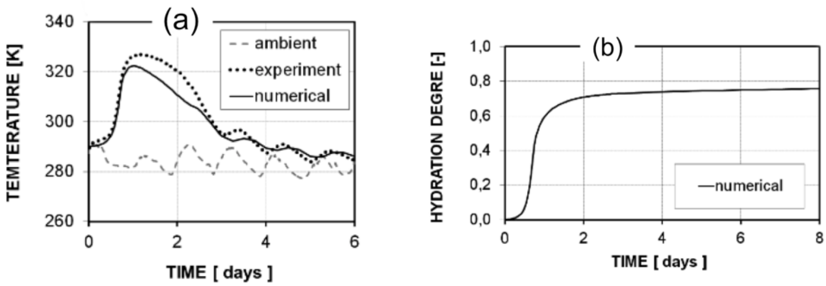

Figure 2. Evolution of temperature (a) and hydration degree (b), in the central point of the beam.

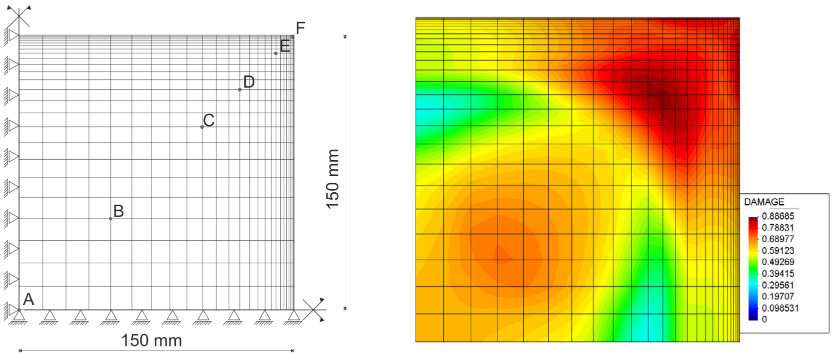

Figure 3. Cross section of the square column: geometry and FE mesh used in the computation (left); distribution of total damage at the end of the simulation, 82 min, (right).

References

1. F. Pesavento, D. Gawin, B.A. Schrefler, Acta Mech, **201**, 313–339 (2008)
2. D. Gawin, F. Pesavento, B.A. Schrefler, Int. J. Solids Struct., **84** (13), 1927–1944 (2011).
3. F. Pesavento, B.A. Schrefler, G. Sciumè, Arch Comput Method E **24**, 423–448 (2017)

Deformability of the masonry subjected to shearing due to vertical displacements

Adam Piekarczyk[1,*]

[1]Silesian University of Technology, Civil Engineering Faculty, Department of Building Structures, Gliwice, Poland

1 Introduction

Forces causing shear of masonry walls in a vertical direction (perpendicular to the bed joints) are usually the result of uneven displacements suffered by structural elements adjacent to these walls. The movements may result from deformations of the subsoil transferred by foundations to the masonry structure or deflections of ceiling system members on which the walls are supported [1], [2].

2 Materials, specimens and test stand

The first series of specimens was made of solid clay brick with a mean normalised compressive strength of 23.3 N/mm^2 and prescribed cement-lime mortar with a volumetric ratio of components 1:1:6 and mean compressive strength 9.74 N/mm^2. Autoclaved aerated concrete (AAC) with a mean normalised strength of 3.11 N/mm^2 and system mortar for thin joints with a mean compressive strength of 18.8 N/mm^2 were used to make the second series of specimens.

The solid clay brick specimens had a width of ca. 129 cm and a height about 141.5 cm. The specimens made of AAC blocks were ca. 125 cm wide and about 151 cm high.

The scheme of the test stand is shown in Fig. 1. Masonry specimens were monolithised with the external and internal middle column of the stand. The displacements of the internal column were caused by the force F using a hydraulic cylinder. The tests were carried out with simultaneous vertical compressive stress σ_c with a constant value induced using steel tendons under N_c force (see Fig. 1).

Wall deformations represented by angles θ were calculated based on changes in the length of measurement bases forming a square measurement system with a side length equal to 600 mm on both surfaces of specimens.

3 Test results

Figure 2 presents graphs of the dependence of shear wall stiffness G_v on the value of shear stress τ. Compressive stresses σ_c accompanying shear were 0.3, 0.6, 0.9 and 1.5 N/mm^2 (N-03, N-06, N- 09, N-15) for brick walls and 0.9 N/mm^2 for specimens made of AAC blocks (A-09). In the case of walls made of both materials, the tests were also carried out without the participation of σ_c stress (N-00, A-00).

* Corresponding author: Adam.Piekarczyk@polsl.pl

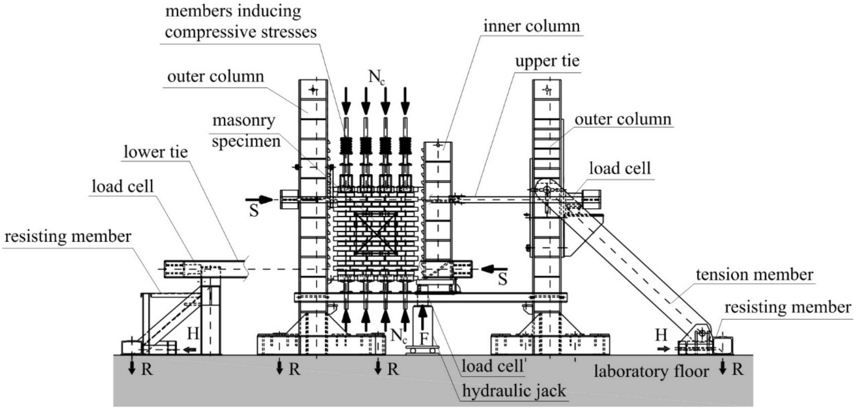

Fig. 1. Test stand.

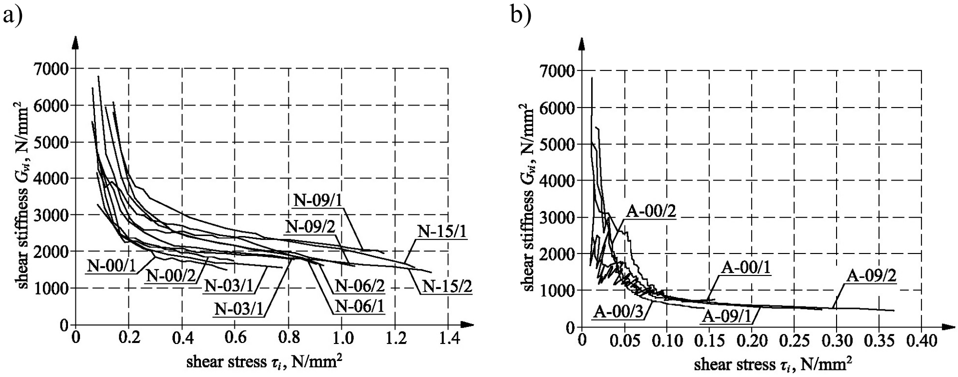

Fig. 2. Graphs showing the dependence of deformability on the value of shear stress for a wall made of: a) solid clay bricks, b) AAC blocks.

4 Conclusions

Based on the results of tests performed in the described scope, it can be stated that:

- the dependence of wall stiffness sheared in the vertical direction on shear stresses in strongly non-linear; stiffness decreases rapidly with increasing load;
- the stiffness of the walls is greater the higher the compressive stress σ_c the that accompany shear, especially for brick masonry;
- compressive stress σ_c (with values from the analysed range) have a positive effect on the crack resistance and load-bearing capacity of the vertically sheared masonry.

References

1. Piekarczyk A., The influence of compressive stress on the load-bearing capacity of masonry subjected to vertical displacements. IOP Conference Series: Science and Engineering, 4711 (2019)
2. Kubica J., Piekarczyk A., Tests of vertically sheared clay brick masonry walls with and without bed joint reinforcement. Proceedings of 13th International Brick/Block Masonry Conference, Amsterdam (2004)

Failure of load-bearing masonry walls supported by a deflecting structure

Adam Piekarczyk[1,*]

[1]Silesian University of Technology, Civil Engineering Faculty, Department of Building Structures, Gliwice, Poland

1 Introduction

A few millimetre deflections of the ceiling (displacement of foundations) on which masonry walls are supported may lead to cracking [1], [2]. In the considered situation, the deflections result from permanent and imposed loads transmitted by the walls to the ceiling structure, the dead weight of the materials laid on the ceiling and service load. In the case of RC ceilings, the deflection will additionally increase over time due to deformations resulting primarily from creep and shrinkage, after the masonry walls have been erected.

The article presents the values of loads on the upper surface of masonry walls, deformations and the pattern of cracking accompanying the formation of the first visible cracks and at failure.

2 Materials, specimens and test stand

The specimens were made of calcium-silicate blocks group 1 according to PN-EN 1996-1-1 standard with a mean normalised compressive strength of 21.8 N/mm^2 and thin layer mortar with a mean compressive strength of 12.5 N/mm^2.

Full-scale masonry walls were tested, approximately 455 cm long, 245 cm high and 18 cm thick. Walls without openings (Type A), with a single door opening (Type B), with two door openings (Type C) and with door and window openings (Type D) were tested.

The test stand is shown in Fig. 1. The walls were built directly at the stand on a slender steel beam (item 8), supported along entire length at that time. An RC ring-beam (item 4) was laid on the upper surface of the wall. The wall was loaded through transverse beams with forces F (item 2, 3). The load on the upper wall surface caused the steel support beam to deflect. The low flexural stiffness of the support allowed for additional deflections (item 10, 11, 12, 13), which reflect the deflections of the ceiling resulting from its direct load and delayed deformations.

3 Test results

Table 1 summarises the values of ultimate stress caused by the load of the upper wall surface σ_u, the accompanying deflection in the centre of the support span $\delta_{u.1/2}$, the ratio of the deflection $\delta_{u.1/2}$ to the support span L and the masonry deformation angle θ_u in the conventionally named left "L" and right "R" field. The results are collated for walls of Type B and D. Fig. 2 shows how these walls were cracked at failure.

[*] Corresponding author: Adam.Piekarczyk@polsl.pl

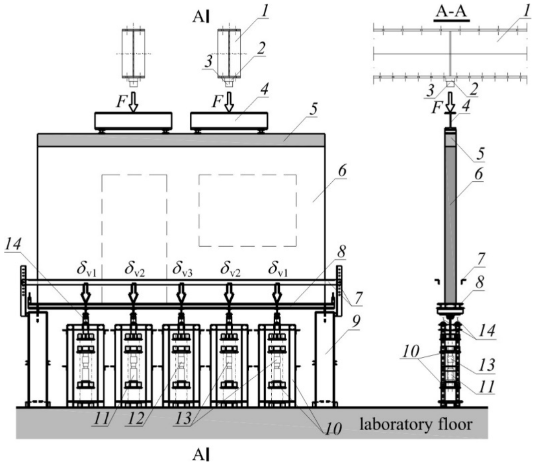

Fig. 1. Test stand: *1* – steel frame, *2* – force gauge (500 kN), *3* – hydraulic jack (500 kN), *4* – steel crossbeam, *5* – reinforced concrete rim, *6* – tested wall, *7* – system for measuring the vertical displacements, *8* – flexible wall support, *9* – external support of the beam, *10* – system enforcing vertical displacements, *11* – hydraulic jack (150 kN), *12* – force gauge (100 kN), *13* – force gauge (50 kN), *14* – screws for fixing the deflections.

Table 1. Test results for selected masonry walls.

Specimen	Area		σ_u, N/mm^2	$\delta_{u.1/2}$, mm	$\delta_{u.1/2}/L$	θ_u, mm/m
B-1	„L”	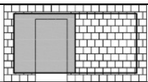	0.391	11.2	1/402	12.2
	„R”	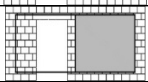				1.15
D-1	„L”	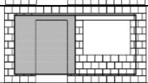	0.458	15.0	1/300	2.60
	„R”	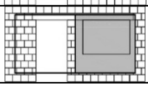				10.5

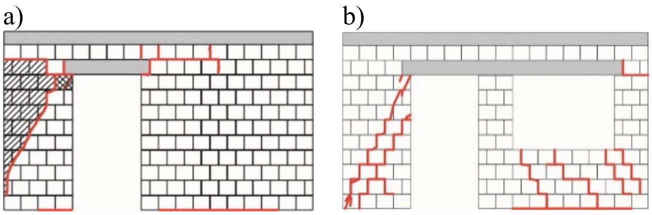

Fig. 2. Cracking pattern at failure for: a) B-1, b) D-1 walls.

References

1. Piekarczyk A., Cracking and failure mechanism of masonry walls loaded vertically and supported by deflecting structural member. IOP Conference Series: Science and Engineering, 471 (2019)
2. Drobiec Ł., Kubica J., Zapobiegania zarysowaniom ścian murowanych opartych na stropach żelbetowych (Prevention of cracking of masonry walls supported on reinforced concrete floors – in Polish), *Materiały Budowlane*, 4/2006

Strength parameters and mechanical properties of lightweight concrete on sintered aggregate

Anna Rogowska[1,*] and *Paweł* Lewiński[1]

[1]Building Research Institute – ITB, Filtrowa 1, 00-611 Warszawa, Poland

1 Introduction

The purpose of the test program is to determine the mechanical properties of lightweight concrete on sintered aggregate. The general research project includes testing for both short-and long-term properties. The subject of this paper is the determination of the short-term properties. The results of rheological tests will be presented in a separate publication.

The issue of lightweight aggregates has been studied extensively in a number of significant publications, including [1]. These presented the properties of aggregates and concretes based on ash aggregates, as well as lightweight concretes. Work [2] describes in detail the properties of lightweight concretes, including concretes on the same aggregates as those discussed in the present research.

The aggregate material comes from the recycling of ashes from power plants, which yield granules after processing. A program for testing the strength parameters and properties of lightweight concrete on sintered aggregate of particularly favourable features was developed. The research was planned based on two concrete mixes, analogous to the ones in [3]. Due to the lack of standards and difficulties in implementation, tensile tests are performed rarely and so far have not produced reliable results [1]. For this reason, ITB Instruction № 194/98 [3] was utilised. Knowledge of the tested parameters is necessary when designing prestressed structures according to standard [5], as well as accepting proven values for static calculations when designing complex engineering structures, including pre-stressed elements made of lightweight concrete.

2 Schedule and implementation of research

A series of tests was carried out in the ITB Laboratory of Building Structures, Geotechnics and Concrete. As a result of these tests, the following parameters were determined: secant modulus of elasticity and cylinder strength of concrete, cube strength of concrete, axial tensile strength, splitting tensile strength, flexural strength and concrete shrinkage (in rheological tests, developed over time). Concrete maturity is the most important element for its strength parameters. The experimental research began when the concrete was mixed. Concrete was produced in a concrete plant by means of a specialised mixer ensuring the homogeneity of the mix. After casting the samples in forms and ensuring the appropriate laboratory conditions, the tests were carried out in accordance with the following procedures (the test equipment provided first class accuracy):

– secant modulus of elasticity of concrete in accordance with [6]
– compressive strength according to [7]
– axial tensile strength according to [3]
– splitting tensile strength according to [8]
– flexural strength according to PN-EN [9]

* Corresponding author: a.rogowska@itb.pl

– shrinkage in accordance with [3].

According to the schedule, strength tests were performed after 7, 14, 28 and 60 days, and shrinkage tests in a period ranging from 1 to 8 days, every 2 days; from 8 to 28 days, every 4 days; and from 28 to 60 days, every 10 days.

3 Analysis of test results and conclusions

The performed tests allowed to determine the aforementioned strength parameters of concretes on lightweight aggregate originating from ashes. In this work, the test results include readings taken within two months of making the mixtures. The entire research process is expected to last about 500 days after making the samples. The results obtained do not differ significantly from the results presented in paper [3]. The mutual empirical relations of concrete tensile strength and secant elasticity modulus in relation to compressive strength, as well as the development of these parameters and their mutual relationship through time were determined. The results are presented in the form of analytical formulas and graphs.

The preliminary research results obtained give a broader view of the possibilities of using lightweight concrete on sintered aggregate in modern construction and the development of its strength parameters over time. The presented results are useful for the correct design of lightweight concrete structures and components, especially pre-stressed structures. It should be remembered, however, that the results were obtained in laboratory conditions. When using these results in practice, it is necessary to take into account the actual conditions in which the concrete will be situated.

Reuse of waste materials is now an environmental priority. As a result, the reuse of ashes for the production of concrete aggregate may, in the future, reduce the mining of raw materials and the use of natural aggregates in construction. The preservation of natural deposits also contributes to environmental protection.

References

1. L. Domagała, *Structural lightweight aggregate concrete* (in Polish), Monografia 462 (Wydawnictwo Politechniki Krakowskiej, Kraków, 2014)
2. S. Chandra, L. Berntsson, *Lightweight aggregate concrete* (Elsevier, 2002)
3. M. Mieszczak and L. Domagała, *Lightweight aggregate concrete as an alternative for dense concrete in post-tensioned concrete slab*, Mat. Sci. For. **926 (**2018)
4. L. Brunarski, *Testing of mechanical properties of concrete on samples made in moulds* (in Polish), Instrukcja 194/98 (ITB, Warszawa, 1998)
5. EN 1992-1-1: 2004 Eurocode 2: Design of concrete structures – Part 1-1: General rules and rules for buildings
6. EN 12390-13:2013 Testing hardened concrete. Determination of secant modulus of elasticity in compression
7. EN 12390-3:2019 Testing hardened concrete – Part 3: Compressive strength of test specimens
8. EN 12390-6:2009 Testing hardened concrete – Part 6: Tensile splitting strength of test specimens
9. EN 12390-5:2019 Testing hardened concrete – Part 5: Flexural strength of test specimens

Analysis of failure modes of bonded TRC elements used in structural strengthening systems

Edoardo Rossi[1,*], *Peter* Harsányi[1], *Tamás* Mészöly[1], and *Norbert* Randl[1]

[1]Carinthia University of Applied Sciences, Faculty of Civil Engineering and Architecture, Spittal an der Drau, Austria

1 Introduction

Textile Reinforced Concrete (TRC), also known as Textile Reinforced Mortar (TRM), Fabric Reinforced Cementitious Matrix (FRCM) or Inorganic Matrix-Grid composite (IMG), is a composite material consisting of high strength fibers (e.g. carbon, glass, basalt, etc.), arranged in yarns, which form a fabric or a grid that is embedded in a fine cementitious matrix. Its mechanical characteristics make it a viable material for strengthening and retrofitting concrete elements and structures. The achievable performances of the retrofitted elements, however, strongly depend on the bond properties between TRC and the concrete substrate and on the ability of the system to transfer stress among the interconnected parts. For such a reason, recently, RILEM technical committee published guidelines defining a test method for the characterization of TRC to substrate bon [1]. This guideline was taken as a reference to perform an experimental campaign investigating the behavior of carbon textile fabric embedded in different cementitious materials, as well as the effect, in terms of failure mode, of mechanical anchorages positioned on the bottom of the specimen.

2 Materials and Method

Nine concrete prisms were cast as substrates for the specimens. They were roughened by waterjetting. After maturation of the concrete substrate, the TRC overlay was cast upon them. The textile used in this campaign was a solidian GRID Q142/142-CCE-25 made of carbon filaments. Two different cementitious compounds were used to produce the matrix: TF10 PAGEL/TUDALIT fine concrete and an Ultra High Performance Concrete (UHPC) mixture developed on the basis of previous studies [2,3]. Furthermore, a mechanical anchorage, consisting of one Hilti X-M8H P8 setting bolt, was placed in the bottom part of 3 specimens, at approximately a distance of 50 mm from the end of the textile layer and centred with respect to the horizontal direction. A summary of the tested specimens is reported in Table 1.

Table 1. Test Series.

Specimen Series	Matrix	Mechanical Anchorage	N° of Specimens
P_SB_#	Pagel	Yes	3
P_#	Pagel	No	3
U_#	UHPC	No	3

Each specimen had a height of 400 mm, a width of 150 mm and a depth of 150 mm for the substrate. The textile layer was 100 mm wide and 950 mm long, of which 200 mm were used for clamping and 300 mm were embedded in the cementitious matrix, as well as bonded to the

* Corresponding author: e.rossi@cuas.at

substrate. The bonded TRC element had a thickness of approximately 10 mm and was placed on the substrate at a distance from the top and the sides of 50 mm and 25 mm, respectively. Figure presents the dimensions of the test layout, as well as a picture of the test set-up.

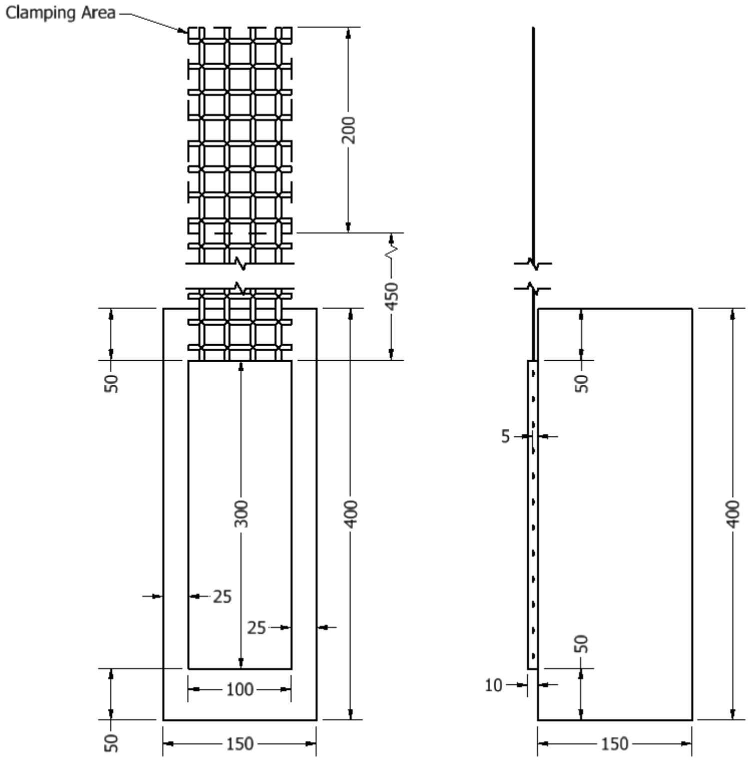

Figure 1. Geometry of the specimens.

The measurements were performed using a Digital Image Correlation (DIC) system. The results were evaluated in terms of failure modes, crack patterns, and force-slip curves. The slip was measured as the relative displacement between the vertical yarns and the concrete substrate. The results obtained through this experimental campaign show how a different concrete recipe, as well as the presence of a mechanical anchorage, influence both the maximum load and the crack pattern.

References

1. G. de Felice, M. A. Aiello, C. Caggegi, F. Ceroni, S. De Santis, E. Garbin, N. Gattesco, Ł. Hojdys, P. Krajewski, A. Kwiecień, M. Leone, G. P. Lignola, C. Mazzotti, D. Oliveira, C. Papanicolaou, C. Poggi, T. Triantafillou, M. R. Valluzzi, and A. Viskovic, Mater. Struct. **51**, (2018)
2. M. Ricker, F. Häusler, and N. Randl, Eng. Struct. **136**, 345 (2017)
3. T. Mészöly and N. Randl, Eng. Struct. **168**, 119 (2018)

Comparison of laboratory tests with numerical Finite Element Method (FEM) of composite beams with prefabricated surfaces with notches

Grzegorz Sadowski[1,*] *Piotr* Wiliński[1], and *Anna* Halicka[2]

[1]Politechnika Warszawska, Wydział Budownictwa, Mechaniki i Petrochemii, Politechnika Warszawska, Polska
[2]Politechnika Lubelska, Wydział Budownictwa i Architektury, Polska

The subject of this paper is a bent composite element formed by concrete over-poure of a beam prefabricate, with the upper surface of prefabricate shaped with notches. The composite beam subjected to testing consisted of: a prefabricate with dimensions of 25 cm x 15 cm x 300 cm, which surface was made in the form of notches with a spacing of 80 mm and filler concrete with a thickness of 7 cm. The main (bottom) reinforcement of beams consisted of ribbed bars 3Ø20 mm of B500B steel, and as stirrups ribbed bars Ø8 mm of B500B steel were used with a spacing of 8 cm in support zones (112 cm on both sides of the element), while in the compressed part of beam their spacing was 11 cm. In addition, between the layers of concrete made at different times, a stapling reinforcement (two-arm stirrups) in the form of ribbed bars Ø6 mm of B500B steel with a spacing of 16 cm was applied. Beam testing was carried out, among others, with the use of DIC method (digital image correlation). The results of laboratory tests of beams were used to calibrate the virtual model of the composite beam with the finite element 3D method. At different levels of beam load, individual components concerning the calculation of shear resistance in the plane of composite according to fib Model Code 2010 prestandards, i.e. adhesion with interlocking of aggregate, friction between concrete (shear friction effect) and dowel action were analysed.

The virtual model of composite beam was created using the Abaqus program. In order to reproduce the concrete work, a model of plastic concrete with CDP (Concrete Damage Plasticity) destruction was used. The cooperation between reinforcement and concrete was achieved using the "embedded" function. The contact between the prefabricated and filler concrete was modelled using a surface-to-surface of "exponential" form. The cohesive interaction between the concretes was modelled using the "traction-separation" function. The model calibration process was carried out by changing the parameters of stress on the cohesive surface and contact displacement. The calibration was found to be satisfactory, obtaining a similar value of load, at which the filler concrete was separated from the prefabricated concrete in the element tested with the use of imaging method.

Scratching between the prefabricated and filler concrete was observed at a load of approximately 110 kN. Both the tests and virtual beam model have shown that scratches occur on one side of notches. Mutual displacement of layers results in subsidence of the adhesive joint on one side of notch and increase of mechanical overlapping on the other side of notches. As the load increases, scratching between the concrete appears on next notches in the direction of support.

The FEM analysis showed that a significant increase in stress in a staple reinforcement occurs only when the contact is scratched. Scratches of joint and the appearance of tensile forces in the staple reinforcement refer to the mandrel effect, which was taken into account in the fib Model Code 2010 prestandard. In addition, in the analyzed element, as a result of shear

* Corresponding author: grzegorz.sadowski@pw.edu.pl

slippage in the contact plane, connectors indirectly generate shear friction. In the virtual model the shear friction concentration on the notches was observed in a place where the stapling reinforcement occurs.

Both the beam testing with the imaging method and the analysis of virtual FEM showed that the occurrence of scratches at the contact between the prefabricated element and filler concrete is strongly influenced by diagonal cracks arising from the shear. They determine when and where scratches occur between concrete slabs laid at different times.

The virtual model of composite beam and its calibration on the basis of available laboratory tests allow for a deeper analysis of the actual work of tested element. The FEM analysis showed that the proportions of individual components taken into account in the calculations of contact shear resistance are variable and depend to a large extent on the slip intensity in the contact zone. Stress concentration in the contact area depends on the prefabricated surface and the location of stapling reinforcement between the concrete.

Pilot mechanical fracture properties of concrete with lunar aggregate simulant

Stanislav Seitl[1,2*], *Petr* Miarka[1,2], *Iva* Rozsypalová[2], *Kateřina* Pokorná[2], *Zbyněk* Keršner[2], *Jacek* Katzer[3], and *Paweł K.* Zarzycki[4]

[1]Institute of Physics of Materials, Academy of Science of the Czech Republic, Zizkova 22, Brno 602 00, Czech Republic,
[2]Faculty of Civil Engineering, Brno University of Technology, Veveri 331/95 Brno 602 00, Czech Republic
[3]Faculty of Geodesy, Geospatial and Civil Engineering, University of Warmia and Mazury in Olsztyn, Heweliusza 4, 10-720 Olsztyn, Poland
[4]Faculty of Civil Engineering, Environmental and Geodetic Sciences, Koszalin University of Technology, Śniadeckich 2, 75-453 Koszalin, Poland

1 Introduction

The surface of the Moon is covered with a debris blanket, called the regolith, produced by the impacts of meteorites. It ranges from fine dust to blocks several meters across. The fine-grained fraction is usually referred to as the lunar soil [1].

The aim of contribution is evaluate mechanical fracture properties of concrete with lunar aggregates simulant (LAS). The LAS in question was developed by P.K. Zarzycki and J. Katzer after their studies of lunar soil simulants [2]. The investigated and compared properties were the bulk density, the flexural strength, compressive strength, the modulus of elasticity, the fracture toughness, the fracture energy, and the fatigue properties presented by Wöhler curve were tested during the research programme.

2 Material and methods

The properties of LAS were as follows: density 4.700 kg·dm^{-3}, loose bulk density 2.413 kg·dm^{-3}, median diameter [3] 0.193 mm.

The analysed mixture composition of concrete with LAS is introduced, then the mixture composition per 1 m^3 is following: cement mortar based on LAS. Portland, cement (450 kg) + water (225 kg). The amount of LAS was added by volume (to match the volume of standardized sand when adding 1350 kg) due to higher density of LAS.

Bulk density of hardened cement composite based on LAS after 28 days of curing was 3.290 kg·dm^{-3}.

The experimental measurement of mechanical fracture properties started at 224 days due to performance of parallel fatigue experiments. Before fatigue tests the bulk density of hardened cement composite based on LAS was 3.056 kg·dm^{-3}. Compressive strength performed on the rest of samples used for static test on start of fatigue experimental campaign was 39.4 MPa and at the end of fatigue campaign was 41.5 MPa.

The specimens for fracture tests had nominal dimensions of 40 × 40 × 160 mm and were cut in the middle of the span to 1/10 (6 specimen) and to 1/3 (6 specimen) of the specimen height. The specimens were subjected to three-point bending tests (see Fig. 1 left) in which diagrams showing force vs. deflection in the middle of the span and force vs. crack mouth opening

* Corresponding author: seitl@ipm.cz

displacement were recorded. After the processing of these diagrams, the values obtained for the static modulus of elasticity, the effective fracture toughness, the effective toughness and the specific fracture energy were determined using the Effective Crack Model [4], and the Work-of-Fracture method [5]. After the fracture experiments had been performed, compressive strength values were determined from one part of each specimen remaining after testing (Fig. 1 right) for informational purposes.

Fig. 1. Illustration of the test configuration used for the fracture testing of specimens in three-point bending (left), and for the subsequent compressive test (right); span was 140 mm.

3 Conclusion

The mechanical fracture and fatigue properties of concrete with lunar aggregate simulant were measured and analysed. Investigated concrete showed higher values of mechanical fracture properties compared to concrete with classical aggregate.

Financial support provided by the Czech Science Foundation (GACR) under project No. 19-09491S (MUFRAS) is gratefully acknowledged.

References

1. Seweryn, K.; Skocki, K.; Banaszkiewicz, M.; Grygorczuk, J.; Kolano, M.; Kuciński, T.; Mazurek, J.; Morawski, M.; Białek, A.; Rickman, H.; et al. Determining the Geotechnical Properties of Planetary Regolith Using Low Velocity Penetrometers. *Planet. Space Sci.* 2014. https://doi.org/10.1016/j.pss.2014.05.004
2. Zarzycki, P. K.; Katzer, J. Multivariate Comparison of Lunar Soil Simulants. *J. Aerosp. Eng.* 2019. https://doi.org/10.1061/(ASCE)AS.1943-5525.0001075
3. Katzer, J. (2012) 'Median diameter as a grading characteristic for fine aggregate cement composite designing', *Construction and Building Materials*, 35. doi: 10.1016/j.conbuildmat.2012.04.050
4. B.L. Karihaloo, Fracture Mechanics and Structural Concrete. New York: Longman Scientific & Technical, 1995
5. RILEM Technical Committee 50-FMC, Determination of the fracture energy of mortar and concrete by means of three-point bend test on notched beams. Materials and Structures, 18(4) (1985) 285–290
6. H. Šimonová, B. Kucharczyková, I. Havlíková, S. Seitl, Z. Keršner, Key Engineering Materials 592-593, 801–804, (2014)
7. S. Seitl, P. Miarka, H. Šimonová, P. Frantík, Z. Keršner, J. Domski, J. Katzer, Periodica Polytechnica Civil Engineering, 63(1), 152–159, (2019)

Thermal performance of rice husk ash mixed mortar in concrete and masonry buildings

Kajanan Selvaranjan[1,*], *Aaruga* Selvaratnam[1], *J.C.P.H.* Gamage[1], and *G.I.P.* De Silva[2]

[1]Department of Civil Engineering, University of Moratuwa, Srilanka
[2]Department of Materials and Science Engineering, University of Moratuwa, Srilanka

1 Introduction

Rice Husk (RH) is an agricultural waste which is produced in huge amounts from the milling process of paddy rice. Rice husk ash (RHA) is a by-product material obtained from the combustion of rice husk. The amorphous silica (84% - 90%) rich RHA has a wide range of applications. This research investigates the possibility of utilizing RHA in the process of developing a mortar with low thermal conductivity to enhance the thermal comfort in concrete and masonry buildings. A total of thirty combinations of RHA were considered in the development process. The thermal conductivity of mortar was determined by Lee's Disc method, and the results were compared to the data for conventional mortar as well as commercial thermal insulation materials. The results indicate a significant reduction in thermal conductivity in the mortar developed with RHA.

2 Methodology

2.1 Specimens preparation

In this study, following materials used for mortar preparation;

- Cement (OPC)
- Sand
- Three different type of Rice Husk
    1. Rice Husk Powder: obtained by grinding the pure rice husk.
    2. Low carbon Rice Husk Ash (RHA): Rice husk was burnt around 600°C using Furnace.
    3. High carbon Rice Husk Ash (RHA): Rice Husk was burnt in open air under uncontrolled condition.

Mortar sample preparation: Mortar mixture proportion are reported in Table 1 and the water cement ratio and cement sand ratio were kept equal to 0.5 and 1:3 respectively. Three types of RHA were used as sand replacement at 10, 20, 30, 50, 70, 80, and 100 % by weight in mortar mixtures.

* Corresponding author: Kajansss22@gmail.com

Table 1. Mix proportions and consistency of mortars.

Mix designation	RHA (%)	Cement (kg/m^3)	Sand (kg/m^3)	RH Powder (kg/m^3)	LRHA (kg/m^3)	HRHA (kg/m^3)	Water (kg/m^3)
M0	0	450	1350	0	0	0	225
M10	10	450	1215	135	135	135	225
M20	20	450	1080	270	270	270	225
M30	30	450	945	405	405	405	225
M50	50	450	675	675	675	675	225
M70	70	450	405	945	945	945	225
M80	80	450	270	1080	1080	1080	225
M100	100	450	0	1350	1350	1350	225

2.2 Thermal conductivity

To check the thermal conductivity samples were prepared in cylinder shaped moulds (60 mm) in diameter and 5 mm in thickness. After 28 days of curing in water, the specimens were tested using Lee's disc method. In each case the average of 3 samples were tested.

2.3 Scanning electron microscopy (SEM) and X-ray Diffraction (XRD)

Raw materials and interfacial zones between cement paste and RHA were observed by means of SEM. The crystalline phases of natural sand and RHA were investigated using XRD technique.

3 Conclusion

It is interesting to note that the use of RHA as fine aggregate replacement improved the thermal insulation. Since the thermal conductivity of mortar made with 100 % RH powder, HRHA and LRHA were reduced by 69.19 %, 63.47 % and 56.23 % respectively.

The author wishes to acknowledge the technical staff of Structural Testing Laboratory and Building Materials Laboratory of the University of Moratuwa for their assistance and support extended during the experimental work. And the financial support provided to the undergraduate research projects and NRC grant (NRC/PPP/18/01) is greatly appreciated.

References

1. H. Nguyen, S. Gallardo, F. Bacani, H. Hinode, Q. Do and M. Do, "Evaluating thermal properties of geopolymer produced from red mud, rice husk ash and diatomaceous earth," 2017
2. J. MacMullena, Z. Zhanga, E. Rirschb, H. N. Dhakala and N. Bennetta, "Brick and mortar treatment by cream emulsion for improved water repellence and thermal insulation," 2011
3. J. S. Patel, D. K. B. Parikh and P. A. R. Darji, "Study on Concrete Using Fly Ash, Rise Husk Ash and Egg Shell Powder," 2017
4. P. Kapur, "Thermal Insulations from Rice Husk Ash, an Agricultural Waste," 1980
5. S. M. S. Kazmi, S. Abbas, M. J. Munir and A. Khitab, "Exploratory Study on the Effect of Waste Rice Husk and Sugarcane Bagasse Ashes in Burnt Clay Bricks," 2016

Application of virtual models for estimating concrete properties

Piet Stroeven[1], and *Marta* Słowik[2,*]

[1]Faculty of Civil Engineering and Geosciences, Delft University of Technology, Stevinweg 1, 2628 CN Delft, the Netherlands
[2]Department of Structural Engineering, Faculty of Civil Engineering and Architecture, Lublin University of Technology, Nadbystrzycka 40, 20-618 Lublin, Poland

1 Introduction

In the paper the virtual model called "compucrete" is presented. This is a model of the real concrete made by the computer. The model was constructed to reduce efforts and time when analysing various properties of cementitious materials. It has been applied already to estimate concrete properties like Young's Modulus and tensile strength [1,2]. Going from the meso- to the micro-level, also porosimetry has been conducted on the basis of which permeability has been estimated. This paper will concentrate on the quality of the model. Possible applications of the model for estimation of concrete properties are discussed in the paper as well.

2 Network analysis

The paper shortly resumes the successive modules jointly composing the concept behind the construction of the "compucrete", successively, particle packing by dynamic DEM (Discrete Element Model), hydration simulation by XIPKM (Extended Integrated Particle Kinetics Method), assessment of structural features of the hardened material by DRaMuTS (Double Random Multiple Tree Structuring), measuring structural features by SVM (Star Volume Method) – Fig.1. The development of the sequence of these modules – and their application – is basically the product of a series of PhD studies realized at Delft University of Technology under supervision of P. Stroeven.

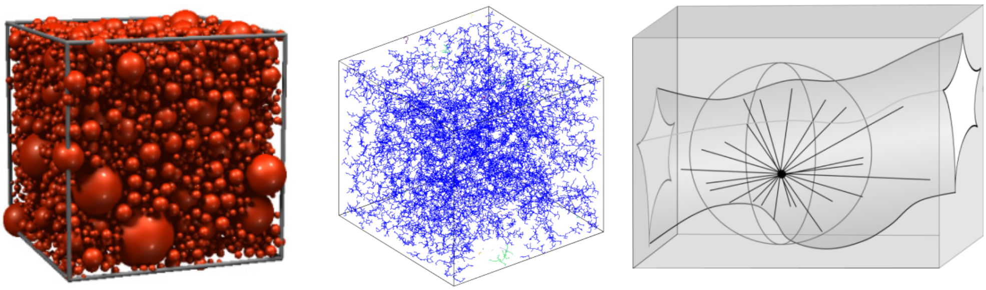

Fig.1. Steps of computing: particle packing, pore delineation, size measuring.

* Corresponding author: m.slowik@pollub.pl

A new development of the model is connected with nano-packing of cement nodules to better mimic the hydration process, and improving the input parameters for the permeability estimation process [3]. The effectiveness of the modified virtual model was discussed on the basis of a permeability estimation process. The performed analysis also focused on porosimetry of cement paste. The fact that the water saturation degree in a sample has a significant influence on obtained data was taken into account. The effect of interfacial transition zone (ITZ) percolation on permeability was discussed as well.
As shown in the paper, the water saturation degree can be varied in the presented model. Obtained results were found in a good agreement with published data demonstrating the reliability of the approach. Next, it was demonstrated that the controversial issue of ITZ percolation on permeability could be solved on the basis of the virtual concrete. Finally, the approach is very appropriate for studying the effects of mineral admixtures on properties of concrete. Recapitulating, it can be concluded that the presented virtual model is economic and versatile [4].

3 Possible application of the model

The successful application of the presented virtual model to the water permeability estimation seems to be promising for achieving further progress in analyzing properties of cementitious materials. In the next research approach, with a potential use of the "compucrete", pores as well as microcracks could be taken into consideration to wider describe water permeability. Furthermore, the virtual model could be applied for discussing fracture parameters of concrete, for example fracture energy that governs the processes of microcracks and pores coalescing in the active fracture process zone (as it is described in the literature, for example [5, 6]). Particularly, the effect of the total porosity as well as the type and the size of aggregate on fracture energy of concrete is worth dealing with, since there is still no consensus on the influence of aggregate granulation and concrete porosity on cracks' formation in concrete structures.

References

1. He, H., Stroeven, P., Stroeven, M., Sluys, L.J. (2012) Influence of particle packing on elastic properties of concrete. Mag. Concr. Res., 64(2), 163–175
2. He, H., Stroeven, P., Stroeven, M., Sluys, L.J. (2011) Influence of particle packing on fracture properies of concrete. Comp. Concr., 8(6), 677–692
3. Stroeven, P., Li, K., Le, L.B.N., He, H., Stroeven, M. (2015) Capabilities for property assessment on different levels of the micro-structure of DEM-simulated cementitous materials. Constr. Build. Mats., 88, 105–117
4. Stroeven, P., Słowik M. (2019) Economic and reliable estimation of cementitious materials properties on the basis of virtual models. In: Brittle Matrix Composites 12, Institute of Fundamental Technological Research, Warsaw, 35–44
5. Słowik, M. (2006) The Analysis of Crack Formation in Concrete and Slightly Reinforced Concrete Member in Bending. In: Brittle Matrix Composites 8, Woodhead Publishing Ltd., Cambridge, ZTurek Research-Scientific Institute, Warsaw, 351–360
6. Słowik, M., Błazik-Borowa, E. (2009) The Influence of Aggregate Size on the Width of Fracture Process Zone in Concrete Members. In: Brittle Matrix Composites 9, Woodhead Publishing Ltd., Cambridge, and IFTR, Warsaw, 429–438

Crack mechanisms in concrete – from micro to macro scale

Marta Słowik[1,*], *Piet* Stroeven[2], and *Amanda* Akram[1]

[1]Department of Structural Engineering, Faculty of Civil Engineering and Architecture, Lublin University of Technology, Nadbystrzycka 40, 20-618 Lublin, Poland
[2]Faculty of Civil Engineering and Geosciences, Delft University of Technology, Stevinweg 1, 2628 CN Delft, the Netherlands

1 Introduction

Cracking is acknowledged to be a major aspect of concrete behavior. The internal structure of hardened concrete is intensely micro-cracked before loading. Once loaded, the further developed crack structure is submitted to environmental influences endangering structural integrity. Under loading we observe micro-cracks to grow and, upon further load increase, to coalesce until they form a macro-crack. At still higher loadings, the macro-crack can grow and spread leading to material fracture. Taking into account that concrete is a brittle material, the analysis of crack mechanisms in concrete, both on micro as well as macro level, is of paramount importance in the theory of concrete structures.

2 Micro and macro cracks analysis

When investigating crack mechanisms in normal strength concrete, it can be observed that concrete is intensely micro-cracked in the so called virgin state. Micro-cracks are mostly situated at the aggregate grain surfaces as the result of high stresses due to evaporation of pore water (Fig. 1.a). Loading is demonstrated leading to growth and coalescence of these micro-cracks to yield global damage characteristics typical for the loading type and intensity ([1]). A higher strain concentration under loading is observed in an active zone of the specimen where microscopic cracks tend to grow and coalescence. This zone is called the fracture process zone (FPZ) and it is often referred to as a progressive microcracking zone between the real crack and the non-cracked portion of concrete (Fig. 1.b).

Crack mechanisms are still subject of continuing studies both on micro- as well as macro-level. It has been demonstrated that the basis of nonlinear fracture mechanics can be applied to describe the phenomenon of concrete work, in particular the fictitious crack model proposed by Hillerborg [2] has appeared very useful in analysis of concrete cracking. The model describes tensile concrete behavior (strain-softening phenomenon) and fracture parameters of concrete like the shape of the σ–δ curve and fracture energy G_F.

* Corresponding author: m.slowik@pollub.pl

a) b)

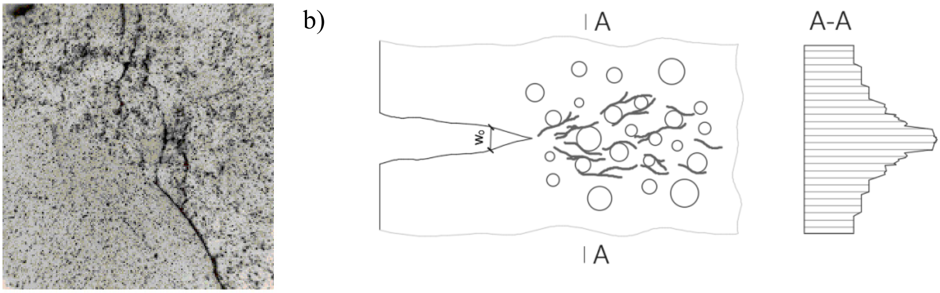

Figure 1. Crack mechanisms in concrete: a) interface microcrack of large spherical grain enters matrix where vertically oriented surfaces of smaller particles are pre-cracked in an “en échelon” array; b) under loading a higher strain concentration is observed in the fracture process zone, microcracks concentrate along weak interfaces surrounding the grains of aggregate and then join and propagate through the cement matrix, so that finally a macrocrack develops.

The application of softening model in Finite Element Method analysis allowed to deeper describe fracture processes connected with formation of failure crack in concrete member. Additionally, it may explain the higher crack resistance observed during the experiments comparing to cracking forces calculated on the basis of linear elastic theory. Differences in mechanisms of crack’s formation in members of different reinforcement ratios has been demonstrated to explain the higher cracking resistance in reinforced concrete member comparing to a plain concrete one [3]. The significant progress with describing size effect was possible after performing numerical simulations using of the fictitious crack model.

The performed numerical analyses [4] have shown that the width of the fracture process zone does have an influence on the FEM results. However, no consistent rules are available to take the width of microcracked zone in account while modeling concrete structures. Also no definite conclusions can be drawn as far as the influence of aggregate size on the width of the fracture process zone.

Although significant progress in recognizing crack mechanisms in concrete has been achieved, there are still some aspects that should be resolved in depth, for example the role of aggregate particles on crack development. This problem is supposedly associated with (sub-level) micro-crack formation resulting from the virgin state, and predominantly leading to partly debonded aggregate grains at the start of the test. This latter phenomenon is definitely depending on aggregate size as it has been demonstrated in the paper.

References

1. P. Stroeven, Some observations on micro-cracking in concrete subjected to various loading regimes, Engrn. Fract. Mech., 35(4/5), pp. 775–782 (1990)
2. A. Hillerborg, M. Modeer, P. E. Petersson, *Analysis of Crack Formation and Crack Growth in Concrete by Means of Fracture Mechanics and Finite Elements*, Cement and Concrete Research, Vol. 6, 773–782 (1976)
3. M. Słowik, *The analysis of failure in concrete and reinforced concrete beams with different reinforcement ratio*, Archive of Applied Mechanics, Vol. 89, pp. 885–895 (2019)
4. M. Słowik, *Numerical analysis of the width of fracture process zone in concrete beams,* Computational Materials Science. 50, pp. 1347–1352 (2011)

Fractal dimension analysis of three-point bend test specimens

Jakub Sobek[1,*], *Petr* Frantík[1], *Tomáš* Trčka[2], and *David* Lehký[1]

[1]Brno University of Technology, Faculty of Civil Engineering, Brno, Czech Republic
[2]Brno University of Technology, Faculty of Electrical Engineering and Communication, Brno, Czech Republic

1 Introduction

The aim of this paper is to analyze fractal geometry of fracture surfaces of concrete specimens tested in a three-point bending (3PB) configuration (RILEM 1985). This type of test is characterized by higher level of constraint at the tip of a propagating crack. Presented study is a part of the research focused on development of a complex multilevel approach for experimental–computational determination of mechanical fracture parameters of concrete which is a typical and frequently used quasi-brittle material in civil engineering practice. A total of 42 specimens of different sizes, depths of notches and test configurations were tested in laboratory. Half of the specimens were tested in 3PB configuration. This set consists of specimens with three different nominal sizes and two depth of notches (shallow and deep). Fifteen representative specimens were chosen out of this set for fractal dimension analysis. Their fracture surfaces were scanned by 2D optical profilometry (Ficker & Martišek 2012) and analyzed by FracDiM software (Frantík 2019), created in Java programming language. Software provides values of fractal dimensions for each scanned row and their values are close to value of line dimension.

2 Analysed specimens

A total of 15 fracture surfaces of 15 tested specimens were selected for fractal dimension analysis. All specimens have the same width of 100 mm but differ in width and depth. Six specimens are of small size (with depth of 100 mm), three of medium size (200 mm) and three of large size (300 mm). Length of each specimen is four times its width. Specimens were made of C30/37 concrete with maximum aggregate grain size of 16 mm.

3 Optical profilometry in 2D

Determination of the fracture surface profile was done by the optical profilometry (which is widely used in a lot of industrial applications). It is a non-destructive and non-contact method how to analyse changes in a surface plane. Laser 2D profilometer operates generally with a defined wavelength semiconductor laser and uses principle of the laser triangulation for two-dimensional profile detection on different target surfaces. The diffusely reflected light from the laser line is replicated on a sensitive sensor matrix by a high-quality optical system and evaluated in two dimensions. Obtained output is values in a two-dimensional coordinate system. The distance of 50 μm was selected between the scanned lines and the spacing between adjacent points was also set to 50 μm within one line. Typical illustration of cracked ligament area can be seen in Fig. 1.

* Corresponding author: jakub.sobek@vut.cz

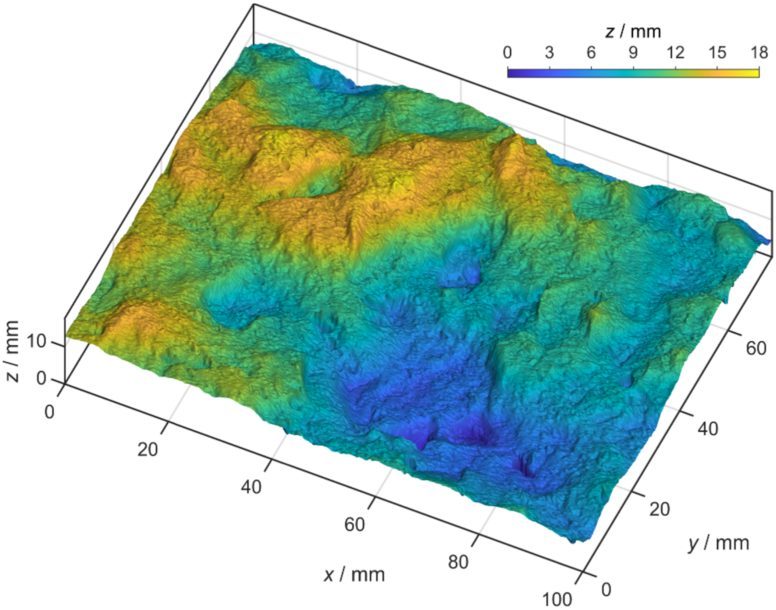

Fig. 1. Typical image of scanned area of interest of ligament's profile, dimension *z* represents depth.

4 Evaluation of fractal dimensions and conclusions

Data of all scanned lines (their depths) served as inputs to FracDiM software. The walking divider method (Richardson 1961) was used together with adjustable arc length dimension and a transformation according to Mandelbrot (1967). Software analyses fractal dimensions sequentially (row by row) and is also able to provide error of calculation. Results of fractal analyses for all selected specimens are compared and discussed with respect to specimen sizes, depth of notches etc.

The financial support from Czech Science Foundation (GACR) project MUFRAS No. 19-09491S is gratefully acknowledged.

References

1. T. Ficker, D. Martišek, Digital fracture surfaces and their roughness analysis: Applications to cement-based materials, Cement and Concrete Research **42**, (2012) 827–833
2. P. Frantík, *FracDiM* software (2019), http://www.kitnarf.cz
3. B. Mandelbrot, How Long Is the Coast of Britain? Statistical Self-Similarity and Fractional Dimension, Science **156**, 3775 (1967) 636–638
4. B. Mandelbrot, *Les objets fractals. Forme, hasard et dimension* (Flammarion, Paris, 1975)
5. L. F. Richardson, The Problem of Contiguity: An Appendix to Statistics of Deadly Quarrels, General System Yearbook **6**, (1961) 139–187
6. RILEM TC-50 FM, Determination of the fracture energy of mortar and concrete by means of three-point bend tests on notched beams, Mater. Struct. **18**, 107 (1985), 287–290

Shear tests on GFRP reinforced concrete beams

Damian Szczech[1,*], and *Renata* Kotynia[1]

[1]Lodz University of Technology, Department of Concrete Structures, Al. Politechniki 6, Lodz, Poland

1 Introduction

Fibre reinforced polymer (FRP) bars have been increasingly used as one of the main substitutes for traditional steel reinforcement, especially in reinforced concrete structures. This paper presents the results of experimental tests and the analysis of variable parameters of concrete beams reinforced with FRP composite bars.

This paper aims to investigate the shear failure mechanisms in beams reinforced with longitudinal and transverse glass fibre reinforced polymer bars. The objective of the study was to investigate the influence of three main changeable parameters on the shear strength of GFRP reinforced concrete beams in comparison to a beam without shear reinforcement: longitudinal reinforcement ratio, transverse reinforcement ratio and the influence of stirrup diameter and spacing with the same shear reinforcement ratio.

2 Experimental program

The presented research results contain a part of a more extensive research program consisting of 22 beams. The paper presents the results of tests performed on seven beams with various variable parameters affecting the value of shear strength. Two longitudinal reinforcement ratios and three transverse reinforcement ratios were used. The closed GFRP stirrups with two different bar diameters and three different spacings were used for shear reinforcement. Both types of reinforcement were made of the GFRP bars with single braid ribs. Structural steel reinforcement was also used in the beams to avoid shear failure on opposite support region of the beam. For comparison, the same additional beams were tested only with longitudinal GFRP reinforcement in order to reliably compare the load capacity of the element with transverse reinforcement in relation to the element without the stirrups. Detailed variable parameters of the analysed beams are summarised in table 1.

Table 1. Variable parameters of analysed beams.

Beam name	Tensile reinforcement	Longitudinal reinforcement ratio	Stirrups diameter	Stirrups spacing	Transverse reinforcement ratio
TG-525-8/250	5ϕ25	2.91%	8 mm	250 mm	0.16%
TG-525-8/200	5ϕ25	2.91%	8 mm	200 mm	0.20%
TG-528-8/250	5ϕ28	3.69%	8 mm	250 mm	0.16%
TG-528-8/200	5ϕ28	3.69%	8 mm	200 mm	0.20%
TG-528-8/120	5ϕ28	3.69%	8 mm	120 mm	0.33%
TG-528-12/270	5ϕ28	3.69%	12 mm	270 mm	0.33%
TG-528-N	5ϕ28	3.69%	beam without stirrups		

* Corresponding author: damian.szczech@p.lodz.pl

The same concrete with a maximum aggregate grain diameter of 8 mm was used for each beam. The mean value of experimental compressive concrete strength was 39.5 MPa.

The three-point loaded beams had a shear span-to-depth ratio (*a/d*) equal to 3.15 referring to the slender beams. All single-span simply-supported beams had a T-section with 400 mm in height and an axis span of 1800 mm. The static scheme of the beams with details of their geometry and reinforcement is shown in Figure 1.

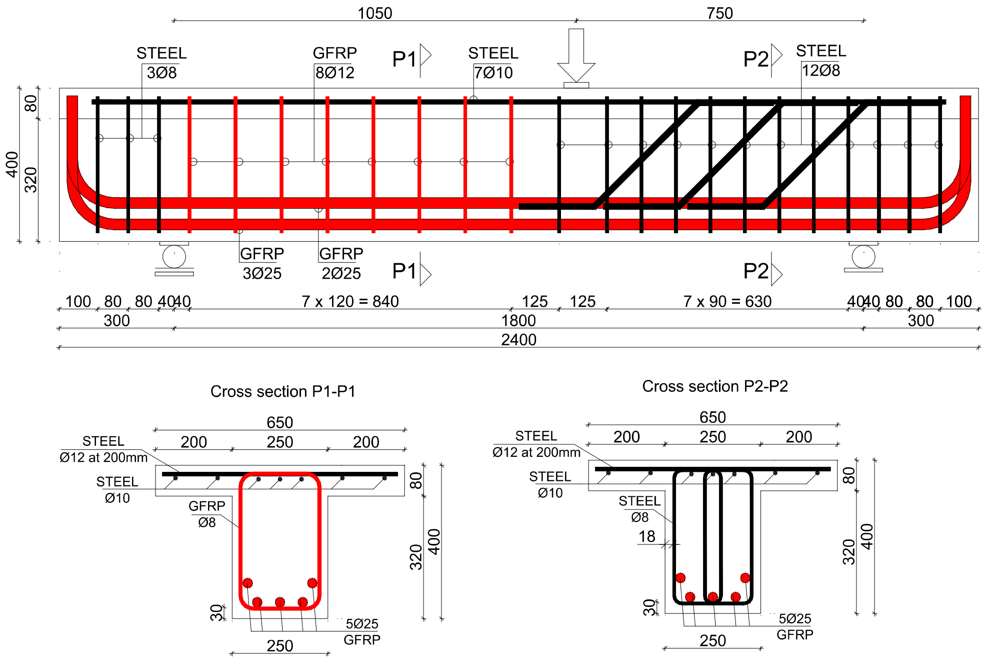

Figure 1. Geometry of beams with reinforcement.

The mechanisms of cracking, deformation and failure of the tested beams were analysed. Deflection of the elements and the differences in the strains of longitudinal reinforcement and stirrups are presented and discussed. Additionally, the paper contains an analysis of the calculated results of the tested beams in relation to the design shear capacity according to the existing codes: Eurocode 2 standards (CEN/TC 250/SC), Italian standard (CNR-DT-203/2006), American standard (ACI 440.1R-15) and Canadian standard (CAN/CSA-S806-12).

References

1. W. Zhao, K. Maruyama, H. Suzuki. RILEM Proceedings. CHAPMAN & HALL, 1995
2. H. Nakamura, H. Takeshi. Doboku Gakkai Ronbunshu 1995.508 (1995)
3. N. Duranovic, K. Pilakoutas, P. Waldron. Non-met. (FRP) rein. for con. struc. 2 (1997)
4. E. Shehata, R. Morphy, S. Rizkalla. Canadian Journal. of Civil Eng. 27.5 (2000)
5. P.A. Whitehead, T.J. Ibell. ACI Structural Journal 2005;102(2)
6. J. Hegger, J. Niewels, M. Kurth. FRPRCS-9 Sydney, Australia, July 2009
7. E. Oller, A. Marí, J. Bairán, A. Cladera. Composites part B, vol. 74, 2015
8. E. A. Ahmed, E. F. El-Salakawy, B. Benmokrane. ACI Struct. Jour. 2010 no. 107-S06

Experimental tests of RC beams flexural strengthening with NSM CFRP strips

Damian Szczech[1,*], *Łukasz* Krawczyk[1], and *Renata* Kotynia[1]

[1]Lodz University of Technology, Department of Concrete Structures, Al. Politechniki 6, Lodz, Poland

1 Introduction

In recent years, the strengthening technique based on near surface mounted (NSM) laminates of fibre reinforced polymer (FRP) has been used to increase the load capacity of concrete elements. The paper presents test results of reinforced concrete beams strengthened in flexure with carbon fibre reinforced polymer (CFRP) strips using the NSM technique, which is based on the application of the FRP reinforcement into the grooves cut in the concrete cover of the RC elements.

The NSM technique confirms higher flexural and shear strengthening effectiveness than the externally bonded reinforcing (EBR) technique. The efficiency of both method depends on the bond behaviour, which is better in the case of the NSM technique mainly due to the greater contact area between the strip and the concrete. This is especially clear if a degree of the longitudinal steel reinforcement is low. The strengthening of RC structures in flexure using CFRP composites mounted into the concrete cover showed high strengthening efficiency both in the ultimate and serviceability limit states.

2 Experimental program

The four full-scale reinforced concrete beams with a cross section of 200 x 400 mm and an axis span of 3600 mm were tested under four-point loading. The analysed beams were a part of the wider research programme contained of 9 beams. The tensile reinforcement consisted of 2 steel bars with 14 mm diameter (longitudinal reinforcement ratio equal to 0.43%). The top reinforcement of all beams was designed in the form of 2 steel bars with a diameter of 10 mm. Transverse stirrups with a diameter of 6 mm at a spacing of 150 mm were used as the shear reinforcement. The concrete cover of the main reinforcement was 31 mm. Figure 1 shows the beam geometry and static scheme.

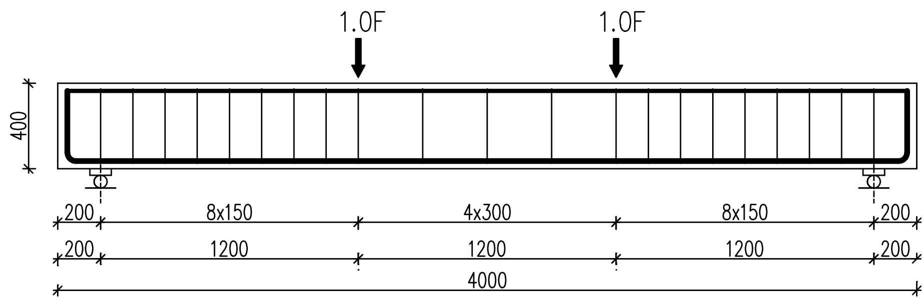

Figure 1. Geometry of beams with reinforcement.

* Corresponding author: damian.szczech@p.lodz.pl

For the flexural strengthening of the reinforced concrete beams, CFRP laminates with a cross section of 2.5 mm x 15 mm were installed into a groove of 6 mm x 19 mm in cross section cut in the concrete cover along the beam's length. The main value of Young's modulus for the CFRP laminate was equal to 168 GPa. The first beam was strengthened with one CFRP strip under its own weight, while the second RC beam was strengthened under preloading bending moment of 30 kNm (in 46% of total load capacity of the unstrengthened beam). The third of the beams was strengthened with two strips under 30 kNm bending moment load as well. One of the RC beams was tested without any strengthening. All analysed beams with reinforcement are shown in Figure 2. The mean value of experimental compressive concrete strength was 40 MPa. The details of strengthening configuration with are presented in Fig. 3.

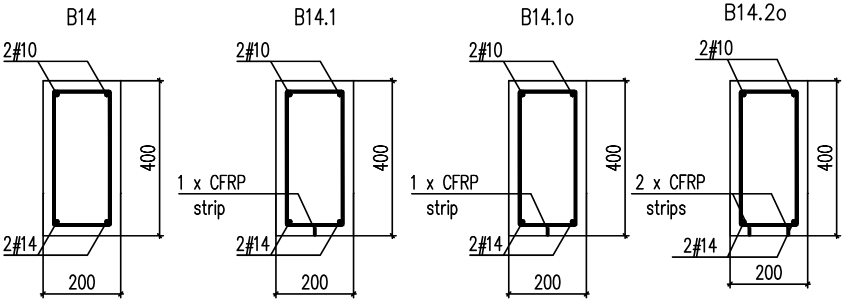

Figure 2. Cross section of tested beams with steel reinforcement.

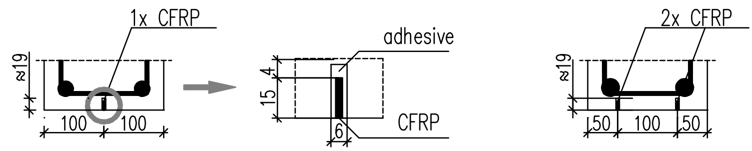

Figure 3. Strengthening configuration with NSM CFRP strips.

All the strengthened beams failed by rupture of the CFRP laminates after the tensile steel yielding. The mechanisms of cracking, deformation and failure modes of the tested beam elements were analysed. Deflection of the elements and differences in the beams ductility are discussed in the paper. The most important test result refers to the high strengthening efficiency of NSM technique. The influence of the NSM reinforcement ratio is analysed in the paper in details.

References

1. A. Bilotta, F. Ceroni, E. Nigro, M. Pecce. Composite Structures, 2015
2. M. Rezazadeh, I. Costa, J. Barros, Composite Structures, 2014
3. M. Przygocka, R. Kotynia, K. Lasek, Proceedings of AMCM, 2014
4. R. Kotynia, K. Lasek, M. Staśkiewicz, Journal of Composites for Construction, 2013
5. M. Badawi, K. Soudki, Construction and Building Materials, 2009
6. J. Barros, S. Dias, J. Lima. Cement and Concrete Composites, 2007
7. J. Barros, A. Fortes, Cement and Concrete Composites, 2005

Mechanical performance of FRP-RC flexural members subjected to fire conditions

Elżbieta Szmigiera[1], *Kostiantyn* Protchenko[1,*], *Marek* Urbański[1], and *Andrzej* Garbacz[1]

[1]Warsaw University of Technology, Faculty of Civil Engineering, 16 Armii Ludowej av., 00-637 Warsaw, Poland

1 Introduction

The implementation of Fibre-Reinforced Polymer (FRP) bars as an alternative solution to traditional methods of reinforcement has become a fascinating issue both theoretically and practically. This topic has garnered attention mainly due to the relatively significant mechanical properties of the bars in the longitudinal direction, the ease of handling, and a high corrosion resistance. The latter can potentially influence the concrete cover thickness, since the bars` properties are not affected considerably by aggressive environments.

On the other hand, one of the main concerns that limit the widespread adoption of these materials in reinforced concrete (RC) structures is their unexplored response to elevated temperatures. As suggested in literature, the behaviour of FRP reinforcement at elevated temperatures can differ from conventional means and depends on the glass transition temperature of the resin. When the temperature in the resin reaches this point, it becomes unable to redistribute the stresses along the fibres, however the fibres continue to withstand loading until the next threshold at which fibres begin to degrade is reached, which is essentially the failure of the structure. Therefore, the fire resistance of FRP reinforcement and FRP-RC structures is an important topic that needs careful analysis before being implemented in RC structures.

Presented and discussed are experimental results for full-scale FRP-reinforced beams subjected to different fire scenarios; some samples were loaded and heated simultaneously, and some were heated at the first stage and then, after a cooling phase, loaded until failure to check their residual strength. In addition, different reinforcement ratios and bar types were used.

2 Hybrid FRP reinforcement

The distinct mechanical behaviour of FRP bars makes designing structures with FRP reinforcement differ from RC design. Properties of FRP bars vary depending on the constituents used and can be adjusted to desirable design situations, cost-efficiency, and environmental attributes for a new developed Hybrid FRP (HFRP) type.

The specimens were reinforced with different FRP bars, such as: BFRP, HFRP, and nano-Hybrid FRP (nHFRP) bars. Producing hybrid bars is analogous to the process of producing other commercially available FRP bars, where a part of the fibres is physically substituted with another fibre type. The selected fibres were basalt and carbon bounded in epoxy resin. For the nHFRP bars, the matrix was modified by adding a four-component 1300 System® to the epoxy resin. A detailed overview on the mechanical properties of HFRP and nHFRP bars utilized for this work is provided in [1-2].

* Corresponding author: k.protchenko@il.pw.edu.pl

3 Fire resistance testing

For this investigation, it is necessary to distinguish two testing groups, namely standard testing and the testing of residual properties of beams.

3.1 Testing of residual properties of the beams

Six full-scale beams were used for testing; three of them were first loaded at 50% of their ultimate strength capacity, then unloaded before being heated in a furnace and allowed to cool, and finally reloaded flexurally until failure. The other three beams were used as reference for the evaluation of the residual strength of tested beams. The results show an atypical behaviour observed in HFRP and nHFRP bar reinforced beams, where after a certain temperature threshold the deflection begins to decrease.

3.2 Standard fire resistance testing

The experimental work involved the preparation of 12 FRP-RC beams. Six of the beams were tested under typical conditions in accordance with a standard heating curve ISO-834 (1990); the specimens were heated and simultaneously loaded in a four-point test by a sustained load until failure, six other beams were used as reference specimens and were not subjected to heating. Beam failure was caused in different ways, beams reinforced with BFRP bars were destroyed by reinforcement failure while those reinforced with hybrid FRP bars were destroyed by concrete crushing. Figure 1 shows that the temperature caused the HFRP bars to burn, however fibres continued to withstand loading. The BFRP-reinforced beams obtained a maximum temperature of 900 °C, compared to beams reinforced with hybrid FRP bars which reached 300-500 °C at failure. Moreover, the highest ductility that was registered was obtained for BFRP reinforced beams, where the maximum deflections reached approximately 16 cm.

Figure 1. Uncovered HFRP Bars (by removing the clear cover after testing).

References

1. E. Szmigiera, K. Protchenko, M. Urbański, A. Garbacz. Innovative HFRP Bars. MATEC Web of Conf 2018, 196, 1–6.
2. E. Szmigiera, K. Protchenko, M. Urbański, A. Garbacz. Mechanical Properties of Hybrid FRP Bars and Nano-Hybrid FRP Bars. Archives of Civ Eng 2019, 65(1), 97–110.

Modification of early strength parameters of concrete containing fly ash and admixture of nano C-S-H as a possible application in 3D printing of concrete buildings

Bartosz Szostak[1*], and *Grzegorz L.* Golewski[1]

[1]Lublin University of Technology, Poland

1 Introduction

The construction industry has been growing faster in recent years. 3D printing of concrete buildings is becoming more common. The development of this innovative technology is associated with the need to develop new techniques and materials. A very important parameter of the material from which houses are printed is its early compressive strength and plasticity. Currently, chemical modification and geopolymer concretes are used to improve mortar parameters. At the moment these are expensive solutions, and some of them are additionally not ecological.
In the paper, the authors present the tests results of traditional cement mortars with the addition of siliceous fly ash (FA) and C-S-H nano-admixture.
The use of FA has a positive effect on the economic (cement replacement) and ecological aspect (reduction of the CO_2 production to the atmosphere). In addition, the use of FA causes better plasticity of the mixture. The use of the C-S-H nano-admixture has a positive effect on shortening the setting time and a rapid increase in the strength of mixtures without losing their subsequent properties, which is presented in the research described in the paper.

2 Experimental research

In the experimental study, the authors compared chosen mechanical and physical parameters of the reference cement pastes (without the C-S-H nano-admixture) and those with the addition of silica FA and C-S-H nano-admixture. On this basis, the impact of FA and nano-admixture on the selected parameters of the cement paste in the early maturation periods was determined – after 4, 8, 12, 24, and 72h.
In addition, the same parameters were tested after 28 days to determine the effect of the additives and admixtures used, on the final parameters of the mix.
The following tests were carried out on previously prepared samples: the compressive strength test on a hydraulic press, the test of setting time and the test of cement matrix shrinkage.
Four types of mixtures were used in the study, differentiated in terms of a FA content and admixture of the C-S-H crystals. The water-binder ratio and the amount of additives and admixtures used result from previous experimental studies of the authors.
The following types of mixtures were used in the tests:

- 0% content of fly ash and 4% of C-S-H: FA-0 CSH-4,
- 20% content of fly ash and 4% of C-S-H: FA-20 CSH-4.
- 0% content of fly ash and 0% of C-S-H: FA-0 CSH-0,
- 20 % content of fly ash and 0% of C-S-H: FA-20 CSH-0.

* Corresponding author: b.szostak@pollub.pl

Fly ash negatively affects the early strength parameters of cement pastes. Significant influence of the C-S-H nano-admixture was observed. After 8h, the strength of the FA-0 CSH-4 and FA-20 CSH-4 samples was nearly 4 times higher than the reference samples. After 72 hours and 28 days, the strength parameters of the mixtures were already similar.
During the setting time study, the FA was found to delay the start of hydration process. The use of the nano-admixture, on the other hand, reduces this time by almost half and reduces the negative impact of fly ash. Both the addition of ashes and admixture do not adversely affect the length of the setting time – they do not shorten it, allowing to build the proper microstructure.
In the initial maturation period (about 10 days), the presence of FA and C-S-H nano-crystals did not significantly affect the shrinkage value. Visible differences were only observed after 10 days. Based on the research, it was found that the use of nano-admixture together with FA significantly reduces the value of shrinkage compared to other mixtures.

3 Conclusions from the research

Based on the experimental research, it was found that:

- The use of the C-S-H nano-admixture has a positive effect on the compressive strength parameters of cement pastes in the early periods. In the first periods tested, the increase in strength was even several times, then gradually decreased. After 72 hours, the influence of nano-admixture was negligible.
- The use of the C-S-H nano-admixture significantly speeds up the start of the setting time of the cement without shortening the whole process.
- The use of the C-S-H nano-admixture and FA had a positive effect on the cement matrix shrinkage. Samples with the 20-4 designation were characterized by the smallest shrinkage of all samples tested.
- The proposed modification of concrete can be used in the technology of 3D printing of buildings

References

1. Le, T T.; Austin, S A.; Lim, S; Buswell, R A.; Gibb, A G. F.; Thorpe, T: Mix design and fresh properties for high-performance printing concrete. Mater Struct 45 (8), p. 1221–1232 2012
2. Pacewicz, K; Sobotka, A; Gołek, Ł: Characteristic of materials for the 3D printed building constructions by additive printing. MATEC Web Conf. 222 (3), p. 1013, 2018.
3. Paul, S Chandra; Tay, Y Wei Daniel; Panda, B; Tan, M Jen: Fresh and hardened properties of 3D printable cementitious materials for building and construction. Archives of Civil and Mechanical Engineering 18 (1), p. 311–319, 2018
4. Sadowski, Ł: Results Obtained at the Nano-scale, w: Multi-scale approach for layered systems made of cement composites, red. Sadowski Łukasz, t. 101.: SPRINGER (Advanced Structured Materials), p. 149–154, 2019
5. Szostak, B; Golewski, G L.: Effect of Nano Admixture of CSH on Selected Strength Parameters of Concrete Including Fly Ash. IOP Conf. Ser.: Mater. Sci. Eng. 416, p. 12105, 2018
6. Van Der Putten, J; Deprez, M; Cnudde, V; Schutter, G de; van Tittelboom, K: Microstructural Characterization of 3D Printed Cementitious Materials. Materials (Basel, Switzerland) 12 (18). DOI: 10.3390/ma12182993

Assessment of the early-age strains and stresses in 2D restrained self-stressed members

Viktar Tur[1], and *Volha* Sannikava[2,*]

[1]Brest State Technical University, Department of Concrete Technology and Building Materials, 224017 Brest, Republic of Belarus
[2]Brest State Technical University, Department of Geotechnics and Transport Communications, 224017 Brest, Republic of Belarus

1 Introduction

Expansive concrete is widely used both for compensation of shrinkage stresses and creation of compressive stresses in structural concrete members. Considerable application area of ones concerns the elements with two-way or three-way restraint conditions. Although the existing design models predict the stress-strain parameters of self-stressing elements in a variety of ways, the comprehensive assessment of restrained expansion strains and corresponding self-stresses is an important task during the design of expansive concrete elements under 2D or 3D confinement.

2 Theoretical background of the design model in case of 2D restraint conditions

The paper proposes the design model for the assessment of expansion strains and self-stresses in case of two-way restraint conditions at the early age of expansive concrete. The concept of the proposed design model is based on the modified early age strains development model (MSDM) for the case of uniaxial restraint arrangements [1]. The main assumptions of the proposed model are as follows:

1) restrained expansion strain at any i-*th* time interval is an algebraic sum of free expansion strain, elastic strain, creep strain at i-*th* time interval and additional strain caused by the restrictive force induced by the restraint at (i-1)-*th* time interval;
2) the presence of confinement in orthogonal directions is considered utilizing the Poisson's ratio for only elastic part of expansive concrete deformations;
3) equilibrium condition between resultant forces in restrictive reinforcement and expansive concrete section takes place in directions x and y at any i-*th* time interval.

In general case restrained expansion strains in direction x and y are calculated in accordance with the expressions:

$$\begin{cases} (\Delta\varepsilon_{s.x})_i = \dfrac{D_{x.i}}{D_{x.i}+1}\left((\Delta\varepsilon_{cf})_i - \sum\limits_{j=1}^{i-1}\left[(\Delta\sigma_{c.x})_j \cdot \dfrac{\Delta\varphi(t_i,t_j)}{E_{c.28}}\right]\right) - \dfrac{\sum\limits_{j=1}^{i-1}(\Delta\sigma_{c.x})_j}{E_c(t_{(i-1)+1/2})} \\ (\Delta\varepsilon_{s.y})_i = \dfrac{D_{y.i}}{D_{y.i}+1}\left((\Delta\varepsilon_{cf})_i - \sum\limits_{j=1}^{i-1}\left[(\Delta\sigma_{c.y})_j \cdot \dfrac{\Delta\varphi(t_i,t_j)}{E_{c.28}}\right]\right) - \dfrac{\sum\limits_{j=1}^{i-1}(\Delta\sigma_{c.y})_j}{E_c(t_{(i-1)+1/2})} \end{cases} \quad (1)$$

* Corresponding author: volhasann@gmail.com

$$\begin{cases} D_{x.i} = \dfrac{E_c(t_i)}{\left(1+\dfrac{E_c(t_i)}{E_{c.28}}\cdot\varphi(t_{i+1/2},t_i)\right)\cdot E_{s.x}\cdot\rho_{s.x}} \\ D_{y.i} = \dfrac{E_c(t_i)}{\left(1+\dfrac{E_c(t_i)}{E_{c.28}}\cdot\varphi(t_{i+1/2},t_i)\right)\cdot E_{s.y}\cdot\rho_{s.y}} \end{cases} \quad (2)$$

In formula (1) v is the Poisson's ratio at the early age of expansive concrete. All other parameters in formulas (1) and (2) should be defined according to [1, 2].

The total self-stresses and restrained expansion strains in the x-direction and in the y-direction at given time interval are defined by:

$$\begin{cases} \left(\sigma_{c.x}\right)_i = \left(\sigma_{c.x}\right)_{i-1} + \left(\Delta\sigma_{c.x}\right)_i \\ \left(\sigma_{c.y}\right)_i = \left(\sigma_{c.y}\right)_{i-1} + \left(\Delta\sigma_{c.y}\right)_i \end{cases}; \begin{cases} \left(\varepsilon_{s.x}\right)_i = \left(\varepsilon_{s.x}\right)_{i-1} + \left(\Delta\varepsilon_{s.x}\right)_i \\ \left(\varepsilon_{s.y}\right)_i = \left(\varepsilon_{s.y}\right)_{i-1} + \left(\Delta\varepsilon_{s.y}\right)_i \end{cases} \quad (3)$$

Verification of the model in the case of two-way restrained conditions was carried out based on the three series of the expansive concrete plane specimens with the mesh reinforcement in the mid-depth of the cross-section. The restraint rate in the principal axes directions was taken as the variable parameter of samples. The development of restrained expansion strains and stresses, that are defined experimentally and calculated according to the proposed model and model Ito et.al [2], for the series I is presented in figure 1.

Figure 1 demonstrates a good agreement between experimental data and those are defined according to the proposed design model.

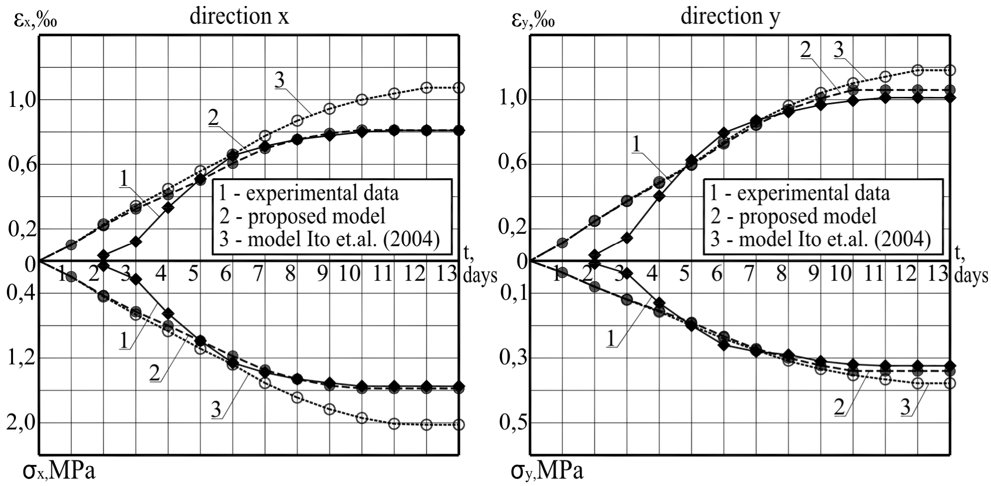

Figure 1. The restrained expansion strains and stresses in the directions x and y for the series I.

References

1. Semianiuk V., Tur V., Herrador M. F., Paredes G. M. Early age strain and self-stresses of expansive concrete members under uniaxial restraint conditions. Construction and building materials, 2017; 131: 39–49
2. Ito H., Maruyama I., Tanimura M., Sato R. Early age deformation and resultant induced stress in expansive high strength concrete. Journal of Advanced Concrete Technology, 2004; 2(2): 155–174

Cement concrete modular pavement implementation for pedestrian and bicycle path

Audrius Vaitkus[1], *Judita* Gražulytė[1], *Viktoras* Vorobjovas[2,*], and *Ovidijus* Šernas[1]

[1]Vilnius Gediminas Technical University, Road Research Institute, Linkmenų str. 28, 08217 Vilnius, Lithuania
[2]Vilnius Gediminas Technical University, Department of Roads, Saulėtekio ave. 11, 10223 Vilnius, Lithuania

1 Introduction

In Europe the most popular pavement type of pedestrian and bicycle paths are asphalt concrete, interlocking concrete paver blocks and unbound granular mixture. In urban areas pedestrian and bicycle paths should be incorporated ensuring harmony with the surrounded area, expressing local community's individuality and improving safety and comfort. These issues are achieved using colored asphalt concrete and different laying patterns of interlocking concrete paver blocks. However, these solutions are old fashioned and do not reflect nowadays society needs and innovativeness. Cement concrete modular pavements also known as precast concrete pavements designed for pedestrian and bicycle paths address these problems. This type of pavement consists of prefabricated concrete slabs that are transported to the project site only after the curing period when the desirable concrete strength is achieved and installed on a prepared foundation. Slabs fabrication in a plant enables to achieve different pavement texture and style what is one of the most important factors designing pedestrian and bicycles paths in urban areas. In addition to other advantages of slabs fabrication in a plant such as better concrete quality, controlled concrete curing conditions, elimination of materials segregation etc., concrete modular pavements are easily removable – mechanically independent – what is the crucial aspect to get access to underlying utilities for repair and replacement.

2 Experimental plan

In Lithuania, the width of pedestrian paths should be not less than 1.5 m and bicycles paths should be at least 1.00 m for one traffic lane and 2.0 m for two traffic lanes in streets, local roads or along them. Due to that, and ensuring easy transportation, handling and installation it was found that optimal dimensions of concrete slab are 1.0 m in length and 1.5 m in width. The slab dimensions were selected considering not only predominant loads, but also slab extraction from precasting moulds and handling with vacuum lift (see Fig. 1 b)).

The required bearing capacity and resistance to cracking during transportation and handling were achieved by using micro and macro synthetic fibers. It allowed to produce 5 cm thickness slabs (see Fig. 1 a)). All slabs, except one, were produced using designed C30/37 concrete and exposure class risk of freeze and (or) thaw attack – XF4. One slab was produced of exposed aggregate concrete using the same designed C30/37 concrete.

* Corresponding author: viktoras.vorobjovas@vgtu.lt

a) b) c)

Fig. 1. Prefabricated cement concrete slabs (a), their installation using vacuum lift (b) and constructed pedestrian pathway (c).

During the production of cement concrete slabs it were performed quality control procedure testing the compressive and flexure strength.

These thin prefabricated synthetic fiber reinforced cement concrete slab were produced with different texture and curing (hardener) type. Seven different combinations of modular pavement were developed, constructed and tested in 20 m length pedestrian pathway in Vilnius city (see Fig. 1 (c)).

It were measured indirect compressive strength using Schmidt hammer, medium profile depth, estimated texture depth and slip resistance in the constructed test site.

3 Results

The use of synthetic micro and macro fibers for cement concrete reinforcement allowed to decrease cement concrete slabs thickness to 5.0 cm and to ensure designed compressive and flexure strength. Nevertheless, analysis of quality control data and research of constructed modular pavement shows, that the method of this thickness slabs fabrication using spot compaction is inappropriate and vibration table must be applied. Also, the paper presents and analyzes the performance characteristics of the constructed pedestrian pathway.

This project has received funding from the European Regional Development Fund (project No 01.2.2-LMT-K-718-01-0044) under grant agreement with the Research Council of Lithuania (LMTLT).

A comparative study of the provisions of ACI: 318-08 and is: 456-2000 building codes for design of flat slabs

Sayed Wafiullah[1,*]

[1]Division of Reinforced Concrete Structures, Institute of Building Materials and Structures, Faculty of Civil Engineering, Cracow University of Technology

ACI 318-08 and IS: 456-2000 building design codes are the two foremost design codes of reinforced concrete structures in Afghanistan. A detail comparative study will help Identify differences of both codes and would substantiate their validity in deigning flat slabs, hence a comparative analysis of these codes are warranted.
The study will provide insights to the structural design engineers to compare economic and safety aspects of both codes in the form of loading combination, thickness, deflection, internal forces magnitudes and required amount of reinforcement. The study aims to investigate the flexural and shear behavior of reinforced concrete flat slabs for both codes in the elastic range under the basic principles of limit states design. This type of study is essential for a complete and proper understanding of building code requirements and design procedures of flat slabs.
The research is organized in two parts, part 1 commences with an introduction, general design concept and the advantages of using flat slab as the type of floor construction. After that, various design approaches for flat slabs are discussed, followed by a comprehensive study of flexural and shear behavior of the flat slabs. Part 2 consist of A Case study for Designing multi panel flat slab using ROBOT Finite Element package, Direct Design Method, and Equivalent Frame Method in order to facilitate parametric comparison of ACI:318-08 and IS:456-2000.
The set of variables, such as amount of reinforcement, bending moment and shear force values, Deflection magnitude, and slab thickness obtained from the analysis and design result were compared among each other's and highlighted the possible advantages and disadvantages of both codes.

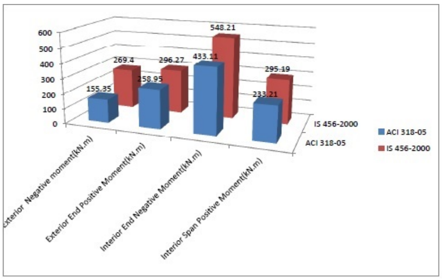

Fig 8.3 graphical comparison of longitudinal moments obtained by Direct Design Method.
The moments obtained by IS 456-2000 is within 20% on average higher compare to ACI 318-05 using direct design method of analysis.

By comparing IS456-2000 and ACI 318-08 we concluded that both codes require the designer to satisfy the minimum thickness requirement, However designing flat slab based on IS 456-2000 will provide higher Bending moment, shear force and torsional moments and accordingly

* Corresponding author: sayedwafiullah2017@gmail.com

higher area of longitudinal reinforcement area (within the range of 15% for column strip) compared to ACI 318-05.
Moreover Designing based on ACI 318-08 will require to augment the slab with shear reinforcement, however the thickness in IS 456-2000 is sufficient large and No need for shear reinforcement.

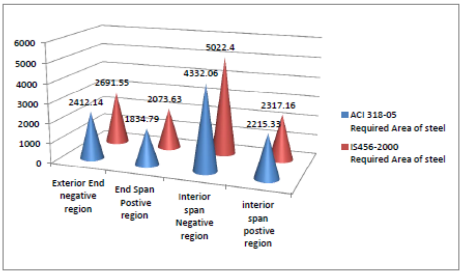

Fig 8.5 graphical comparison of Required Area of steel in mm^2 for column strip along line 2 in East west Direction.

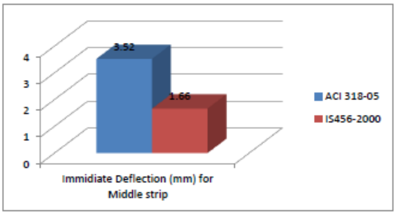

Fig 8.9 graphical comparison of immediate deflection in interior panel.

References

1. MacGregor, J.G., Reinforced Concrete Mechanics and Design, Fifth Edition, Prentice – Hall international, Inc., New Jersey, 2002
2. Nilsson, A.H., Darwin D., Dolan C.W., Design of Concrete Structures, Thirteenth Edition, The McGraw – Hill Companies, 2004
3. Mc Cormac, J.C., Design of Reinforced Concrete, Fifth Edition, John Wiley & sons, Inc., New York, 2001
4. Dayaratnam, P., Design of Reinforced Concrete Structures, Oxford & IBH, New Delhi, 2010
5. Gambhir, M.L., Design of Reinforced Concrete Structures,SPHI Learning Private Limited, New Delhi, 2010
6. Pilla, S.U., Menon, D., Reinforced Concrete Design, First Edition, Tata McGraw-Hill, New Delhi, 1998
7. Mastofinejad, Davood, Reinforced Concrete Structures, Volumes 1,2, Danish publishers, Asphahan, Iran, 2010
8. ACI 318-05, Building Code Requirments for Reinforced Concrete, The American Concrete Institute, Detroit, 2005
9. ACI R 318-05, Commentary on Building Code Requirments for Structural Concrete, The American Concrete Institute, Detroit, Michigan, 2005
10. IS 456-2000, Code of Practice for Plain and Reinforce Concrete, Bureau of Indian standards, New Delhi, 2000

Ductility and internal forces redistribution in lightweight aggregate concrete beams

Tomasz Waśniewski[1,*], and *Ewelina* Kołodziejczyk[2]

[1]Lodz University of Technology, Department of Concrete Structures, Lodz, Poland
[2]Lodz University of Technology, Department of Concrete Structures, Lodz, Poland

1 Introduction

The ductility of the reinforced concrete elements can be defined as the ability to plastic deformation, in the area of permissible loads and also above it. High ductility means that the structure can transfer loads despite the overloading of its critical sections. Admittedly, excessive displacements and deflections may occur, but the load capacity of the structure will be maintained. In the statically indeterminate systems, adequate ductility ensures the ability to rotate of critical cross-sections, which allows the proper redistribution of the internal forces.
Lightweight Aggregate Concrete (LWAC) is typically defined as concrete having a density smaller than or equal to 2200 kg/m^3 and can be obtained by mixing natural or artificial lightweight aggregates [1]. There is a general scepticism regarding the use of lightweight aggregate concrete (LWAC) for structural applications. This concern is attached to the more brittle material behaviour which leads to lower ductility [2–5].
This article presents a numerical parametric analysis of the behaviour of the reinforced LWAC cross-sections under the immediate load taking into account the density of the LWAC concrete, concrete strength and tensile reinforcement ratio.
Using the moment–curvature relationship as a sectional constitutive law, numerical analysis of the deformations and internal forces redistribution of double-span beams made of LWAC and reinforced with different reinforcement ratio is presented.

2 Calculation assumptions

In this study, the fibre model of the reinforced section is used according to [6] to determine M-κ relationships. This method assumes a non-linear material model of compressed concrete, tension stiffening rule and non-linear model of steel reinforcement.
Numerical analysis of the beams was conducted in OpenSees, an open–source non-linear finite element method framework. One dimensional element, with three degrees of freedom at each end, were used. Bending stiffness in the integration points was calculated based on the sectional moment–curvature relationship.

3 Results and conclusions

Figure 1 shows the comparison of the M-κ relationships for lightweight (LWAC) and normal weight concrete (NWC) for two values of the tensile reinforcement ratio and three values of compressive strength of the concrete.

* Corresponding author: tomasz.wasniewski@p.lodz.pl

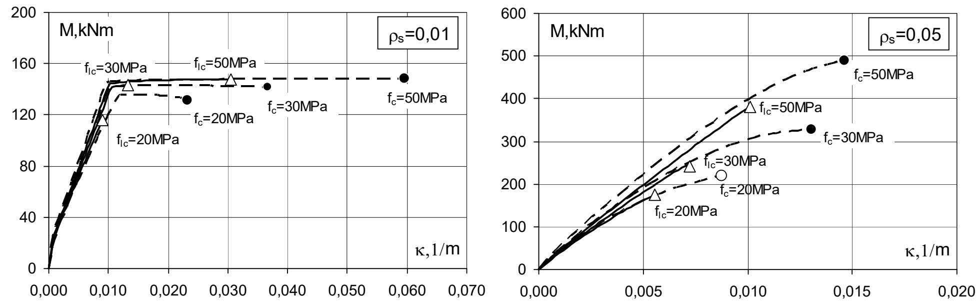

Figure 1. M-κ relationships for cross-sections made of LWAC and NWC.

Analysis of the cross-sections shows a strong influence of the low ultimate compressive strains of the LWAC on the ultimate curvature. It can be noticed in almost all sections reinforced with low reinforcement ratio (ρ_s=0,01) steel yielding occurs and the load-bearing capacity is the same. Only for the cross-section made of lightweight concrete with the lowest compressive strength, the reinforcement does not yield and the load capacity is reduced. However, the length of the plastic branch of the M-κ relationship for sections made of lightweight concrete is much shorter and the ultimate curvature much smaller. This translates directly into the ductility of the cross-section, which is less for lightweight concrete.

In the case of over-reinforced (ρ_s=0,05) sections, the difference in load-bearing capacity is visible between the sections made of lightweight and normal concrete. This is because the ultimate bending capacity of the cross-section, in this case, depends on the ultimate strains of the compressed zone of the concrete. In cross-sections made of lightweight concrete, the ultimate curvatures are also smaller, which leads to less ductility.

Limited deformability of the cross-sections made of lightweight concrete strongly influences the ability to form the plastic hinges and limits the redistribution of internal forces in indeterminate systems.

References

1. European Committee for Standarization. EN 1992-1-1 Eurocode 2: *Design of concrete structures – Part 1-1: General rules and rules for buildings.* (CEN, Brussels, 2004)
2. J.A. Øverli, T.M. Jensen Increasing ductility in heavily reinforced LWAC structures, Engineering Structures Volumes 62–63, 15 March 2014, Pages 11–22
3. N.F. Carmo, H. Costa, T. Simões, C. Lourenço, D. Andrade Influence of both concrete strength and transverse confinement on bending behavior of reinforced LWAC beams, Engineering Structures Volume 48, March 2013, Pages 329–341
4. D. Dias-da-Costa R.N.F. Carmo, R. Graça-e-Costa, J. Valença, J. Alfaiate, Longitudinal reinforcement ratio in lightweight aggregate concrete beams, Engineering Structures, Volume 81, 15 December 2014, Pages 219–229
5. J.A. Øverli, Towards a better understanding of the ultimate behaviour of LWAC in compression and bending, Engineering Structures Volume 151, 15 November 2017, Pages 821–838
6. A. Czkwianianc, M.E. Kamińska *Metoda nieliniowej analizy żelbetowych elementów prętowych, Studia z zakresu inżynierii nr 36*. (Institute of Fundamental Technological Research Polish Academy of Sciences, Warsaw, Poland, 1993)

Condition assessment of cemented materials using deconvolution on laser vibrometer measurements

Piotr Wiciak[1,*], *Giovanni* Cascante[1], and *Maria Anna* Polak[1]

[1]Univeristy of Waterloo, Department of Civil and Environmental Engineering, Waterloo, Ontario, Canada

Current non-destructive ultrasonic techniques (NDT) are based mostly on wave velocity analysis [1, 2]. While current techniques can identify severe damage, they fail to detect early deterioration. Therefore, the proposed method, based on the propagation of surface waves, takes into account not only changes in wave velocity but also changes in wave attenuation. In practical/field applications, access to a structure is often limited to one side only (i.e. concrete slabs, vacuum building walls). Thus, surface wave analysis is a natural solution. To improve the reliability of wave attenuation measurements, responses of ultrasonic transducers are measured using a high-frequency Doppler laser vibrometer.

An ultrasonic output of the tested sample should be treated as a convolution of the input signal sent to the specimen, coupling between the transmitter and the specimen, specimen characteristics, coupling between the receiver and the specimen, and finally the receiver's characteristic. In this study, the receiver coupling is eliminated by using a non-contact laser vibrometer. The main interest of NDE is the condition of the tested object. The object characteristic is given by (Eq. 1):

$$H_{OBJECT} = Y/X, \tag{1}$$

where: H_{OBJECT} is the transfer function of a tested element; X and Y are the measured input and output signals (as a function of frequency). Therefore, it is critical to know the properties of the input signal (i.e. perform a calibration process). It can be assumed that coupling can be accounted for with the calibration of the transducers. The response of the 54-kHz ultrasonic transducer used in this study is presented in Fig. 1.

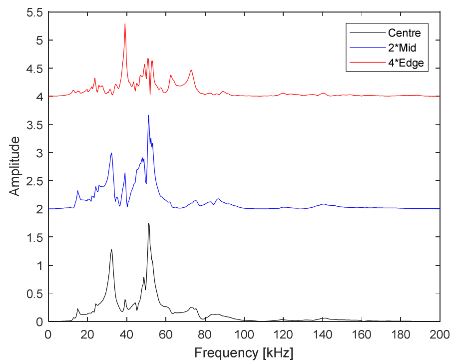

Figure 1. Frequency response of 54 kHz ultrasonic transducer.

* Corresponding author: pwiciak@uwaterloo.ca

Laboratory experiments are conducted on concrete beams in two conditions: intact and damaged and a half-space medium made of cemented sand, which includes a localized defect (i.e. void). The intact concrete specimen is the reference specimen with no induced damage. The damaged concrete specimen is subjected to freeze and thaw cycles to induce distributed micro-cracking (representing early damage). Based on obtained transfer function, the damage index is evaluated based on spectral relative difference for two material conditions. The damage index plots for both concrete specimens and cemented sand specimen are presented in Fig. 2.

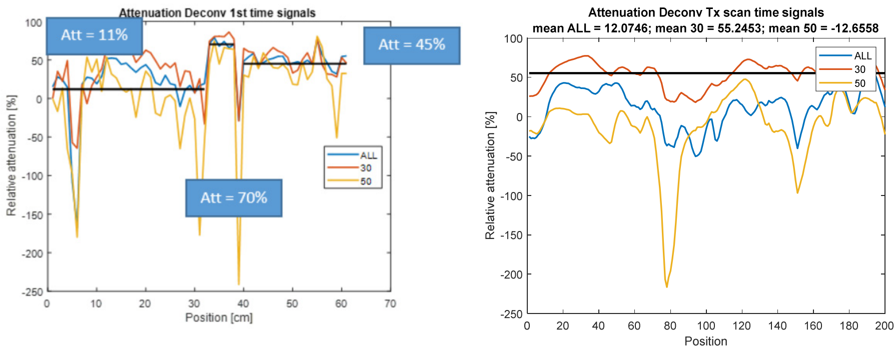

Figure 2. Damage index calculated for cemented sand (left) and concrete specimens (right).

The damage index proposed in the methodology, based on the deconvolution technique improving signal analysis (i.e. the time signals have a simpler form and are easier to analyze), offers a significant distinction between different material conditions (up to 70%). Moreover, the proposed technique has been successfully applied to both distributed (i.e. micro-cracks) and localized (i.e. void) defects.

References

1. McCann, D.M. and Forde, M., 2001, *Review of NDT methods in the assessment of concrete and masonry structures*, NDTE International, vol. 34, pp. 71–84
2. Popovics, J.S., 2003, *NDE techniques for concrete and masonry structures*. Prog. Struct. Engng Mater., vol. 5, pp. 49–59

Structural testing of compression members reinforced with FRP bars

Maria Włodarczyk[1,*]

[1]Warsaw University of Technology, Faculty of Civil Engineering, 00-637 Warszawa, al. Armii Ludowej 16, Poland

1 Introduction

Fibre Reinforced Polymer (FRP) bars are a dynamically developing products in the construction building market. The FRP bars are increasingly used as an alternative to steel reinforcement in concrete structures. Their wide applicability is due to their properties such as high strength, resistance to corrosion, easy cutting, etc. [1].

For many years, research has been conducted on the identification of properties and the possibility of application of BFRP (Basalt Fibre Reinforced Polymer), GFRP (Glass Fibre Reinforced Polymer), CFRP (Carbon Fibre Reinforced Polymer), HFRP (Hybrid Fibre Reinforced Polymer) bars in structural members as the alternative to steel reinforcement. Due to linear stress-strain relationship for composite bars vast majority of the research and analyses concerns elements in bending [2–4], while for compressed elements with composite reinforcement there is a lack of extensive research, with a very few works [5,6], among others. However, there is an increasing requirement to assess the suitability of this reinforcement in compression elements.

This paper presents results of experimental tests of concrete columns reinforced with BFRP and HFRP bars.

2 Experimental testing

The research includes structural elements that have been subjected to axial compressive force. The experimental programme consisted of the columns with the cross-section dimensions 150×150 mm and height of 750 mm reinforced with BFRP, HFRP bars. In each of the elements, the stirrups were made of bars with a diameter of 6 mm, of the same material as bars of the longitudinal reinforcement. The tensile strength for BFRP bars ranged from 1103 to 1153 MPa and the elastic modulus from 43.87 to 48 18 GPa. In case of the HFRP bars the tensile strength was between 1139 and 1278 MPa while the elastic modulus was between 73.57 and 73.89 GPa. The concrete class C35/45 was used with a compressive strength in the range from 45.64 to 60.94 MPa that was measured on cubic samples.

It was observed that the compression members with BFRP and HFRP reinforcement collapsed by crushing concrete. For elements with BFRP bars the experimental ultimate force (N_n) ranged from 906 to 1001.50 kN, while for the elements with HFRP bars from 905.50 to 972.20 kN. The predicted theoretical ultimate force (N_R) was 1026.90 kN for columns with BFRP bars and 1371.15 kN with BFRP bars, respectively.

Based on the performed analysis the recorded values of the experimental ultimate forces N_n it can be concluded that for all elements the experimental ultimate force is smaller than the calculated theoretical bearing capacity N_R. However, the difference between the result is less

* Corresponding author: maria.wlodarczyk@il.pw.edu.pl

prominent if a larger diameter of the longitudinal reinforcement bars has been used or for the elements in which the stirrup spacing was reduced.

3 Analysis of results and conclusions

The axial compressive force and longitudinal deformation in the reinforcement bars were recorded during the carried out experiments. Strains were measured in bars located on the opposite sides of columns. The representative results for the tested columns are shown in Fig. 1. Force-strain diagrams for the columns with BFRP bars are shown in Fig. 1a, while for the columns with HFRP reinforcement are presented in Fig. 1b. The ultimate capacity is about 15% higher for columns with HFRP reinforcement than for columns with BFRP bars. However, reported strains at the limit load (ductility) are slightly larger for columns with BFRP bars than in case of columns with HFRP reinforcement.

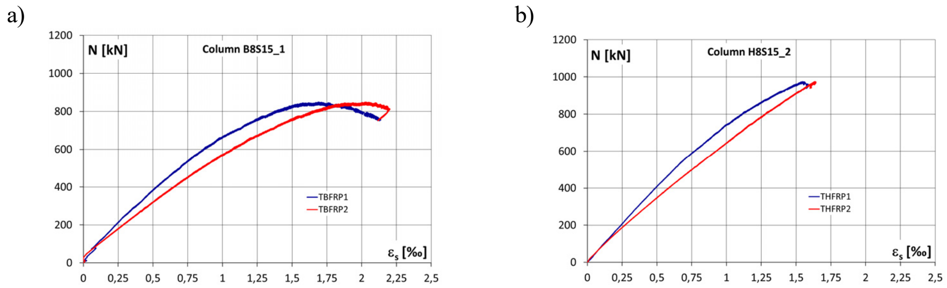

Fig. 1. Axial force vs strain measured in the main reinforcement bars: a) columns with BFRP; b) columns with HFRP.

The performed tests confirm applicability of the FRP bars in compressive elements, although a larger number of tests is needed to investigate the possible range of their application. Reported discrepancy between the measured and the predicted limit load requires additional research on formulation of the calculation procedures and reinforcement detailing (e.g. stirrup spacing) in the regarded structural elements. Design procedures supposed to be validated on a large population of typical structural elements.

Experimental tests were carried out under the grant NCBiR, PBS3/A2/20/2015 - Innowacyjne hybrydowe zbrojenie kompozytowe FRP do konstrukcji infrastrukturalnych o podwyższonej trwałości (HFRP).

References

1. *fib* Bulletin 40, *FRP reinforcement in RC structures*, (2007)
2. A. Garbacz, E. Szmigiera, K. Protchenko, M. Urbański, Springer, (2018)
3. Håkan Nordin, Björn Täljsten, Composite Part B: Engineering, Elsevier, vol. **35**, (2004)
4. C.A. Neagow, L. Gil, M.A. Pérez. Construction and Building Materials, vol. **101**, part 1, (2015)
5. Y. Kusumawardanigsih, M.N.S. Hadi, Composite Structures, Cost **3987**, Elsevier, (2010)
6. M. Soghair Hosny, H. Ahmed Mahmoud, M. Abdel-Hafez Atif, Ahmed Ibrahim, H. Ramadan, Al-Azahar Engineering, Ninth International Conference, AEIC (2007)

Risk, robustness, vulnerability – properties that determine the safety of concrete structures

Szczepan Woliński[1,*]

[1]Rzeszow UT, Chair of Building Structures, ul. W. Pola 2, 35-04 Rzeszow, Poland

1 Introduction

Statistics of failures and collapses of concrete structures clearly indicate that only occasionally they are resulting from actions or events covered under the standard structural analysis. Most often causes of structural catastrophes are due to human errors, exceptional situations or series of disadvantageous events. In Eurocode 1–7 on accidental actions, the ability of a structure to withstand catastrophic events without being damaged to an extent disproportionate to the original cause is called as robustness. Conversely, a structure which can be easily affected by any damage is called vulnerable. A good measure of these properties is the direct and indirect risk that allows for a reliable assessment of the safety of structures. The paper presents the procedure of risk assessment using the frequency-consequences acceptance matric and quantification of the structural robustness and vulnerability. That procedure is illustrated through numerical example of risk, robustness and vulnerability impact on safety of the uncomplicated reinforced concrete structure.

2 Assessment of risk, robustness and vulnerability that determine structural safety

Although the explicit risk assessment is not easy to carry out, it can help to classify and compare different methods of increasing the robustness and decrease the vulnerability and improve the quality of structures, especially for buildings of high consequence classes. The probability and consequence analysis related to the assessment of robustness and vulnerability usually contains statistical, fuzzy and fuzzy-statistical information on basic variables and parameters. Using the concept of fuzzy numbers, fuzzy statistics and a scheme of approximate reasoning the subjective and qualitative information related to input variables, calculation methods, manufacturing processes, professional knowledge and intuition necessary for risk analysis and assessment can be taken into account in design process of building structures. The risk associated with direct consequences due to exposure is the recommended measure of structural robustness. The risk due to all indirect consequences represents the vulnerability and the total risk characterizes the safety of a structure. The proposed fuzzy index of robustness was defined as follows [1, 2]:

$$\tilde{I}_R = \frac{\sum_i \tilde{R}_{Dir_i}}{\sum_i \tilde{R}_{Dir_i} + \sum_i \tilde{R}_{Ind_i}} \tag{1}$$

where $\tilde{R}_{Dir_i}$ is the direct fuzzy risk associated with the initial damage to a structure due to the i-action or event and $\tilde{R}_{Ind_i}$ is the indirect fuzzy risk associated with the subsequent system failure due to the same action or event. To simplify the calculations fuzzy variables and parameters

* Corresponding author: szwolkkb@prz.edu.pl

have been represented by means of fuzzy numbers $X = (m_{x,} \alpha, \beta)$; where α and β are left-sided and right-sided range of a membership function around $m_{x,}$. The robustness index takes values $0 \leq \overline{I}_R \leq 1$. If the risk is due to direct consequences only, the system is completely robust and $\overline{I}_R = 1$. If the risk is due to indirect consequences, the structural system has no robustness and $\overline{I}_R = 0$ and is completely vulnerable.

3 Acceptable risk

In the predominant opinion a measure of acceptable or tolerable risk should be based on human, economic and environmental values and expressed in the socio-economic terms. Generally, methods of risk acceptance may be divided into two categories; *implicit* methods of the comparative character which make use of qualitative risk criteria from similar structures and scenarios for other cases and sectors of industry and *explicit* methods, based on direct evaluation of risk acceptance. The frequency-consequence matric corresponding to the target reliability levels recommended in Eurocode 1990 and proposed fuzzy measures of failure consequences [2] have been applied in calculation of risk, robustness, vulnerability and to assess their impact on safety of the reinforced concrete frame structure.

4 Conclusions

The approach presented in the paper utilizes qualitative and quantitative information on materials properties, topology, accidental actions and different types of hazards treat to a structure as well as information on the influence of direct and indirect consequences, structural robustness and vulnerability expressed in terms of risk. It makes possible to carry out the complex analysis and to estimate the safety of a structure.

Structural risk should be analyzed and evaluated by means of quantitative criteria to identify possible hazard scenarios, probabilities of the undesired events and to estimate costs of damages and their indirect consequences. The complex analyzes of the structural risk makes possible to design safe structures, especially these classified to the higher classes of consequences.

References

1. M. H. Faber, *Framework for risk assessment of structural systems*, Proceedings of Workshop COST26: Urban habitat constructions under catastrophic events. Czech TU Prague 2007, 359–367
2. Sz. Wolinski, *Risk based approach to service life assessment of building structures,* Proceedings of Seminar: Sustainability of Constructions, Dresden, 2008, 4.43–4.51
3. Sz. Wolinski, *Defining of the structural robustness,* Bull. Pol. Ac.: Tech. 61 (2013) 137–144

Buildings of the John Paul II Center – a challenge for civil engineering and architecture

Bogumił Wrana[1], and *Jan* Wrana[2,*]

[1]Krakow University of Technology
[2]Lublin University of Technology

The John Paul II Center (CJPII) facilities – a 'symbolic temple' – with Małe Błonia park, also known as the 'Nie lękajcie się' ('Do not be afraid') Center is located in Krakow-Łagiewniki, on a post-soda lime deposit burrow, created from products of the former 'Solvay' Krakow Soda Plant. This area is known as the 'Białe Morze' ('White Sea'), and it is situated in a natural valley of the river Wilga, between the hill of St. Joseph in the north and the Borkowska Mountain in the southwest. The post-soda lime, as a ground base for the Center facilities, is unique worldwide – therefore it constituted a challenge for civil engineering.

Figure 1. John Paul II Sanctuary, Krakow (photographed by J. Wrana).

[*] Corresponding author: j.wrana@pollub.pl

Figure 2. John Paul II Sanctuary, Krakow (photographed by J. Wrana).

The limestone deposit burrow is approx. 15 m high; it retained its original consistency and color – white pulp – to this day. The CJPII buildings are geotechnical category 3 structures, developed on a foundation slab that is 0.8 m thick, and in the center section – 0.45 m thick. The slab is supported by 200 CFA-type reinforced concrete drilled piles with diameters of 1000 mm and 650 mm, which are up to 25 m long. The load-bearing structure of the Center facilities is a reinforced concrete frame-coating skeleton.

The symbolism of this urban setting (e.g. the scale of the Wadowice market square), situated on a grid consisting of 200 piles, at a post-industrial site – lime deposits securing its survival – in combination with architectural solutions referring to places related to the life of John Paul II (Wawel Cathedral, St. Mary's Church) and natural material solutions (brick and white stone) referring to methods of combining them, and used in facades of the John Paul II Center buildings.

Application of ultrasonic pulse velocity test to concrete assessment in structures after fire

Julia Wróblewska[1,*], *Robert* Kowalski[1], and *Michał* Głowacki[1]

[1]Warsaw University of Technology, Civil Engineering Faculty, Institute of Building Structures, Al. Armii Ludowej 16, 00-637 Warsaw, Poland

1 Introduction

In fire conditions, an unsteady heat transfer occurs in the cross-section of reinforced concrete elements. Their surface heats up faster than their interior. As a result, concrete has non-uniform properties in the element cross-section. The greatest degradation of concrete (e.g. compressive strength reduction) occurs in the near-surface area. In the external layer of element cross-section, the concrete is usually damaged to such an extent that it should be considered destroyed. When assessing a structure after fire, it is crucial to determine the thickness of this layer.

The standardized [1] UPV (ultrasonic pulse velocity) method is commonly used for in situ concrete testing. The time of travel of compressional waves propagating in concrete between the transmitting and receiving transducers is measured. In normal conditions, concrete compressive strength can be estimated from the wave velocity measurements using correlation relationships. They are based on a correlation of the ultrasonic pulse velocity with the value of concrete modulus of elasticity and the moisture content. According to [2], the UPV method can also be a good indicator of the degree of concrete damage in structures after fire. As a result of chemical and physical processes occurring in concrete exposed to high temperature, the Young's modulus of concrete decreases, together with the amount of contained water.

From a practical point of view, when assessing concrete in situ, it is usually suitable to use an indirect ultrasonic method in which both transducers are applied to one surface of the element. This allows testing structural elements with only one-sided access. The paper presents a description and results of a study aimed at verifying the applicability of the indirect UPV test to preliminary assessment of concrete quality in structures after fire.

2 Experimental study

Four 160x200 mm reinforced concrete beams were exposed to high temperature on one side (from the bottom) for 60, 120, 180 and 240 minutes. One beam was unheated. Lateral surfaces of the elements were thermally insulated to ensure a one-way heat transfer in the cross-section. As a result of FEM calculations, maps of temperature fields in the cross-section were generated. There was a good compatibility of temperature measurements in the heated elements with the calculated values.

A Pundit PL-200 with point contact exponential transducers was used in ultrasonic tests. This allowed performing the measurements without the necessity of grinding the concrete surface (deteriorated in high temperature) and without the use of a coupling agent.

* Corresponding author: j.wroblewska@il.pw.edu.pl

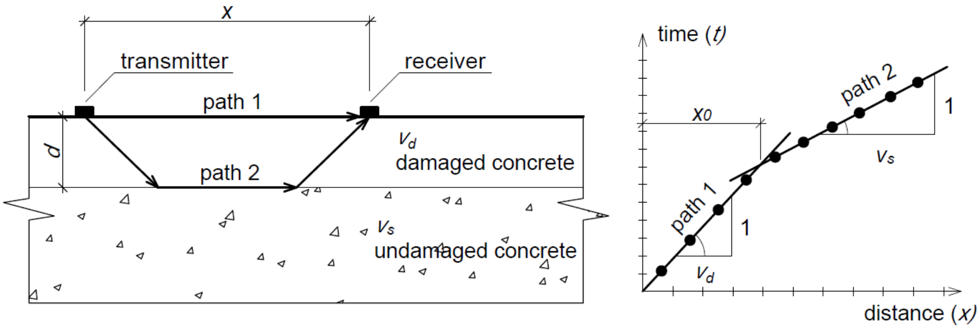

Fig. 1. Scheme of ultrasonic pulse velocity measurement and the assessment of damaged concrete layer thickness using the indirect ultrasonic method (acc. to [2]).

In order to estimate the thickness of the external concrete layer characterized by lower strength parameters, an indirect UPV method was used (Fig. 1) [2]. Both the transmitter and receiver were applied to the same heated surface of the beams. In this way, ultrasonic wave propagation in the near-surface area was analyzed. The travel time of waves was measured for varying distances between the transducers. The results were presented on the diagram of the travel time (t) dependence from the distance (x) between the transducers. For heated beams, a characteristic change in diagram slope was observed for the ordinate marked x_0. This is the distance between the transducers for which travel time of waves in the surface layer (path 1 – lower wave velocity (v_d) in damaged concrete) is equal to travel time in deeper layers of cross-section (path 2 – higher wave velocity (v_s) in undamaged concrete). Thickness (d) of the damaged concrete layer in every beam was estimated according to the formula [2]:

$$d = \frac{x_0}{2}\sqrt{\frac{\upsilon_s - \upsilon_d}{\upsilon_s + \upsilon_d}}\ . \qquad (1)$$

The elements were also examined using direct ultrasonic test, i.e. applying transducers to the lateral, opposite surfaces of the element. Variability of wave velocity measured across the beam section at different distances from the heated edge was analyzed. There was a good compatibility of the estimation of destroyed concrete layer thickness obtained with the direct and the indirect method. The calculated depth in the cross-section at which the undamaged concrete was located increased with the heating duration. However, due to relatively high scattering of the results and their complex interpretation, a full confirmation of suitability of the indirect UPV method for estimating the thickness of destroyed external concrete layer in structural elements after fire was not obtained.

References

1. EN 12504-4:2004. Testing concrete. Determination of ultrasonic pulse velocity
2. ACI 228.2R-98. Nondestructive test methods for evaluation of concrete in structures

Nonlinear Finite Element Analysis of punching shear strength of reinforced concrete slabs supported on L-shaped columns

Qing Zhang[1], *Graeme J.* Milligan[1,*], and *Maria Anna* Polak[1]

[1]University of Waterloo, Department of Civil and Environmental Engineering, Waterloo, Ontario, Canada

1 Introduction

The punching shear behavior of reinforced concrete slabs supported on L, T and cruciform-shaped columns has not been extensively studied even though most current design codes include design provisions for such connections. The derivation of these provisions is unclear. Empirical data of punching failures of slabs supported on L, T or cruciform shaped columns is limited due to the cost and time required to test specimens with slab thickness and column sizes commonly used in practice.

The punching shear behavior of interior L-shaped slab-column connections subjected to static concentric loading with or without slab openings is analyzed using a plasticity based nonlinear finite element model (FEM) in ABAQUS. The FEM is similar to others used at the University of Waterloo to study punching and was calibrated considering the 9 isolated slab-column specimens tested by Hawkins, Fallsen and Hinojosa (1971). These 9 specimens were tested to study the impact of column rectangularity on punching shear, and the results were used in the calibration of the ACI 318 provisions.

In this paper a brief summary of previous punching shear research of slab-column connections is provided. Additionally, a brief discussion of the FEM calibration is provided. Finally, a comparison of the predicted load-deflection response, crack patterns, shear stress distribution in the slab along the column perimeter and comparison to predictions from ACI 318-19 and Eurocode 2 (2004) (EC2) is provided.

2 Finite Element Analysis of isolated slab-column connections

In this paper the punching shear behaviour of the four isolated slab-column specimens shown in Figure 1, and one specimen without an opening, are analyzed to verify the critical perimeter assumed in ACI 318-19 and EC2 (also shown in Figure 1). It is hypothesized that the diagonal portion of the critical perimeter is ineffective due to shear stresses concentrations near the outer corners of the L-shaped column. The impact of slab openings at various locations around the L-shaped column is also studied. If the diagonal portion of the critical perimeter is ineffective the capacity of specimens L1x6-1x4i, and L1x6-1.2x1.2i and L1x6-1.2x1.2o should be similar to that of the connection without an opening (L1x6-0).

A comparison of the predicted load-deflection, where the deflection is measured at the location shown in Figure 1, is provided in Figure 2. A comparison of the predicted load capacity from the calibrated FEM, ACI 318-19 and EC2 is provided in Table 1. As seen in Figure 2 and Table 1 the impact of the inner openings is minor, with a maximum decrease in capacity of 4.9% for specimen L1x6-1x4i, whereas openings located along the outside of the column, as in specimen L1x6-1x4o, significantly decrease the connection capacity (16.9% decrease). An analysis of the shear stress distribution in the slab verifies that the slab near the inner portion of the column is subjected to very low stress, which renders this portion of the slab ineffective in

* Corresponding author: milligan@uwaterloo.ca

transmitting load to the column. As shown in Table 1 ACI 318-19 and EC2 (2004) greatly overpredict the punching capacity of all specimens.

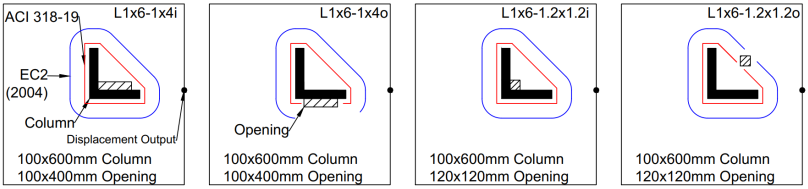

Figure 1. Hypothetical slab-column specimens considered in study.

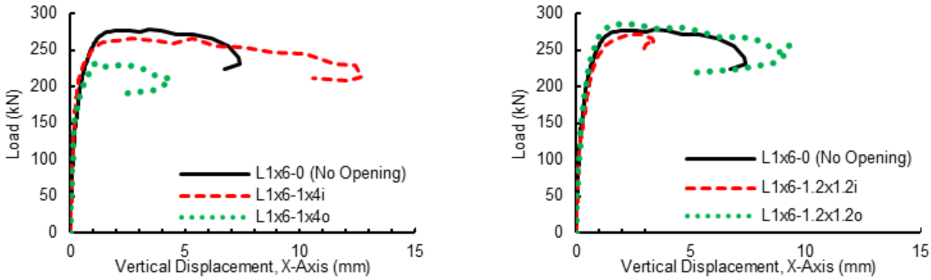

Figure 2. Comparison of predicted load displacement response.

Table 1. Comparison of punching capacity predicted by FEM, ACI 318-19 and EC2 (2004).

Specimen	Opening Size	V_{FEA} (kN)	V_{ACI} (kN)	V_{EC2} (kN)
L1x6-0	None	279.3	523.3	479.1
L1x6-1x4i*	100x400	265.5	523.3	479.1
L1x6-1x4o	100x400	232.1	436.3	372.1
L1x6-1.2x1.2i*	120x120	271.7	523.3	479.1
L1x6-1.2x1.2o	120x120	286.4	509.6	450.7

*Required reduction in critical perimeter unclear. Full critical perimeter used in calculations

3 Conclusions and discussions

The results of the FEA suggest that the effective loaded area around L-shaped columns assumed in ACI 318-19 and EC2 (2004) are incorrect. Both standards are found to greatly overpredict the punching capacity of slabs supported on L-shaped columns compared to the FEA predictions.

The authors would like to thank the Natural Sciences and Engineering Council of Canada, NSERC, and the University of Waterloo for funding this research.

References

1. ACI Committee 318. (2019). Building Code Requirements for Structural Concrete (ACI 318-19) and Commentary on Building Code Requirements for Structural Concrete (ACI 318R-19). Farmington Hills, MI: American Concrete Institute
2. European Committee for Standardization. (2004). Eurocode 2: Design of concrete structures - Part 1-1: General Rules and Rules for Buildings. Brussels, Belgium
3. Hawkins, N. M., Fallsen, H. B., & Hinojosa, R. C. (1971). Influence of Column Rectangularity on the Behavior of Flat Plate Structures. ACI Special Publication, 30, 127–146

Impact of workmanship on load-bearing capacity and durability of masonry structures

Joanna Zięba[1,*], *Izabela* Skrzypczak[2], and *Lidia* Buda-Ożóg[1]

[1]Department of Building Structures, Faculty of Civil Engineering and Environmental Engineering, Rzeszow University of Technology, Poznańska 2, Rzeszow 35-084, Poland
[2]Department of Geodesy and Geotechnics, Faculty of Civil Engineering and Environmental Engineering, Rzeszow University of Technology, Poznańska 2, Rzeszow 35-084, Poland

1 Introduction

Masonry structures are a type of structure that is constantly widely used in construction. Thanks to modern engineering tools, we can easily check the limit state of masonry elements. However, in the light of today's requirements, checking only the limit state is not a sufficient step in the design process. The basis in the design of the structure is sufficiently safe and reliable design of the structure. Regardless of the material chosen for the wall, its main function is to transfer loads to the lower parts of the structure and therefore must be properly designed. Errors in masonry structures can occur both at the design and execution stages.

2 Quality of workmanship of wall

The construction of masonry elements is based on a number of basic assumptions, including the class of execution of works. Eurocode 6 [1] distinguishes between 2 classes of execution of works: class A and class B. The construction designer decides about the class of masonry works. It is of great importance in designing, because it is the basis for determining the partial factor for the wall.

To illustrate the difference in the bearing capacity of masonry walls resulting from the appropriate class of execution of works in masonry, an example of calculation of bearing capacity for a wall made of autoclaved aerated concrete blocks (AAC) of one of the Polish producers was presented. The difference in the computational strength of the masonry, taking into account various classes, is equal to about 15%. The work also shows the impact of the masonry class and units category on the level of reliability. The presented bills show how important wall construction is for design.

3 The "verticality" of the wall

Most wall cracks can be avoided by improving the quality of work performed. Execution of masonry structures significantly affect the load-bearing capacity, formability and durability. Design recommendations provided in the standards for checking the limit states are only valid if the wall meets the relevant construction requirements. Only then can the simplifications adopted in the computational models ensure an appropriate level of safety. Deviations of the made masonry structure from its assumed shape and location should not exceed the values

* Corresponding author: j.zieba@prz.edu.pl

given by the manufacturer of building materials and in the design documentation. Examples of maximum deviations declared by the manufacturer are given in Table 1.

Table 1. Permissible deviations.

Position	Maximum deviation
on each floor	**± 20mm**
at the height of the building with three or more floors	**± 50mm**
vertical shift	**± 20mm**

4 Geodetic methods of inventorying verticality of walls

Control geodetic measurements, which include the measurement of deviations from the vertical plane of the facade walls of the building, are made in order to obtain information about the geometry of the object and determine deviations from their location. In the scope of measurement regarding deviations of facade walls from the vertical plane, the following methods of geodetic measurements have been the most common so far [2]: straight line method, plumbing method, angular spatial indentation method, angular spatial indentation method from 3 positions, 3D polar method.

5 Summary

The consequences of mistakes made during masonry walls can be very different. Sometimes it will be a leaning wall or harmless cracks, other times it will be thermal bridges or even serious wall cracks. Although we are probably not able to design, execute and operate masonry facilities with a full guarantee of the appearance of cracks and other defects, a significant part of these damages can be eliminated at the design, construction and operation of the facility.

References

1. EN 1996-1-1:2004 Eurocode 6: Design of masonry structures - Part 1-1: General rules for reinforced and unreinforced masonry structures. 2004 CEN
2. J. Ćwierz, W. Cinal, A. Kampczyk: *„Pomiar odchyleń ścian elewacji budynku od płaszczyzny pionowej”,* doi: 10.17512/znb.2016.1.04

Digital fabrication in the process of creation of the parametric concrete fencings

Marcin Giedrowicz[1,*]

[1]Wydział Architektury Politechniki Poznańskiej

1 Background and the task

Concrete fencings in Poland are continuously very popular and attract ever growing interest since the 90-ties of the last century, providing budgetary alternative for fences made of steel, timber and brickwork. Among many advantages of precast concrete fencings are their durability, easy and quick production, short time of a purchase order execution at the building site and low price. Not without reason, concrete fences quickly became cheap substitute for the fencings commonly used in Poland – that in general, directly refer in its form to their more noble archetypes. Consequently, aesthetics of the concrete fences is disputable to say the least, and often criticized in architectural circles. Amidst many critical opinions aimed at them the most important seems to be the one telling about decline of the public area aesthetics and pushing traditional solutions out from villages.

The main research and design objective was to elaborate a catalog of concrete fencing designs that would be included in the commercial offer of the Poznań-based producer of precast concrete products. The job entrusted was of a complex nature, that included: elaboration of the catalog of concrete fencing patterns in the form of digital models, preparation of the fence mock-ups in scale 1:25 by means of 3D printing, making the fence prototypes in scale 1:1, with assistance of CNC technology, making the casting moulds based on the wooden prototypes. Design of the collection developed was supposed to be characterized by a fresh look on the material such as concrete and the most up-to-date design, assisted by CNC technology and parametric designing methods. The conception of the investor was the new collection of fences that was supposed to be supplied to more demanding customers, who not only will appreciate the design of the fence but also place it in the appropriate area. This conceptual thinking concerning new designs was based on the idea, that the new product should find its place only in the urban or suburban areas, where it can be a complementation of the modern architecture.

2 Methods

The first stage of the designing process consisted in creation of a large collection of fence designs, according to the investor's guidelines, relating to technological limitations and costs of production. The standard solution in creation of fencings is a panel with dimensions of 50 × 200 × 4.4 cm – most often 4 pieces of the panel are laid one upon the other, until repeatable surface area of 200 × 200 × 4.4 cm is obtained. A set of 4 panels that make a pattern is placed in the concrete columns with the tee bar cross-section, and then multiplied according to a plot perimeter. In consequence, the elaborated patterns were subjected to evaluation according to their commercial attractiveness and ability to be produced by casting method. This stage of work was carried out in close cooperation with the investor, who excluded those patterns that did not give hope for high sale and that generated too many production problems. The basic problems related to commercial attractiveness included:

---

* Corresponding author: marcin.giedrowicz@put.poznan.pl

– using too many openings (decrease of viewing insulation, lacking privacy on the building plot being fenced),
– too expressive or complicated form (requiring 4 different casting moulds to be built, each with dimensions of 50 × 200 × 4.4 cm in order to obtain one repeatable pattern with dimensions of 200 × 200 × 4.4 cm),
– using too large openings (lacking barrier against animals or possible burglars).

The most important technological problems included:
– selection material for fabrication of a prototype (that enable to mould using solvents and chemical substances),
– selection of right technology to fabricate a prototype (additive and subtractive methods were considered),
– the designs difficult for transportation (susceptibility to breaking when stacking panels flat one upon the other),
– too thin side edges and corners (making reinforcement with steel bars impossible),
– in the topology, using a pattern of right, obtuse and interior angles,
– using too small openings (not possible to be precisely cast from concrete).

In result of analyses carried out, 4 fencing designs were singled out with the following trade names: NEO PRL – single-element design which is the modern interpretation of the railway fencing from the era of socialist Poland.

STRIPE – simple, minimalistic, single-element design with horizontal stripes, easily setting in the contemporary residential and service housing. ATTRACTOR – complicated four-component design developed in the Grasshopper program, using the „Attractor" type algorithm. WAVE – two-element design developed in the Grasshopper program, using the „Tween Curve" type algorithm. The second stage of the work consisted in precise elaboration of geometry of individual fences, and then producing their trial mock ups in scale 1:25 – for this purpose 3D printing technology was applied, in type FDM and the Zortrax M200 printer. Produced patterns did not arouse fears or objections of the investor, who permitted to continue the works. The third, most complicated stage of the work was production of the fence prototypes - it was decided to use subtractive fabrication and wood-like material in the form of MDF boards. The prototype fences produced were intended to serve at the later stage of works as the positives to make casting moulds from fiber glass and steel. The first two fence designs (NEO PRL and STRIPE) did not make significant technological problems - they were produced by means the two and half axis CNC mill planer. In both cases the double MDF board was used, with dimensions of 200 × 50 × 2.2 cm, placed one upon the other and integrated with wood screws. The entire working path of the mill was elaborated sequentially in Rhinoceros / Grasshopper, CorelDraw and ArtCAM programs. The ATTRACTOR design of the fence, generated in the Grasshopper program consisted of as many as 4 individual elements with dimensions of 200 × 50 × 4.4 cm, which together contained in itself 124 unique openings. The next significant technological limitation was the relatively small size of the openings – causing that wet concrete in the casting mould took on both, narrow and longitudinal shape. In consequence, small mass of concrete placed in the narrow space could not be removed from the mould undamaged. This situation was solved by making holes, the angle of inclination of their internal wall was within the span of 80 to 85°. Despite many attempts and many ideas of how to make cuts at so small inclination angle, and the 2.5-axis mill, it appeared to be impossible or absolutely too time consuming. In result, the decision was made to engage to this task the 6-axis KUKA KR 60 HA robot arm, controlled by the library of Grasshopper – KUKA prc v2 program. The robot performed 124 openings in 4 subsequent stages of work – the MDF boards were mounted onto the provisional bench by means of clamps. The fourth two-element WAVE design was made using the 2.5 axis mill – despite the fact that the operation also required cutting out of internal walls with the inclination angle not smaller than 80°.

However, specific topology of that design enabled correct cutting to be made using two milling cutter types – the first cut using the flat mill and the second cut using the angular mill with the cutting plane equal to 45°. The last stage of work was to produce pouring moulds using the produced positives – the moulds were made from steel bearings equipped with 4 handles, filled with the impression made from fiber glass.

3 Results

The elaborated casting moulds were supplied to the investor who implemented them in the production line. Moulds before filling them with B30 concrete mix were covered with oily substance, to facilitate separation of concrete from the mould. Process of mould filling and of concrete surface levelling on the vibration table took about 60 seconds for one element. After that time, the solidifying concrete element was separated from its mould and laid in the drying area – the process of independent drying takes about 24 hours. In consequence, trial castings of all developed fence designs were produced - to the satisfaction of the investor, the obtained moulds had no errors or deformations of geometry. Soon, mass production of the developed designs was started - where current statistics demonstrate very high sale of the „STRIPE" design, good sale of the „ATTRACTOR" and „WAVE" designs and low sale of „NEO PRL" design.

4 Conclusions and discussion

At present, the fencing market requires revision of the current standards, adjusting the offer to the expectations of the more demanding customer and to the higher aesthetic values. Concrete fencing can constitute excellent addition to the contemporary urban and suburban architecture – however, under a few conditions:
– use of concrete designs that do not imitate any other material or style,
– conscious application of CNC technology in order to elaborate precise and economical designs,
– treating concrete as the inspiring material, beautiful in itself,
– seeking for modern solutions, driven by technological progress.
In addition, the author represents the opinion that the ban on using concrete fencings in rural areas should be maintained, while demanding that traditional solutions are applied.

References

1. Bonenberg W., Giedrowicz M., Radziszewski K., *"Współczesne projektowanie parametryczne w architekturze"*, Wydawnictwo Politechniki Poznańskiej, Poznań 2019, ISBN 978-83-7775-548-8
2. Kozina I. 2015, Polski Design, Wydawnictwo SBM Sp. Z.o.o. Warszawa, ISBN 978-83-7845-896-8
3. Natividade V. „Digital Design and Fabrication of Freeform Concrete Blocks. The experience of Cobogo Tranca", FABRICATION | Design & Application – Volume 1 – eCAADe 36, Łódź 2018, pages 743–752

An innovative safety format for structural system robustness checking

Viktar V. Tur[1,*], *Andrei V.* Tur[1], and *Stanislav S.* Derechennik[1]

[1]Brest State Technical University, Faculty of Civil Engineering, Brest, Belarus

1 Introduction

Prevention and mitigation of progressive collapse of the damaged structural system immediately after sudden column loss can be achieved using following methods: 1) TF-method (indirect Tying-Force provisions); 2) AP-method (direct Alternate Load Path method); 3) risk-based method; 4) key-element design method. Currently, the EN 1991-1-7 allows the use of indirect TF- method and some guidance is contained in the EN 1992-1-1. The AP-method consists in considering internal forces redistribution throughout the structural system following the sudden loss of a vertical support element based on non-linear analysis. This paper briefly presents the main steps of assessing the robustness of a structural system based on classical energy-conservation approach, while focusing on ensuring the target safety format when non-linear analysis in accidental design situation.

2 Pseudo-static non-linear response of the damaged structural system

According to (Izzuddin et al. 2008), sudden column loss is considered similar in effect to sudden application of the gravity load on the damaged structure with removed column (SDOF-system), consisting of the vertical deflections at the point of the removed column (Fig. 1).

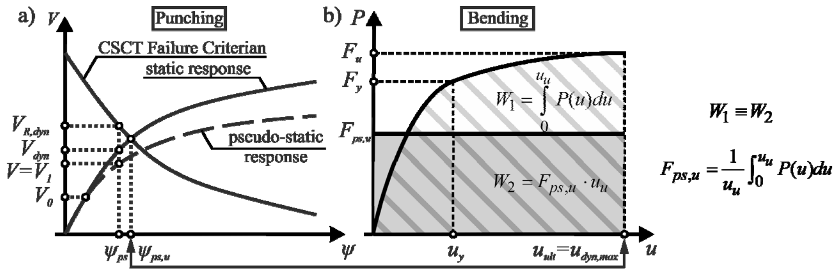

Figure 1. The principle of assessing the robustness of a structural system with flat slabs based on a combined approach.

The following basic assumption is formulated in present paper: *a damaged structural system with SDOF has the required robustness in accidental design situation if the generalized gravity load (F_{st}) applied immediately after sudden column loss, does not exceed ultimate pseudo-static response $F_{ps,u}$ obtained from the equality balance of the external work over dynamic displacement, and internal energy absorbed by the substructure over the ultimate static deflection u_{ult}*. In case of the flat slab robustness assessment, the following combined procedure

* Corresponding author: profturvic@gmail.com

proposed, as it shown in Fig. 1. In accordance with proposed approach, the maximum dynamic displacement $u_{dyn,max}$, which is used for calculation of the pseudo-static ultimate gravity load $P_{ps,ult}$ in case of the bending failure mode is obtained from the corresponding pseudo-static rotation $\psi_{ps,u}$, calculated based on CSCT-model for punching shear (Fig. 1a).

3 Safety format for non-linear response

If the mean rates of occurrence of the accidental event is equal $\lambda_i = 10^{-6}\ldots10^{-5}$, than conditional failure probability for the structural system should be on order of $10^{-2}\ldots10^{-1}$, and the target value of reliability index β_{tag} should be the order of 1.5. Based on the Order Statistic (Non-parametric) Theory of original procedure for estimation of the desired *p-th* percentile of assuming arbitrary given confidence level (γ) was developed and presented in detail in (Tur and Derechennik 2018). According to proposed approach, the estimator of resistance $\hat{R}_{p,\gamma}$ (in term of ultimate pseudo-static response $F_{ps,u}$) of *p-th* percentile with desired confidence level γ can be represented as a normalized linear combination of the first three order statistics:

$$\hat{R}_{p,\gamma} = R_{lowest} - \lambda_{(1),\gamma}\Delta_{2-1} - \lambda_{(2),\gamma}\Delta_{3-2} \tag{1}$$

where $R_{lowest} = R_{(1)}$ is the lowest value of resistance in the ordered sample; $\Delta_{2-1} = R_{(2)} - R_{(1)}$ and $\Delta_{3-2} = R_{(3)} - R_{(2)}$ are nonnegative differences; $R_{(1)}$, $R_{(2)}$, $R_{(3)}$ – first, second and third order statistics, respectively; $\lambda_1 = \lambda(\gamma,n)$; $\lambda_2 = \lambda(\gamma,n)$ – a dimensionless coefficient, which depends sample size n and specified confidence level γ. Values of dimensionless coefficients λ_1, $\lambda 2$ for assessment of the 0.01 percentile with different confidence level γ are listed in Table 1. Global resistance factor is equal:

$$\gamma_{global}(\gamma) = \frac{1 - \lambda_{1(0.5;\gamma)} \cdot (\Delta_{2-1} / R_{lowest}) - \lambda_{2(0.5;\gamma)} \cdot (\Delta_{3-2} / R_{lowest})}{1 - \lambda_{1(0.01;\gamma)} \cdot (\Delta_{2-1} / R_{lowest}) - \lambda_{2(0.01;\gamma)} \cdot (\Delta_{3-2} / R_{lowest})} \tag{2}$$

Table 1. Values of the coefficient λ_1, λ_2 for different confidence level γ for 0.01 percentile estimation (N = 35).

γ	0.1	0.2	0.3	0.4	0.5	0.6	0.7	0.75	0.8	0.9
$\lambda_{1(\gamma)}$	-0.46	-0.28	-0.11	0.09	0.32	0.63	1.05	1.35	1.75	4.32
$\lambda_{2(\gamma)}$	-0.14	+0.03	0.19	0.37	0.58	0.86	1.26	1.53	1.9	4.29

Based on the set of pseudo-static responses, obtained from the full probabilistic analysis of the two-span frame (2×6 m), the following two approaches of determining the global safety factor γ_{glob} were examined: Approach 1 – the values of the factors γ_{Rd} and γ_R were determined separately according to EN 1992-2 and proposed procedure (2), respectively. Then the value of the global safety factor γ_{glob} calculated as the product of $\gamma_{Rd}\gamma_R$; Approach 2 – the value of the global safety factor was determining in accordance with (2) and the model uncertainty considered as the basic variable of the non-linear resistance model.

4 Conclusions

An innovative calibration procedure of the global safety factor γ_{glob} proposed based on Order (non-parametric) Statistics estimation method. A new calibrations procedure gives sufficiently larger values of the global safety factor γ_{glob} than according to EN 1992-2, especially with increasing of the confidence level. When Approach 2 is applied, the model uncertainty can to become the dominant basic variable, whereas according to EN 1992-2, calculation $\exp(\alpha_R \beta V_{Rd})$ when the coefficient of variation V_{Rd} changes from 6.6% to 16.7% leads to a change in the value of factor γ_{Rd} from 1.03 to 1.08 (only!).

References

1. Izzuddin, B. A., Vlassis, A. G., Elghazouli, A. Y., and Nethercot, D. A. (2008), Progressive Collapse of Multi-Storey Buildings Due to Sudden Column Loss – Part 1: Simplified Assessment Framework. Engineering Structures, 30(5), pp. 1308–1318
2. Tur, V. V., Derechennik, S. S. (2018), An Innovation Conformity Criterion for Assessment of the Concrete Strength Under Uncertainty Conditions// High Tech Concrete: Where Technology and Engineering Meet: Proceeding of the 2017 *fib* Symposium, held in Maastricht, The Netherlands, June 12-14, 2017/ D.A. Hordijk and M. Lukovic (eds.) – Springer International Publishing AG, pp. 1628–1635

Macro modelling of infill walls

İsmail Ozan Demirel[1], *Vesile Hatun* Akansel[2], and *Ahmet* Yakut[1,*]

[1]Civil Engineering, Middle East Technical University, Turkey
[2]Civil Engineering, Mugla Universitesi, Mugla, Turkey

Infill walls are known to participate in structural behavior by creating compression struts under lateral loads. In spite of this fact which is proved by experimental investigations, infill walls are considered as non-structural elements in many earthquake regulations and not included in building models during earthquake resistant design. Although two-dimensional geometry and brittle, nonlinear nature of its components make modelling of infill walls difficult, simple strut models have been developed for structural models. In this study, infill walls inside reinforced concrete (RC) frames are idealized with three compression struts where infill wall contribution to rigidity and strength of RC frame is taken into account together with negative effects such as short column formation. The proposed macro model has been calibrated with the results of the cyclic experimental tests on the RC frame infilled with traditional infill wall and improved infill wall with bilateral mesh reinforcement developed at METU Structural Mechanics Laboratories. Finally, calibrated models were applied on a case study frame and the earthquake performances were compared.

[*] Corresponding author: ayakut@metu.edu.tr

Half precast prestressed slab research under short-term and long-term load

Łukasz Drobiec[1,*], *Radosław* Jasiński[1], *Wojciech* Mazur[1], *Artur* Kisiołek[2], *Krzysztof* Grzyb[1], and *Jakub* Zając[1]

[1]Silesian University of Technology, Department of Building Structures, Akademicka 5, 44-100 Gliwice, Poland
[2]Wielkopolska Higher School of Social Sciences and Economics, Institute of Economics, Surzyńskich 2, 63-000 Środa Wielkopolska, Poland

Tests of a full-scale model of slab with dimensions of 6.31 x 6.31 m, built of TerivaPanel panels were carried out under short-term and long-term load. TerivaPanel panels are half precast, prestressed concrete slabs with ribs connected at the bottom. The panels have specially shaped cross connection (shear key) enabling to transfer loads between the panels. The tests were carried out under load placed on the top of the slab. Additionally the load was applied sequentially, measurements were made by electronic method. In one of the stages of long-term testing, the load was applied to one half of the slab to examine the possibility of faulting. The measurements were carried out at monthly intervals, using a geodetic method. The values of vertical displacements at the panel joints (in the middle of the slab) and for central panels along the entire length of the transverse joint were measured.

[*] Corresponding author: Łukasz.Drobiec@polsl.pl

Eco-sustainable construction material: high consistency mortar with biochar additions

Devid Falliano[1,*], *Dario* De Domenico[2], *Salvatore* Quattrocchi[2], *Paolo* Cosenza[2], *Giuseppe* Ricciardi[2], *Luciana* Restuccia[1], and *Giuseppe Andrea* Ferro[1]

[1]Department of Structural, Geotechnical and Building Engineering, Politecnico di Torino, Corso Duca degli Abruzzi, 24, Turin, 10129, Italy
[2]Department of Engineering, University of Messina, Contrada Di Dio, 98166 Sant'Agata, Messina, Italy

This contribution focuses on the design and the characterization of innovative mix designs of high consistency mortars with biochar additions in different percentage with respect to the cement weight. Biochar is a by-product material that gives the cementitious mix a sustainable connotation from an environmental point of view. The mix designs here presented are characterized by a good dimensional stability in the fresh state, peculiarity that gives them the possibility to be extruded and so, to be used in automated construction processes. In addition to the mechanical properties (flexural and compressive strength), the assessment of the CO_2 emission of representative mixes is presented. Different biochar content and maximum diameter of the aggregate are studied, obtaining interestingly indications on these parameters to optimize mechanical properties. Finally, on the basis of the CO_2 emission assessment, some indication about future research work to minimize CO_2 emissions are reported.

[*] Corresponding author: dfalliano@unime.it

A study on the correlation of real and simulated ground motion records-based intensity measures with seismic performance measures

Shaghayegh Karimzadeh[1,*], *Koray* Kadas[1], *Aysegul* Askan[1], and *Ahmet* Yakut[1]

[1]Civil Engineering Department, Middle East Technical University, Turkey

Ground motion simulations are increasingly being used worldwide in earthquake engineering practice. Correspondingly, investigation of their efficiency in estimation of seismic demand parameters is crucial. In this study, a large set of simulated ground motion records in the Western part of North Anatolian Fault Zone (in Turkey) is generated. The ground motion dataset formed involves a wide range of earthquake magnitudes, source-to-site distances, and site profiles. The simulated dataset is prepared using the stochastic finite fault ground motion simulation methodology. In parallel with the simulated dataset, a real ground motion dataset which has similar seismological characteristics with the region of interest is formed. The seismological properties include source mechanism, source-to-site distance and site class. For both simulated and real datasets, alternative ground motion intensity measures representing peak ground motion levels, frequency content and spectral values are assessed. Next, nonlinear time history analyses are performed utilizing a set of single degree of freedom models with a wide period range. Then, the correlations of the ground motion intensity measures with the performance measure in terms of maximum inelastic displacements are studied. Results reveal a strong correlation for the simulated ground motion dataset with the selected engineering demand parameter pointing out the high degree of efficiency of regional ground motion simulation.

[*] Corresponding author: shaghkn@metu.edu.tr

Evaluation of observed seismic damage for the 1999 Duzce earthquake

Shaghayegh Karimzadeh[1], *Ahmet* Yakut[1,*], and *Aysegul* Askan[1]

[1]Civil Engineering Department, Middle East Technical University, Turkey

In 1999, two subsequent destructive earthquakes, Kocaeli (Mw = 7.4) and Duzce (Mw = 7.1), strike the Duzce region in Western Turkey. Extensive building damage was observed in Duzce area in 1999. In the aftermath of the earthquake, a damage database was formed by experts through the field survey. The database includes damage distribution of nearly 500 reinforced concrete buildings. In this study, this damage database is used in order to investigate the correlation of the observed structural damage with alternative ground motion intensity measures. The selected ground motion intensity measures include peak ground acceleration, peak ground velocity, spectral acceleration intensity, spectral velocity intensity, Arias intensity, and Housner intensity. The ground motion intensity measures are determined from the regionally simulated records of the 1999 Duzce earthquake. Simulations are performed at sites where damage assessment data is available. For simulations, the stochastic finite-fault approach based on a dynamic corner frequency approach is used. Correlation of structural damage with ground motion intensity is evaluated through Pearson and Spearman correlation coefficients. In general, varying degrees of correlations are observed between the observed damage and the considered ground motion intensity measures.

[*] Corresponding author: ayakut@metu.edu.tr

Experimental study on shear behaviour of CFRP strengthened out of plane curved reinforced concrete beams

Chinthana Fernando[1,*], and *P.* Gamage[1]

[1]Department of Civil Engineering, University of Moratuwa, Srilanka

Shear performance of Carbon Fibre Reinforced Polymer (CFRP) strengthened concrete curved beams subjected to out of plane bending is an important aspect. A detailed test program was designed in order to determine the shear behaviour of CFRP strengthened horizontally curved RC beams. A total of nine medium scale beam specimens were prepared with 2 m and 4 m curvatures. The non-strengthened control beams were designed to fail in shear mode primarily, by increasing the flexural capacity to sustain the flexure till the beam reaches enhanced shear capacity after installation of CFRP. The test results indicate the dependency of shear strength gain with the curvature of strengthened beams under out of plane loading.

[*] Corresponding author: chinthana.vimukthi@live.com

Longitudinal forces in bearing components of R/C concrete - a generally ignored phenomenon which severely changes the behavior

Piotr Noakowski[1,*]

[1]Bauwesen, TU Dortmund, Exponent GmbH, Germany

Tension forces are practically activated in each concrete beam. The phenomenon is due to the effects of shrinkage and temperature drop which are obstructed by columns, walls, etc. As soon as such actions are distinct and the constraining elements sufficiently stiff, corresponding tension forces and through cracks are produced. Such cracks:

– separate the affected sections and endanger their tightness,
– decrease their stiffness and so produce large deflections,
– may diminish the shear bearing capacity due to the lack of compression zones.

All the phenomena impair frequently the strength and the serviceability of the affected structures. These facts indicate that longitudinal forces shouldn't be ignored in modern design of concrete structures.

* Corresponding author: p.noakowski@exponent.de

Load and resistance factors for prestressed concrete girder bridges

Andrzej S. Nowak[1,*], and *Olga* Iatsko[1]

[1]Civil Engineering, Auburn University, Auburn, AL 36849, United States

There has been a considerable progress in the reliability-based code development procedures. The load and resistance factors in the AASHTO bridge design code were determined using the statistical parameters from 1970's and early 1980's. Load and resistance factors were determined by first fixing the load factors and then calculating resistance factors. Load factors were selected so that the factored load corresponds to two standard deviations from the mean value and the resistance factors were calculated so that the reliability index is close to the target value. However, from the theoretical point of view, the load and resistance factors are to be determined as coordinates of the so-called "design point" that corresponds to less than two standard deviations from the mean. Therefore, the optimum load and resistance factors are about 10% lower than what is in the AASHTO LRFD Code. The objective of this paper is to revisit the original calibration and recalculate the load and resistance factors as coordinates of the "design point" for prestressed concrete girder bridges. The recommended new load and resistance factors provide a consistent reliability and a rational safety margin.

[*] Corresponding author: nowak@auburn.edu

Research on the recycled and hybrid fibre reinforced self-compacting concrete under flexure

Małgorzata Pająk[1,*]

[1]Silesian University of Technology, Civil Engineering Faculty, Akademicka 5, 44-100 Gliwice, Poland

In the present study the fibres coming from the end-of-life tires were investigated to contribute to management of wastes produced by people. The influence of the recycled, glass and polypropylene fibres on the flexural behaviour of SCC was tested. The recycled fibres and their mixture with glass or polypropylene fibres (hybrid mixes) were analysed. The research revealed that the dosage of 1.5% of recycled fibres is highly effective in the SCC matrix. The pronounced increase of the flexural parameters were noted. The values of the residual flexural tensile strengths obtained in the tests classified the R-SCC to be used as a partial replacement of the conventional reinforcement. The addition of other types of fibres to R-SCC caused the enhancement of flexural parameters with no negative effect on the distribution of the fibres.

[*] Corresponding author: malgorzata.pajak@polsl.pl

Effects of polyvinyl alcohol content and fiber length on carbonization behavior of strain-hardening cementitious composite

Xinhua Yang[1,*], and *Zuyun* Luo[1]

[1]School of Civil Engineering and Mechanics, Huazhong University of Science and Technology, Hongshan District, Wuhan 430074, Hubei, China

Due to good tensile hardening performance, strain-hardening cementitious composite (SHCC) has wide application prospects. However, how does polyvinyl alcohol (PVA) affect the durability of materials? In order to answer this question, some carbonization experiments were performed on the SHCC specimens with different PVA content of 0.1%, 0.3%, and 0.5% and different fiber length of 6 mm, 12 mm, and 18 mm at ambient temperature. The statistical results showed that the carbonization depth satisfies approximately normal distribution and the specimens with higher PVA content or shorter PVA fibers have a smaller carbonization depth. Finally, a carbonization model was given for SHCC.

* Corresponding author: yangxinh@hust.edu.cn

List of authors